Physics Library
QC
1
.P5812
V.56
no.7

THE PHYSICAL REVIEW

VOLUME 56 | Second Series | NUMBER 7

OCTOBER 1, 1939

Published for the
AMERICAN PHYSICAL SOCIETY
by the
AMERICAN INSTITUTE OF PHYSICS
Incorporated
LANCASTER, PA., AND NEW YORK, N. Y.

UNIVERSITY OF MICHIGAN LIBRARIES

THE PHYSICAL REVIEW

A journal of experimental and theoretical physics established by E. L. Nichols in 1893

Published by the American Institute of Physics for the

American Physical Society

OFFICERS

President

JOHN T. TATE
University of Minnesota
Minneapolis, Minnesota

Vice President

JOHN ZELENY
Yale University
New Haven, Connecticut

Secretary

W. L. SEVERINGHAUS
Columbia University
New York, New York

Treasurer

G. B. PEGRAM
Columbia University
New York, New York

Local Secretary for the Pacific Coast

PAUL KIRKPATRICK
Stanford University
California

Editor

JOHN T. TATE
University of Minnesota
Minneapolis, Minnesota

BOARD OF EDITORS

JOHN T. TATE, *Editor* — J. W. BUCHTA, *Assistant Editor*

Associate Editors

K. T. BAINBRIDGE	A. L. HUGHES	W. BLEAKNEY
H. P. ROBERTSON	T. H. JOHNSON	G. BREIT
H. B. WAHLIN	F. A. JENKINS	D. M. DENNISON

Manuscripts for publication should be submitted to John T. Tate, University of Minnesota, Minneapolis, Minnesota.

Proof and all correspondence concerning papers in the process of publication, should be addressed to the Publications Manager, American Institute of Physics, 175 Fifth Avenue, New York, New York.

Subscription Price

United States and Possessions and Canada $15.00
Foreign $16.50

Back Numbers

Complete set: Series 2,[1] Vol. 1, 1913–Vol. 54, 1938—$396.00
Yearly rate: $16.50
Single copies: $1.50 each prior to July, 1929; $.75 each after July, 1929.

Subscriptions and orders for back numbers should be addressed to Prince and Lemon Streets, Lancaster, Pennsylvania, or to the American Institute of Physics, 175 Fifth Avenue, New York, New York.

Advertising is not accepted for the *Physical Review* but attention is called to the *Review of Scientific Instruments* and the *Journal of Applied Physics*, companion publications of the Institute, and media through which the field of physics can be reached most effectively. Rates and other information will be furnished on request.

Changes of address and complaints of failure to receive the *Physical Review* in the case of members of the American Physical Society, should be addressed to the Treasurer; in the case of other subscribers, to the Publications Manager. New copies can be sent free in response to complaints of non-delivery only if notice of non-delivery is received within three months of date of issue.

[1] For Series 1 inquire of Physics Department, Cornell University, Ithaca, N. Y.

The Physical Review is published semi-monthly at Prince and Lemon Streets, Lancaster, Pennsylvania.

Entered at the Post Office at Lancaster, Pennsylvania, as second class matter.

Acceptance for mailing at special rate of postage provided for in section 1103, Act of October 3, 1917, authorized September 6, 1926.

Physics
Physics-USA
January
10-10 63
Replace

THE
PHYSICAL REVIEW

A Journal of Experimental and Theoretical Physics Established by E. L. Nichols in 1893

VOL. 56, NO. 7 OCTOBER 1, 1939 SECOND SERIES

Emission of Neutrons by Uranium*

W. H. ZINN, *City College, The College of the City of New York, New York*

LEO SZILARD, *Pupin Physics Laboratories, Columbia University, New York, New York*

(Received August 14, 1939)

Fast neutrons emitted by uranium under the action of thermal neutrons were studied by using a radium-beryllium photoneutron source. The background due to the primary neutrons can be neglected since only a few of the photoneutrons are sufficiently fast to be counted. Data are obtained concerning the energy spectrum of the uranium fission neutrons by recording photographically by means of a linear amplifier and cathode-ray oscillograph the pulses due to helium atoms projected in an ionization chamber. Visual inspection of the record gives an upper limit of the spectrum of 3.5 Mev. The number of neutrons emitted is estimated by analyzing the pulse distribution of hydrogen atoms projected by uranium neutrons in an ionization chamber filled with hydrogen and argon. The number found is brought into relationship with the number of fissions, observed under comparable conditions, in an ionization chamber lined with a thin film of uranium oxide containing a known amount of uranium. In this way it is found that about 2.3 neutrons are emitted per fission. The method used would permit a greater accuracy in the determination of this number than the actual accuracy obtained in the present experiments. This number, together with the fission cross section and the cross section for radiative capture gives the number of neutrons produced for each thermal neutron absorbed in uranium.

WE reported[1] some time ago that fast neutrons are emitted—apparently instantaneously—from uranium under the action of thermal neutrons and we found, as a rough estimate, an average of two neutrons per fission process. This result was obtained by counting the helium recoil nuclei which the fission neutrons project in a helium-filled ionization chamber. The emission of neutrons in the fission of uranium was independently discovered by von Halban, Joliot and Kowarski[2] as well as by Anderson, Fermi and Hanstein,[3] who observed an increase of the thermal neutron density in water in the presence of uranium. Others[4] have investigated the same phenomenon.

Before this "instantaneous" emission had been observed, Roberts, Meyer and Wang[5] discovered a delayed emission of neutrons from uranium which apparently follows a beta-transformation of a half-life period of twelve seconds. We had found that the instantaneous emission was very much stronger than the delayed emission and we assumed that it corresponds to a direct ejection of neutrons from the uranium fragments, without being preceded by a beta-transformation, and that accordingly the time delay involved is far too small to be measured by the usual

* Publication assisted by the Ernest Kempton Adams Fund for Physical Research of Columbia University.

[1] L. Szilard and W. H. Zinn, Phys. Rev. **55**, 799 (1939).

[2] H. von Halban, F. Joliot and L. Kowarski, Nature **143**, 470 (1939).

[3] H. L. Anderson, E. Fermi and H. B. Hanstein, Phys. Rev. **55**, 797 (1939).

[4] G. P. Thomson, J. L. Michiels and G. Parry, Nature **143**, 760 (1939); G. von Droste and H. Reddeman, Nat. Wiss. **20/21**, 371 (1939).

[5] R. B. Roberts, R. C. Meyer and P. Wang, Phys. Rev. **55**, 510 (1939).

UNIVERSITY OF MICHIGAN LIBRARIES

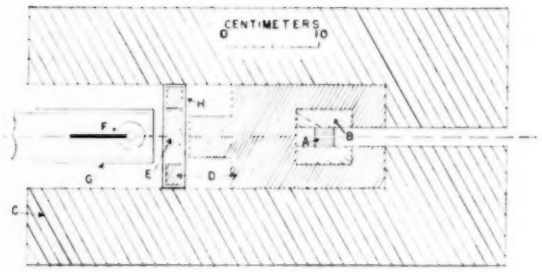

FIG. 1. Arrangement for the observation of the emission of fast neutrons from uranium. *A*—radium; *B*—beryllium block; *C*—paraffin wax; *D*—lead; *E*—uranium cell; *F*—spherical ionization chamber; *G*—cadmium sheet cap; *H*—cadmium sheet shield.

methods. This assumption was based on the arguments that it would be very difficult to explain the great abundance of the instantaneous neutron emission without assuming direct ejection and that no hard beta-rays were observed which should be expected to be present if the neutron emission followed a very short-lived beta-transformation. From direct experimental evidence, however, we could not exclude a delay smaller than one-tenth of a second. Gibbs and Thomson[6] have now shown by direct experiments that the delay is smaller than one-thousandth of a second and this appears to leave little doubt as to a direct ejection of neutrons.

In the present experiments helium recoils were used for investigating the energy distribution of the fission neutrons, but hydrogen recoils were used for estimating the number emitted per fission.

The experimental arrangement is shown in Fig. 1. The source of thermal neutrons was about one gram of radium, *A*, placed in the center of a beryllium block, *B*, and surrounded by a paraffin cylinder, *C*. Fast neutrons emitted under the action of the thermal neutrons by about 430 grams of uranium metal enclosed in the cell *E*, were detected by the spherical ionization chamber, *F*. The pulses from the chamber were fed into a linear amplifier and were made visible by means of a cathode-ray oscillograph. A camera with a moving film was used to obtain a photographic record of the pulses appearing on the oscillograph screen.

Two such records are shown in Fig. 2; one was obtained in the absence and the other in the presence of the cadmium sheet shield, *H*. The shield *H* completely surrounds the uranium and shuts it off from most of the thermal neutrons, leaving a background of pulses which is partly due to particularly fast photoneutrons from the source, and partly due to fission neutrons from the uranium emitted under the action of the few thermal neutrons which pass through the cadmium shield. This background amounts to less than one pulse per minute.

The ionization chamber, which was filled with 10 atmospheres of hydrogen and 8 atmospheres of argon, contained a small amount of nitrogen. By removing the cadmium cap, *G*, from the chamber the nitrogen atoms in the chamber can be exposed to the action of thermal neutrons and

[6] D. F. Gibbs and G. P. Thomson, Nature **144**, 202 (1939).

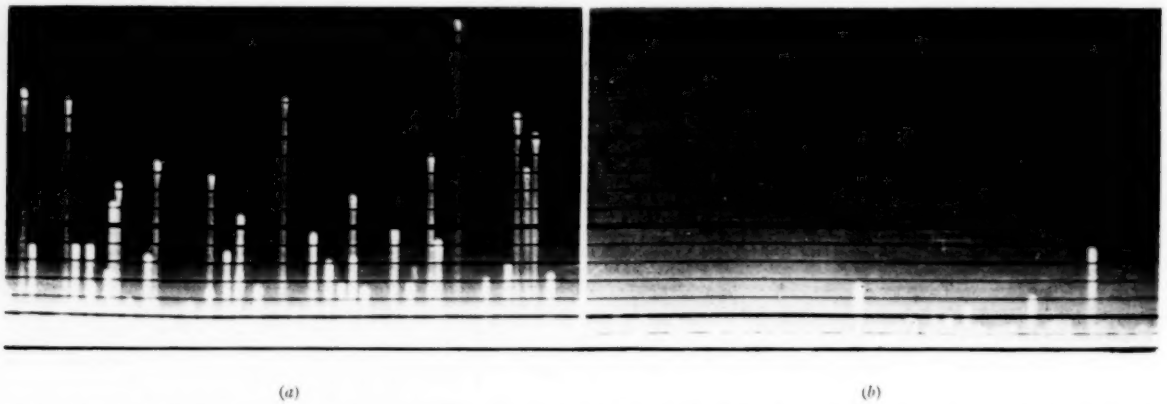

(*a*) (*b*)

FIG. 2. (*a*) Oscillograph record of the fast neutrons from uranium. Cadmium sheet shield, *H* of Fig. 1, absent. Thermal neutrons falling on the uranium in the cell *E*. Ionization chamber filled with 10 atmospheres of hydrogen and 8 atmospheres of argon. (*b*) Record obtained with the cadmium shield *H* shutting off the thermal neutrons from the cell *E*.

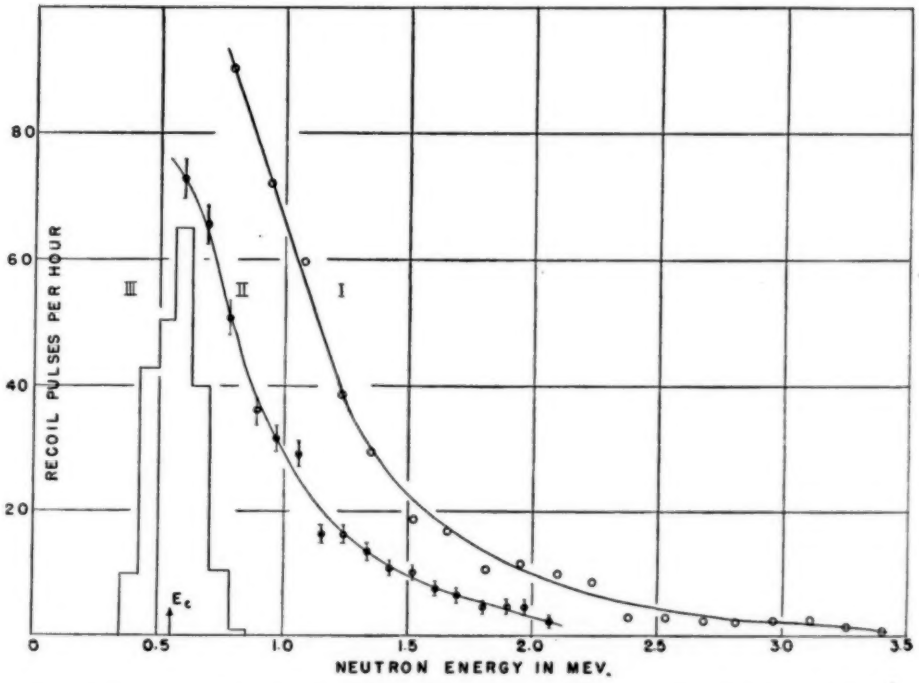

FIG. 3. Curve I: Pulse distribution due to helium recoils. Ionization chamber filled with 10 atmospheres of helium and 10 atmospheres of argon. Curve II: Pulse distribution $P(E)$ due to hydrogen recoils. Ionization chamber filled with 10 atmospheres of hydrogen and 8 atmospheres of argon. Curve III: Pulse distribution due to protons emitted, under the action of thermal neutrons, by a small amount of nitrogen in the chamber filled with 10 atmospheres of helium and 10 atmospheres of argon.

will then emit protons of about 0.6 Mev energy.[7] The pulses due to these protons were recorded and their distribution is shown in curve III of Fig. 3. This curve shows a sharp maximum which should correspond to an energy of about 0.6 Mev, and therefore this curve was used for calibrating the ionization chamber.

In order to find from the observed number of hydrogen recoils the number of neutrons which pass through the chamber it is necessary to know something about the energy distribution of the fission neutrons. This knowledge is required for two reasons. First, the scattering cross section of hydrogen is a function of the neutron energy; secondly, the observed pulse distribution of the hydrogen recoils is cut off at a certain energy E_c, which in this case was 0.55 Mev, in order to avoid the counting of pulses in the region which is affected by the gamma-ray background. Neutrons which have an energy below this cut-off energy, E_c, do not contribute to the recorded pulse distribution and their number has to be determined from the shape of the neutron spectrum, provided this spectrum is known.

If the time required for the collection of ions in the chamber were short compared with the time constant of the amplifier, the size of the pulses recorded by the oscillograph might be considered a fair measure of the energy which the recoil proton loses in the chamber. Even so, the size of the pulses cannot be considered a measure of the initial energy of the recoil protons if these lose only part of their energy in the chamber and are stopped by the walls. Therefore, if $R(E)dE$ is the number of recoil protons having an initial energy between E and $E+dE$, and if $P(E)dE$ is the number of recoil protons which lose in the chamber an amount of energy between E and $E+dE$, these two functions will be rather different in the high energy region where the range of the recoil protons cannot be neglected in comparison with the linear dimensions of the chamber. For the hydrogen-argon filled chamber

[7] J. Chadwick and M. Goldhaber, Proc. Camb. Phil. Soc. **31**, 612 (1935); T. W. Bonner and W. M. Brubaker, Phys. Rev. **49**, 778 (1936); M. S. Livingston and H. A. Bethe, Rev. Mod. Phys. **9**, 344 (1937).

which was used the two functions can be expected to coincide very nearly in the region of the cut-off energy E_c, and can be expected to differ widely for energies above 1.5 Mev.

For this reason helium recoils (which have about $\frac{1}{10}$ the range of recoil protons for equal neutron energies) had to be used instead of hydrogen recoils in order to find the upper end of the energy spectrum of the fission neutrons. Curve I, in Fig. 3, shows the pulse distribution of helium recoils obtained with 10 atmospheres of helium and 10 atmospheres of argon in the chamber. This curve shows that the spectrum of the fission neutrons extends to about 3.5 Mev. Though the existence of a small number of high energy neutrons such as reported by von Halban, Joliot and Kowarski,[8] is not inconsistent with our result, the number of neutrons having energies above 4 Mev appears to be too small to have much bearing on our estimate of the total number of fission neutrons.

Since the calibration of the chamber, which we performed by means of protons, is not entirely satisfactory for correlating the size of the pulses due to helium recoils with the energy of the helium recoils, the helium-argon filled chamber was also calibrated by means of D+D neutrons of 2.5 Mev energy. The two calibrations coincided within the limits of the experimental error.

An estimate of the number of fission neutrons should be based on a count of hydrogen recoils rather than helium recoils since the scattering cross section of helium has a sharp maximum[9] for neutrons of about 1.0 Mev energy, and helium is therefore not suitable for the purposes of a quantitative estimate. It can be shown that, if the neutron-proton scattering is spherically symmetrical in the system of the center of gravity, the number of neutrons $N(E)dE$ which pass through the chamber, and which have an energy between E and $E+dE$, is given by:

$$N(E)=-\frac{E}{H\sigma(E)}\frac{dR(E)}{dE},$$

where $\sigma(E)$ is the scattering cross section of the proton and H is the number of hydrogen atoms in

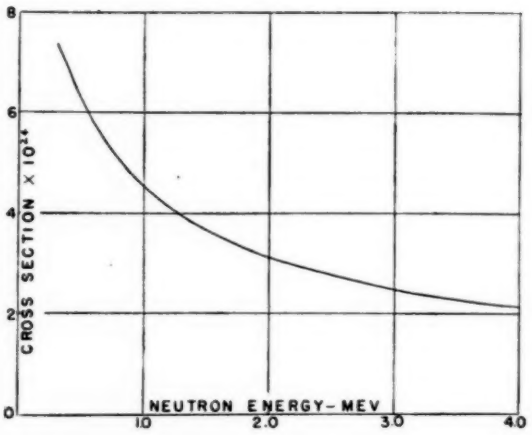

FIG. 4. Neutron-proton cross section as a function of neutron energy according to current theory.

the ionization chamber. From this we derive, for the total number of neutrons, N, passing through the chamber:

$$N=\int_0^\infty N(E)dE=\frac{\alpha}{\sigma_{Av}H}\left[E_cR(E_c)+\int_{E_c}^\infty R(E)dE\right],$$

where α is the ratio of the total number of neutrons to the number of neutrons which have an energy in excess of E_c, and σ_{Av} is an average scattering cross section of the proton, the value of which has to be determined from the energy spectrum of the neutrons. Since we have:

$$\int_0^\infty R(E)dE=\int_0^\infty P(E)dE$$

and since, for the reasons stated above, we have with good approximation:

$$R(E)\backsimeq P(E) \quad \text{for} \quad E\leq E_c,$$

we can express N in terms of $P(E)$ instead of $R(E)$. We then have:

$$N=\frac{\alpha}{\sigma_{Av}H}\left[E_cP(E_c)+\int_{E_c}^\infty P(E)dE\right].$$

Let it now be assumed for the sake of argument that all the neutrons are emitted from a moving uranium fragment which has a mass number of about 120 and a kinetic energy of about 100 Mev. If all the neutrons were emitted from such a moving fragment with a single energy E_0, the energy distribution of the neutrons in the

[8] H. von Halban, F. Joliot and L. Kowarski, Nature **143**, 939 (1939).
[9] H. Staub and W. E. Stephens, Phys. Rev. **55**, 131 (1939).

laboratory reference system would stretch from:

$$E_{\min}=(0.9-E_0^{\frac{1}{2}})^2 \text{ Mev}$$

to:

$$E_{\max}=(0.9+E_0^{\frac{1}{2}})^2 \text{ Mev}.$$

It is easy to see that the neutrons should be uniformly distributed in this energy interval if their distribution is spherically symmetrical in the center of mass system. One obtains accordingly:

$$\alpha=(E_{\max}-E_{\min})/(E_{\max}-E_c)$$

and

$$\frac{1}{\sigma_{Av}}=\frac{1}{E_{\max}-E_c}\int_{E_c}^{E_{\max}}\frac{dE}{\sigma(E)}.$$

Using for $\sigma(E)$ the curve shown in Fig. 4 which has been theoretically derived,[10] the following values of α/σ_{Av} are obtained for various values of $E_{\max}$.

$E_{\max}$	2.0 Mev	3.0 Mev	4.0 Mev
α/σ_{Av}	$0.316\times10^{+24}$	$0.353\times10^{+24}$	$0.388\times10^{+24}$

The variation of α/σ_{Av} with $E_{\max}$ is so slight because of the manner in which both α and σ_{Av} decrease with rising $E_{\max}$.

The value of the expression:

$$E_cP(E_c)+\int_{E_c}^{\infty}P(E)dE$$

was found from the observed pulse distribution (curve II of Fig. 3) to be 13.7 pulses per minute. Since the number H of hydrogen atoms in the chamber was $H=6.9\times10^{+21}$ the number of neutrons passing through the chamber is

$$N=1.98\times10^{-21}(\alpha/\sigma_{Av}) \text{ per minute.}$$

If the cadmium cap G is removed the number of thermal neutrons reaching the uranium cell is increased and the number of fast neutrons passing through the ionization chamber is increased by the same factor. This factor was found to be 1.22 by filling the ionization chamber with pure hydrogen and then counting the hydrogen recoils giving rise to pulses above a certain arbitrarily set level, both in the presence and absence of the cadmium cap. Thus the number of neutrons N^* which pass through the chamber in the absence of the cadmium cap, G, is

$$N^*=2.415\times10^{-21}(\alpha/\sigma_{Av}) \text{ per minute.}$$

From N^* the number, K, of neutrons emitted per minute by the uranium was calculated by taking into account the geometrical factors, including the variation of the thermal neutron density within the uranium cell. K is thus found to be:

$$K=8.25\times10^{-19}(\alpha/\sigma_{Av}) \text{ per minute.}$$

In order to obtain the number of neutrons emitted per fission it is necessary to compare K with the number of fissions, L, which occur in the uranium under the conditions of this experiment. For this purpose both the ionization chamber and the uranium cell were removed and a parallel plate ionization chamber lined with a thick layer of uranium oxide was placed in the position previously occupied by the uranium cell. The number of fissions produced in this chamber was observed and found to be 19 per minute. The chamber was then calibrated by comparing the number of fissions obtained from the thick uranium oxide layer with the number of fissions obtained in the same chamber at the same thermal neutron intensity from a thin layer of uranium oxide containing 1.4 mg of uranium. The calibration was carried out by using a particularly strong neutron source, so as to obtain a sufficiently large number of counts from the thin layer. The ratio of the fission counts from the thick layer and from the thin layer was found to be 29.2, from which it is concluded that 196,000 fissions per minute should take place in the uranium cell containing 427.7 grams of uranium. This would be the number of fissions if the density of the thermal neutrons were not reduced in the uranium cell due to the absorption of such neutrons in uranium. We estimate that the average density of thermal neutrons within the cell is reduced by a factor of 0.715. The number of fissions L actually taking place within the cell is therefore

$$L=140{,}000 \text{ per minute.}$$

In order to estimate the reduction of the average thermal neutron density within the uranium cell leading to the factor of 0.715, we first explored the anisotropy of the thermal neutron radiation near the uranium cell by means

[10] J. Schwinger and E. Teller, Phys. Rev. 52, 286 (1937).

of a rhodium indicator, and then calculated the thermal neutron density within the uranium by assuming the distribution of thermal neutrons to be the same as would result from the superposition of two parallel thermal neutron beams, one directed away from the source and the other towards it, and having an intensity ratio of 3 to 1. We assume exponential absorption for these two beams within the uranium and an exponent corresponding to a half-value thickness in uranium of 14 g per cm^2.

The number of neutrons emitted per fission is

$$K/L=5.9\times10^{-24}(\alpha/\sigma_{Au}).$$

This number should be increased by perhaps 10 percent in order to correct for the fact that $P(E)$ does not exactly coincide with $R(E)$ even for $E\leq E_c$. The magnitude of this correction was estimated by comparing for D+D neutrons of 2.5 Mev energy the observed pulse distribution $P(E)$ with the calculated distribution $R(E)$ in the region of the low recoil energies. Making this correction one finds for ρ, the number of neutrons per fission

$$\rho=6.5\times10^{-24}(\alpha/\sigma_{Au}).$$

Using for α/σ_{Au} the value 0.353×10^{-24} which corresponds to $E_{max}=3$ Mev rather than to the actually observed upper limit of the fission neutron spectrum, one finds

$$\rho=2.3.$$

Since the fission neutrons hardly will be emitted with a single energy E_0, too high a value for α/σ_{Au} would be obtained if the observed value of the upper limit of the energy spectrum were used for E_{max}. In any case the error introduced by the uncertainty of the actual energy distribution of the fission neutrons should be small since one finds for

$$E_{max}=2 \text{ Mev} \quad \rho=2.0$$

and for

$$E_{max}=4 \text{ Mev} \quad \rho=2.5.$$

More serious, however, may be a number of experimental inaccuracies which might conceivably add up to give a considerable error.

The interest in the number of neutrons emitted per fission arose out of its obvious importance from the point of view of the possibility of nuclear chain reactions. At present we have the following set of values: number of neutrons per fission, 2.3; fission cross section,[11] 2.0×10^{-24} cm^2; cross section for radiative capture[12] 1.3 or 1.2×10^{-24} cm^2. According to these values, the number of neutrons emitted by uranium per thermal neutron absorbed should be 1.4, which agrees with the value of 1.5 recently obtained by another method by Anderson, Fermi and Szilard.[13] Too much significance should not be attributed to this agreement, since the values given above are subject to fairly wide experimental errors.

If required the present experiments could be repeated with greater accuracy since the method used is quite capable of being applied with greater precision. Moreover, it gives the number of neutrons per fission independently of the value of the fission cross section which enters into the method used by von Halban, Joliot and Kowarski. These authors report[14] a value of 3.5 ± 0.7 neutrons per fission.

It should be mentioned that it appears to be essential for the method presented here to work with a low background count. The background is due to the primary neutrons and can be kept small by using a photoneutron source. We did not find it possible to obtain quantitative results by using neutrons from radon-beryllium sources or from the D+D reaction on account of the high background count due to the primary neutrons.

We are indebted to Dr. G. N. Glasoe for suggesting the method of obtaining the photographic records and for much valuable advice in this connection, and to Dr. E. T. Booth for determining by means of an alpha-particle count the uranium content of the thin uranium sheet which we used for purposes of calibration. Also, we wish to thank the Department of Physics of Columbia University for the laboratory facilities placed at our disposal and the Association for Scientific Collaboration for enabling us to obtain the radium used in this experiment.

[11] H. Anderson, E. Booth, J. Dunning, E. Fermi, G. Glasoe and F. Slack, Phys. Rev. **55**, 511 (1939).
[12] H. v. Halban, L. Kowarski and P. Savitch, Comptes rendus **208**, 1396 (1939); H. L. Anderson and E. Fermi, Phys. Rev. **55**, 1106 (1939).
[13] H. L. Anderson, E. Fermi and L. Szilard, Phys. Rev. **56**, 284 (1939).
[14] H. von Halban, F. Joliot and L. Kowarski, Nature **143**, 680 (1939).

Induced Radioactivity in Europium

KASIMIR FAJANS AND DAVID W. STEWART*
Departments of Chemistry and Physics, University of Michigan, Ann Arbor, Michigan
(Received August 16, 1939)

Europium oxide has been bombarded with slow neutrons from the cyclotron for periods ranging up to about five months, and with 7-Mev deuterons for much shorter lengths of time. By reduction of the europium to its bivalent state, it has been possible to separate this element from neighboring members of the rare earth group. By slow neutron activation, two periods of induced radioactivity have been produced in europium; one, with a half-life of 9.4±0.2 hours, is assigned to Eu^{152}, in accordance with the results of other investigators. This isotope probably decays both by the emission of negative electrons and by the capture of K electrons. The beta-spectrum, as measured in the cloud chamber, has an upper limit of 1.83 Mev. The second period, produced only after long exposure, has not decayed appreciably in six months. It has been assigned to Eu^{154}. Preliminary studies indicate that K-electron capture may also take place in the decay of this isotope. The upper limit of the beta-spectrum has been found to be 1.0±0.1 Mev. By relatively short deuteron bombardments, the 9-hour period has also been produced, and in addition two new periods of 12±4 minutes and 105±5 minutes have been obtained. These could not be separated from the 9-hour activity by chemical methods, which indicates that they are due also to isotopes of europium, probably to isomeric forms of Eu^{152} and Eu^{154}, not produced appreciably by slow neutron activation.

INTRODUCTION

RADIOACTIVITY induced in europium by the action of neutrons had previously been studied by Sugden,[1] Marsh and Sugden,[2] Hevesy and Levi,[3] and Pool and Quill.[4] Europium, like cerium, differs from other members of the rare earth group in that it may be separated from neighboring elements by a single chemical operation with satisfactory completeness, and for this reason it has been feasible to study more carefully the radioactivity induced in it by deuteron as well as by neutron bombardments. The stable isotopes of europium and adjacent elements are shown in Fig. 1, where the figures refer to percent abundance.

Previous investigators had found in europium a negative-active period of 9.2-hour half-life. On the basis of experiments with fast neutrons, this activity has been shown by Pool and Quill[4] to be due to Eu^{152}. These same experimenters have reported a period of 27 hours, which they observed only after fast neutron activation, and have assigned this to Eu^{150}, which is reported to emit positrons. In the present study, slow neutrons were used to extend the previously known results, and deuterons were also used to search for new radioactive isotopes. Cloud-chamber studies were made of the radiations from certain of the artificially produced radioelements.

MATERIALS AND APPARATUS USED

Europium oxide was obtained from Professor H. N. McCoy, who made the original purification. To remove traces of the lighter elements, such as sodium, the europium was twice precipitated from acid solution by oxalic acid, with ignition each time to the oxide. An examination of the arc spectrum of the material with a Littrow quartz spectrograph failed to reveal impurities of other rare earths, or of any of the common elements.

A further question as to the purity of the material was raised after electroscopic measurements on 0.5-gram samples showed that natural

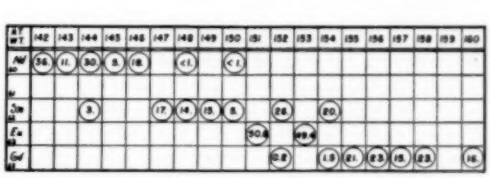

FIG. 1. Stable isotopes with their relative abundance.

* Present address, Department of Chemistry, Columbia University, New York.
[1] S. Sugden, Nature **135**, 469 (1935).
[2] J. K. Marsh and S. Sugden, Nature **136**, 102–3 (1935).
[3] G. v. Hevesy and H. Levi, Kgl. Danske Videnskab. Selskab, Math.-fys. Medd. **14**, No. 5 (1936); also Nature **136**, 103 (1935), **137**, 185 (1936).
[4] M. L. Pool and L. L. Quill, Phys. Rev. **53**, 437–46 (1938).

radioactivity, with an intensity of the order of magnitude of the natural leak of the measuring instrument, was present before bombardment. Tests on larger samples of the europium oxide resulted in the identification of traces of mesothorium, radiothorium, thoron, and subsequent members of the natural thorium series, and a method was devised to remove all detectable natural radioactivity. The method of Kaufman[5] was used, in which a small amount of europium iodate was precipitated to act as a carrier for the less soluble thorium iodate. This was followed by the precipitation in the solution of barium sulfate to act as a carrier of radium and lead isotopes. By repeating this process, and finally reprecipitating the europium, a quantity of material was prepared in which no natural activity of any kind could be detected. This europium oxide was then used for all further experiments.

Deuterons were accelerated in the cyclotron, where a beam of from 10 to 20 microamperes at 7 Mev was usually available for direct bombardments. For the production of neutrons, beryllium was bombarded with larger currents of deuterons at somewhat lower energy.

Measurements of the radioactivity were made with a Lauritsen type electroscope. The sensitivity of this instrument was frequently checked with a standard uranium oxide source, and all readings were reduced to a constant sensitivity.

The sign of the particles emitted and the energy of beta-rays were measured in a cloud chamber 12 inches in diameter, in a magnetic field uniform to about ± 0.5 percent over the volume of the chamber. The chamber was filled with hydrogen, and alcohol and water were used as condensable vapor.

Slow Neutron Activation

Europium oxide was surrounded by paraffin and exposed to neutrons from the cyclotron. The strongest activation was obtained in an exposure which lasted from August, 1938, to January, 1939, during which time the cyclotron was operating intermittently with varying efficiency. This sample showed a strong initial decay in the previously known period, here observed to be 9.4 ± 0.2 hours, and then further decay in an extremely long period. In six months following bombardment, the intensity has remained constant within the experimental error of about one percent. The sample now has an activity about sixty times as great as the background of the electroscope, and further measurements of the decay are being made.

To make certain that the long period activity was not due to remaining traces of the naturally-active contaminant, previously detected and removed, the sample, following bombardment, was dissolved in nitric acid and barium sulfate was precipitated in the solution. The sulfate precipitate carried with it less than one percent of the long period activity, whereas the same treatment had removed almost all of the beta-activity of the natural contaminant. The bombarded sample was also much more active than could be explained on the basis of a remaining trace of radioactive impurity. It may thus be concluded that both periods observed are due to isotopes of europium produced by the capture of slow neutrons. No periods shorter than the one of 9.4 hours could be detected, even in samples bombarded for much shorter intervals of time and measured within five minutes after bombardment.

If, following the work of Pool and Quill,[4] the 9-hour activity is assigned to Eu^{152}, the long period most probably belongs to Eu^{154}. The two observed slow neutron reactions are thus:

$$Eu^{151} + n^1 \rightarrow Eu^{152} + h\nu \qquad (1)$$

$$Eu^{153} + n^1 \rightarrow Eu^{154} + h\nu. \qquad (2)$$

The observation of a new, long-lived radioactive isotope, with its assignment to Eu^{154}, explains the results of Hevesy and Levi[3] and others who have found an abnormally high absorption in europium for slow neutrons without detecting the long period.

Radiations connected with both periods have been examined. The energy spectrum of the 9-hour beta-rays was measured in the cloud chamber in a field of 334 gauss. From a distribution of 840 tracks, the observed upper limit was found to be 1.83 ± 0.05 Mev. This is in agreement with the value of 2.0 Mev found by Hevesy and

[5] L. Kaufman, J. App. Chem. (U. S. S. R.) **9**, 918–24 (1936).

Levi from absorption measurements, but does not agree as well with the value of 2.6±0.4 Mev reported by Naidu and Siday.[6] Subsequent to the present work, the authors supplied a sample of the material to Mr. A. W. Tyler, who has investigated the radiations in a magnetic spectrometer. His value of 1.885±0.012 Mev for the upper limit of the electron spectrum[7] is in good agreement with that reported here.

Absorption experiments on the 9-hour radiation showed that gamma-rays of at least two different energies accompanied the beta-rays. From absorption in aluminum, the softer component was found to have an energy of about 50 kev. If Eu^{152} decayed to Sm^{152} by the capture of a K electron as well as to Gd^{152} by the emission of a beta-particle, the K radiation expected from samarium would have approximately the observed energy. Samples of europium were furnished to Dr. J. R. Richardson, who made a study of the gamma-radiation in the cloud chamber. His results[8] show gamma-ray lines at 45 kev, 0.31 Mev, and 0.9 Mev, and he has concluded that the K-electron capture is a probable process in the decay. Tyler[7] has also found these gamma-ray lines, and in addition three other lines, some of which are internally converted, and which may account in part for the presence of K radiation. It is not yet clear whether the higher energy gamma-rays are associated with an electron capture or with the beta-decay process.

The two decay mechanisms, represented by the equations

$$Eu^{152} \rightarrow Gd^{152} + e^-, \quad (3)$$

$$Eu^{152} + e^- \rightarrow Sm^{152} + h\nu + \text{neutrino}, \quad (4)$$

are in accord with the behavior predicted by Sizoo[9] for three isobaric nuclei of consecutive atomic number, the first and third of which are stable, and the second beta-radioactive.

Radiations from the long period of Eu^{154} have not been studied so completely. The particles emitted were found to be negative electrons, and gamma-radiation was also found to be present. Absorption measurements in aluminum showed that the beta-rays have an upper limit of 1.0±0.1 Mev, and this value has been confirmed by preliminary cloud-chamber measurements. The energy of the gamma-radiation has not been measured because of the low intensity available. Analogous considerations to those above suggest that Eu^{154} may also decay both by the emission of beta-particles and by the capture of K electrons. In this case also, the two product nuclei, Gd^{154} and Sm^{154}, are stable isotopes.

Deuteron Activation

Europium oxide was bombarded with deuterons for periods ranging in length up to about five hours. With the usual currents, this represented a maximum of less than 100 microampere-hours, at from 6 to 7 Mev.

Following bombardment, europium was separated chemically from other elements which might be formed. This was done by passing a solution of europium chloride through a Jones reductor, in which zinc and dilute acid reduced the trivalent europium to its bivalent form, from which it could be precipitated as $EuSO_4$, which is insoluble. The reduction process is a specific separation of europium from almost all other rare earth elements, since other members of the group can be reduced only with much greater difficulty, if at all. The nature of the separation and the conditions under which it is carried out have been described by McCoy.[10] Lanthanum chloride was added before reduction

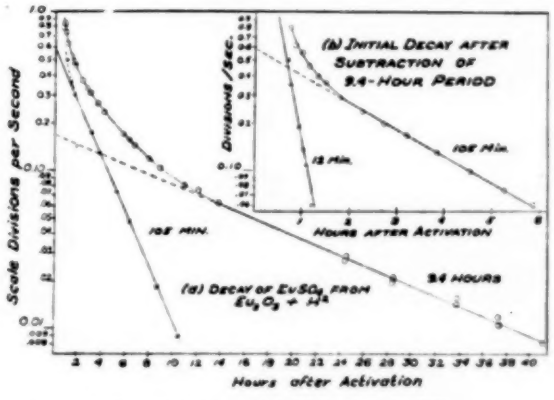

Fig. 2. Decay of Eu from Eu+H^2.

[6] R. Naidu and R. E. Siday, Proc. Phys. Soc. (London) **48**, 332–36 (1936).
[7] A. W. Tyler, Phys. Rev. **56**, 125–30 (1939).
[8] J. R. Richardson, Phys. Rev. **55**, 609–14 (1939).
[9] G. J. Sizoo, Physica **4**, 467–72 (1937).
[10] H. N. McCoy, J. Am. Chem. Soc. **58**, 1577–80, and 2279–81 (1936); **59**, 1131–2 (1937).

to serve as a carrier for the other rare earths, and was reprecipitated as the trivalent oxalate by the addition of oxalic acid, after the removal of the europous sulfate.

The decay of a sample of $EuSO_4$ from Eu_2O_3 activated by deuterons and separated in this way is shown in Fig. 2. The analysis shows three periods of decay: 9.4 ± 0.2 hours, 105 ± 5 minutes, and 12 ± 4 minutes. The decay of the unreduced fraction, which should contain any other rare earths produced by transmutation reactions, showed only these same three periods and in much lower intensity, probably due to small amounts of europium not completely reduced by the zinc.

To investigate whether the periods observed in the $EuSO_4$ were all due to isotopes of europium, the ratio of their initial intensities, corrected for an infinitely long bombardment time, was calculated and compared with the ratio extrapolated from the decay of a sample of europium oxide which was not treated chemically after bombardment. The corrected intensity ratio for the periods 9-hour : 105-minute : 12-minute, was found to be 1 : 1.5 : 10, within the limits of accuracy of the analysis, for both samples. Since the 9-hour period is known to be due to Eu^{152}, from work with neutrons, and since there was no detectable fractionation of the other two activities in the chemical separation, it seems most likely that all three are due to isotopes of europium. In addition, it may be noted that most isotopes in Gd or Sm, to which usual (H^2, n) and (H^2, α) processes from europium might lead, are stable or have known radioactive periods quite different from any of those observed here. This is in accord with the view that the periods observed are due to isotopes of europium.

Deuteron bombardments prolonged enough to produce the long period of Eu^{154} could not conveniently be performed, but the 9.4-hour period from deuteron activation was undoubtedly the same as that assigned to Eu^{152}. The two shorter lived isotopes produced by deuterons were not observed after neutron activation. Chemical evidence, which indicates that they are isotopic with the 9-hour radio-europium, suggests that they may be due to isomeric forms of Eu^{152} and Eu^{154} which, as shown, are produced much more easily by deuterons than by neutrons. It has not been possible to decide to which isotope each period belongs.

We are indebted to Professor H. N. McCoy for the europium oxide used, and to Professor J. M. Cork, Dr. B. R. Curtis, and to other members of the Department of Physics for their interest and cooperation in making the bombardments and the cloud-chamber studies. Mr. Norman Bauer and Mr. William H. Sullivan assisted in purifying the europium and in making cloud-chamber measurements. The investigation was made possible by a grant from the Horace H. Rackham Trust Fund.

Induced Radioactivity in Strontium and Yttrium; Nuclear Isomers in Strontium

DAVID W. STEWART*
Departments of Chemistry and Physics, University of Michigan, Ann Arbor, Michigan
(Received August 16, 1939)

In revising and extending previous work on induced radioactivity in strontium and yttrium, it was found that with stronger activation by deuterons and neutrons, more accurate determinations could be made of the radioactive decay periods, and measurements of beta- and gamma-ray energies could be made with greater certainty. Periods of 2.0 ± 0.2 hours, 14 ± 2 hours, and 82 ± 4 hours were found in yttrium separated from strontium bombarded with 7-Mev deuterons. The first of these periods was assigned to Y^{85}, and the other two either to Y^{85} and Y^{87}, or to isomeric forms of either of these. Periods of 3.0 ± 0.1 hours and 55 ± 5 days, produced in strontium by bombardment of that element with deuterons and neutrons, were assigned to the decay of isomeric forms of Sr^{89}, and the nature of that isomerism was investigated. From measurements in the cloud chamber, the maximum energy of the beta-rays from the 3-hour isomer was found to be 0.60 Mev, those from the 55-day isomer had an upper limit of 1.50 Mev, and the gamma-radiation which accompanied the 3-hour decay was found to have two components, of 0.55 Mev and 1.10 Mev. A tentative energy level diagram suggests that the metastable state of Sr^{89} decays first by the emission of a beta-particle and then by the emission of either one or two gamma-rays. The ground state of Sr^{89} decays directly to the ground state of Y^{89} without the emission of gamma-radiation.

INTRODUCTION

IN a previous paper,[1] radioactivity induced in strontium and yttrium by bombardment with deuterons and both fast and slow neutrons was reported. Radioactive isotopes with half-life periods of 3.0 ± 0.1 hours and 55 ± 5 days, both emitting negative electrons, were found in strontium and were identified with the decay of isomeric forms of Sr^{89}. Periods of 2.0 ± 0.1 hours, positive active, and 60.5 ± 2 hours, negative active, were found in yttrium and were assigned to Y^{88} and Y^{90}, respectively. The beta-ray spectra associated with the four periods were also measured in a 6-inch hydrogen-filled cloud chamber in a magnetic field.

Recently, improvements in the cyclotron have made available more intense beams of deuterons, and hence greater neutron intensities, and it has been possible to extend and revise the work previously reported.

EXPERIMENTAL PART

Arrangements for bombarding targets of strontium and yttrium nitrates, and for separating chemically the resulting activities were the same as reported previously.[1] Deuterons were accelerated in the cyclotron and were available at energies between 6 and 7 Mev, in currents of from 10 to 20 microamperes. Material was exposed to slow neutrons inside paraffin blocks at a distance of about 30 cm from the beryllium target on which the deuterons were allowed to fall.

Measurement of radioactive decay was made on a Lauritsen type electroscope, and on a Wulf string electrometer using an ionization chamber filled with Freon (difluorodichloromethane).

Measurement of beta-ray energies was done in a hydrogen-filled cloud chamber twelve inches in diameter, in a magnetic field uniform to 0.5 percent throughout the chamber. Samples were placed against the inner wall of the chamber and were covered only with thin Cellophane tape. Gamma-rays were measured by observing recoil electrons ejected from a carbon absorber placed diametrically across the chamber. The gamma-ray source was placed behind a lead collimator outside the chamber, in the manner described by Richardson,[2] who also was responsible for the design and construction of the apparatus used. The absorber was of paper, treated with paraffin and lampblack, and having a density of 0.037 g/cm^2. Only those recoil tracks were measured which had an initial direction within $\pm10°$ of the forward direction of the gamma-ray.

Stable isotopes of strontium and yttrium and neighboring elements are shown in Fig. 1, where figures refer to percent abundance of the isotopes.

* Present address, Department of Chemistry, Columbia University, New York.

[1] D. W. Stewart, J. L. Lawson and J. M. Cork, Phys. Rev. **52**, 901–6 (1937).

[2] J. R. Richardson, Phys. Rev. **55**, 609–14 (1939).

UNIVERSITY OF MICHIGAN LIBRARIES

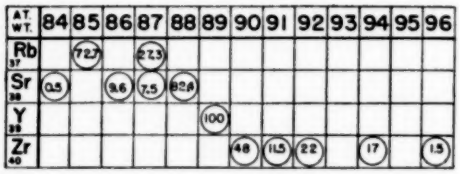

FIG. 1. Stable isotopes with their relative abundance.

RADIOACTIVE ISOTOPES OF YTTRIUM

When pure strontium nitrate was bombarded with deuterons and yttrium separated from the products, a decay such as is shown in Fig. 2 was observed. By analysis, three periods, of 2.0 ± 0.2 hours, 14 ± 2 hours, and 82 ± 4 hours, were identified in a number of duplicate experiments. The shortest period was observed in the cloud chamber to emit positrons, as previously reported, and the two longer periods were found to emit negative electrons. These results indicate that the longer period activity previously obtained in yttrium can no longer be identified with the 60.5-hour period of Y^{90}, and hence there is no further reason to postulate a $Sr^{88}(H^2, \gamma)Y^{90}$ reaction, as suggested in the preliminary report.

The possibility that the 14-hour period might be due to Na^{24}, from a contamination of sodium in the original material, was carefully investigated. The original strontium nitrate was recrystallized four times, twice from nitric acid and twice from water, with centrifuging of the crystals each time. In addition, in other experiments, sodium chloride was added in excess to the sample after bombardment and the usual chemical separation of the radioactive yttrium made from both the strontium and sodium present. In all cases, the three activities remained with the yttrium isotopes.

Since only the 2-hour period was obtained by bombarding yttrium with fast neutrons, the 14- and 82-hour periods cannot definitely be assigned to particular isotopes of yttrium. It is most likely that they are due to Y^{85} and Y^{87}, formed from Sr^{84} and Sr^{86} by (H^2, n^1) reactions, or to isomeric forms of either of these yttrium isotopes. The much greater abundance of Sr^{86}, as a starting material, would suggest Y^{87} as the probable product. The observed negative decay of such an isotope requires the existence of at least one unknown stable isotope of zirconium, or a K-electron capture process, in which the observed beta-particles are actually due to the internal conversion of a gamma-ray following such capture. Present mass-spectrograph data for zirconium show no stable isotopes lighter than Zr^{90}, but it is possible that other, lighter, isotopes may still be found. The radiations from the longer periods were not intense enough at best to be examined conveniently for evidences of K-electron capture, nor were the beta-spectra measured to identify internal conversion electrons.

NUCLEAR ISOMERS IN STRONTIUM

The preliminary identification of the 3-hour and 55-day periods in strontium, produced both by deuterons and neutrons, as due to the decay of isomeric forms of Sr^{89} has been further confirmed. The production of the 3-hour isomer is much favored over the one of 55-day half-life when neutrons are used instead of deuterons, and it has been possible to prepare relatively strong sources of the 3-hour activity almost free from the longer period isomer. These have been used for cloud chamber studies of the beta- and gamma-radiation which accompanies this decay. The 55-day isomer, produced most strongly by

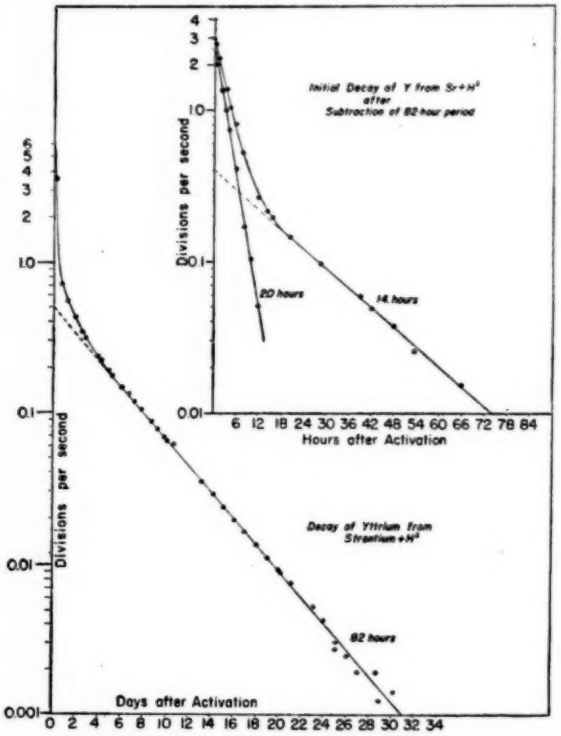
Initial Decay of Y from Sr+H²
after
Subtraction of 82 hour period
Divisions per second
20 hours
14 hours
6 12 18 24 30 36 42 48 54 60 66 72 78 84
Hours after Activation
Decay of Yttrium from
Strontium+H²
82 hours
Days after Activation
0 2 4 6 8 10 12 14 16 18 20 22 24 26 28 30 32 34

FIG. 2. Decay of yttrium from $Sr+H^2$.

deuteron bombardment of strontium, has no gamma-radiation. The upper limits of the two beta-spectra have also been redetermined more accurately. The observed maximum energy for the beta-rays from the 3-hour isomer was found to be 0.60 Mev (Konopinski-Uhlenbeck extrapolation = 0.65 Mev), from a distribution of 794 tracks as shown in Fig. 3. The observed upper limit for the 55-day isomer is 1.50 Mev (K-U extrapolation = 1.82 Mev), as determined

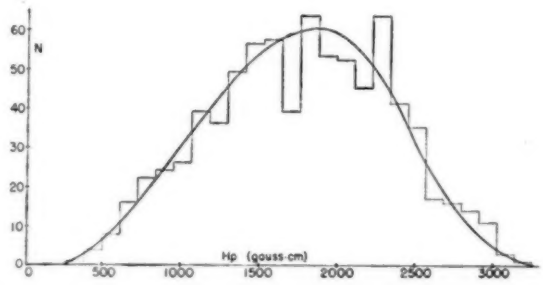

FIG. 3. Beta-rays from Sr^{89} (3-hour). 794 tracks; $H = 222$ gauss; Observed upper limit = 0.6 Mev.

from 551 tracks shown in Fig. 4. These values are in good agreement with the independently determined values reported previously.[1]

The energy of the gamma-rays emitted during the decay of the 3-hour isomer was determined from a distribution of 475 recoil tracks in the cloud chamber. Even with the strongest sources available, the loss of intensity in the collimation process was so great that more than 3000 photographs were required to give this number of measurable recoils, all meeting the requirement as to direction previously described. The distribution of tracks with energy is shown in Fig. 5. From this, at least two components in the gamma-radiation can be identified. The first, corresponding to a maximum recoil momentum given by the point A, has an energy of 0.55 Mev; the second, limited by the point B, corresponds to a gamma-ray of 1.10 Mev. After correcting for the greater probability of recoil ejection by the gamma-ray of lower energy, an intensity ratio of 5 : 1 between the lower and higher energy lines is probably of the correct order of magnitude.

Since it has been shown that the beta-spectra of the two isomers are quite different, and also because the gamma-rays are associated with the

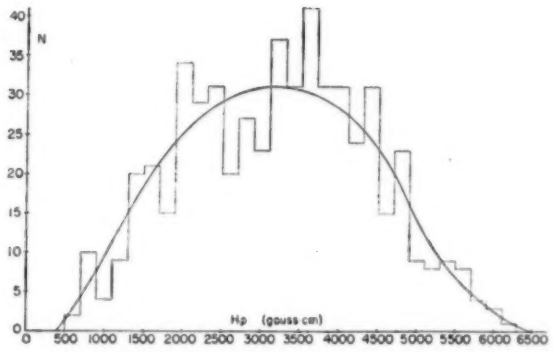

FIG. 4. Beta-rays from Sr^{89} (55-day). 551 tracks; $H = 401.4$ gauss; Observed upper limit = 1.50 Mev.

period of shorter half-life, it must be concluded that the isomers are of the second type described by Bethe.[3] In this type of decay, the isomer corresponding to the metastable state emits a beta-particle directly, following this with the emission of one or more gamma-rays, possibly in a cascade process. If the ground and metastable states of the radioactive nucleus are to be separated by only a small energy difference, the sum of the beta- and gamma-ray energies for the one isomer must be approximately equal to the beta-ray energy of the other isomer. Applying this requirement to the experimental data, an energy level diagram for Sr^{89} and its decay product, Y^{89}, is obtained such as that shown in

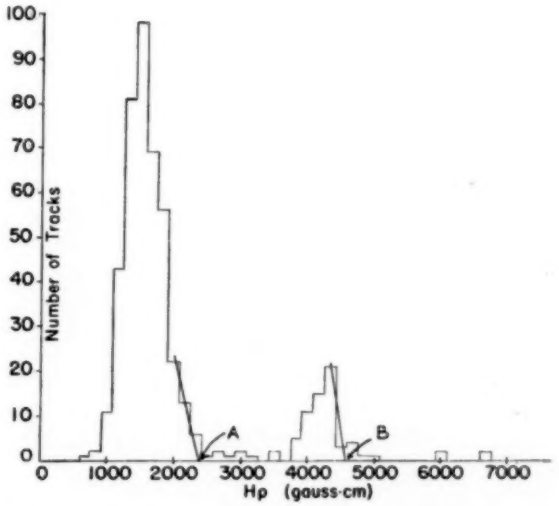

FIG. 5. Recoil electrons from gamma-rays of Sr^{89} (3-hour). Carbon radiator—475 tracks.

[3] H. A. Bethe, Rev. Mod. Phys. 9, 226 (1937).

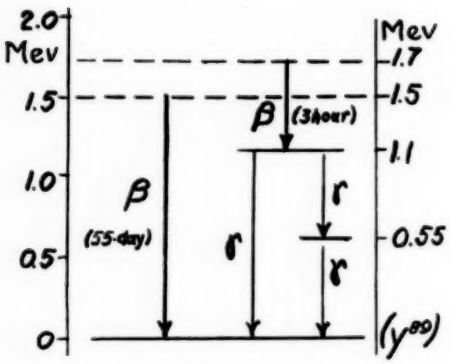

FIG. 6. Suggested energy levels in Sr^{89}.

Fig. 6. Observed values of the upper limits of the beta-spectra are used throughout. Dotted lines indicate possible levels in the radioactive nucleus, and solid lines those in the product.

In this scheme, the separation of the ground and metastable states is found to be 0.2 Mev, and the gamma-decay is assumed to take place in either of two alternative processes. In one, the total energy is dissipated in one gamma-ray of 1.1 Mev; in the other process, two gamma-rays of approximately the same energy (and therefore not resolved in the distribution shown in Fig. 5) are emitted in succession, each of about 0.55 Mev. The larger number of low energy quanta observed suggests that the cascade process is slightly more probable than the emission of the energy in one step. A larger number of tracks would be required to fix more definitely the ratio between the two processes.

ACKNOWLEDGMENTS

The author is indebted to Professor K. Fajans of the Department of Chemistry for his helpful interest and guidance throughout the work reported here. Particular thanks are due to Professors J. M. Cork and H. R. Crane, and to Drs. B. R. Curtis, J. L. Lawson, and Gerald Tape, all of the Department of Physics, for their cooperation. This investigation was made possible by grants from the Horace H. Rackham Trust Fund.

OCTOBER 1, 1939 PHYSICAL REVIEW VOLUME 56

Time Distribution of Cosmic-Ray Bursts

PIARA S. GILL
University of Chicago, Chicago, Illinois
(Received August 2, 1939)

Cosmic-ray bursts recorded with Carnegie model C cosmic-ray meters located at three widely separated stations were analyzed as to their time distribution. These bursts were produced under 12 cm of lead shielding. The results show that the cosmic-ray bursts may be considered as a random series of events. Tests for possible diurnal variations indicate systematic diurnal variations, but the data available are insufficient to make the conclusion certain.

COSMIC–RAY bursts recorded with model C cosmic-ray meters[1] can easily be recognized as a sudden displacement in the positive direction of the electrometer needle trace in the film. A criterion for distinguishing between true bursts and statistical variations which may have the appearance of bursts has been given by Bennett, Brown and Rahmel[2] for bursts recorded with a Carnegie model C cosmic-ray meter. They show that at Chicago a statistical fluctuation corresponding to 0.5 mm deflection of the electrometer needle is found to occur, on the average, once every 42.2 hours, and for 0.75 mm deflection, once every 18,000 hours. Actually 6–8 bursts were observed between 0.5 and 0.75 mm deflection per 42.2-hour period, so only bursts less than 0.5 mm should be omitted for this reason. This estimate of the statistical fluctuations appears to be valid for Huancayo and Cheltenham as well as Chicago. At Teoloyucan, the fluctuations appear to be greater at some times than at others, for some reason not entirely clear. During these disturbed intervals it

[1] A. H. Compton, E. D. Wollan and R. D. Bennett, Rev. Sci. Inst. **5**, 415 (1934).
[2] R. D. Bennett, G. S. Brown and H. A. Rahmel, Phys. Rev. **47**, 437 (1935).

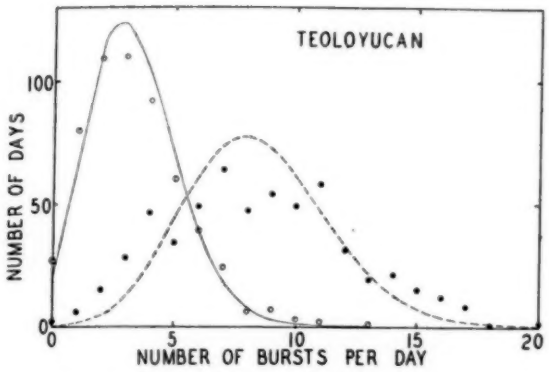

FIG. 1. Test of Poisson's law at Teoloyucan.

is difficult to be certain of the nature of deflections as great as 1 mm. The bursts were classified according to size, and the number of bursts in each such group was counted. Bursts of size 1 are those which correspond to an electrometer deflection between 0.5 mm and 1.5 mm; of size 2, to a deflection between 1.5 mm and 2.5 mm, etc. Because of the difficulty with data at Teoloyucan, it seemed desirable to make two sets of calculations: one for bursts of all sizes, and the other for bursts of size greater than 1.

This paper deals with bursts produced under a shielding of 12 cm of lead. The energy distribution of these bursts has been discussed by Gill and Schein.[3] The data available from three different stations cover, respectively, the periods from February, 1937, through October, 1938, at Teoloyucan; from November, 1936, through September, 1937, at Cheltenham; and from July, 1936, through September, 1936 at Huancayo.

All these data show, at first glance, a rather marked grouping of bursts, which led to the investigation of their time distribution. This grouping might be a consequence of the well-known high probability of short time intervals in a random series of events; or, it might be due to some systematic cause. To test for randomness, the method of Rutherford and Geiger[4] was used. The number of bursts appearing in equal intervals of time was counted, one day being taken as the interval. For a very large number of bursts, Poisson's law is that the probability that n bursts should appear in a given day is given by $x^n e^{-x}/n!$, where x is the average number of bursts per day and n may have any positive integral value from 0 to ∞. Figs. 1, 2 and 3 show the agreement between theory and experiment at all three locations. In each case the broken line gives the theoretical curve and the solid circles, the observed relative frequencies for the bursts of all sizes. The full lines in each case give the theoretical curves and the circles, observed numbers for all the bursts except those of size 1. The number of bursts of all sizes registered during the periods mentioned above and also the number of all bursts except those of size 1, and the average number of bursts per day are given in Table I. In view of the comparatively small

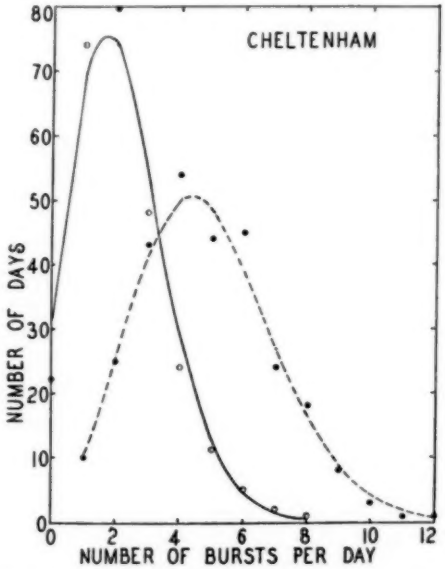

FIG. 2. Test of Poisson's law at Cheltenham.

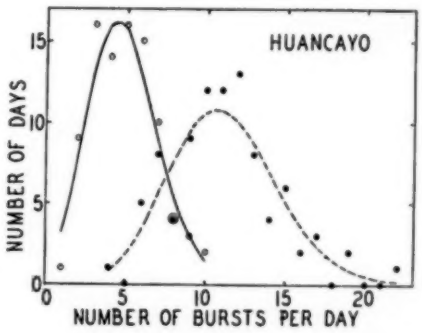

FIG. 3. Test of Poisson's law at Huancayo.

[3] P. S. Gill and M. Schein gave a report on burst frequency as a function of energy at the Symposium on Cosmic Rays in June, 1939, at the University of Chicago. The proceedings of the symposium will appear shortly in the *Reviews of Modern Physics*.

[4] Rutherford, Chadwick and Ellis: *Radiations from Radioactive Substances*, p. 171.

TABLE I. *Number of bursts at Teoloyucan, Cheltenham and Huancayo.*

	TEOLOYUCAN 560 DAYS	CHELTENHAM 276 DAYS	HUANCAYO 90 DAYS
Total number of bursts of all sizes	4710	1332	1004
Average number of bursts of all sizes per day	8.41	4.83	11.16
Total number of all bursts except those of size 1	1874	599	442
Average number of all bursts except size 1 per day	3.34	2.17	4.91

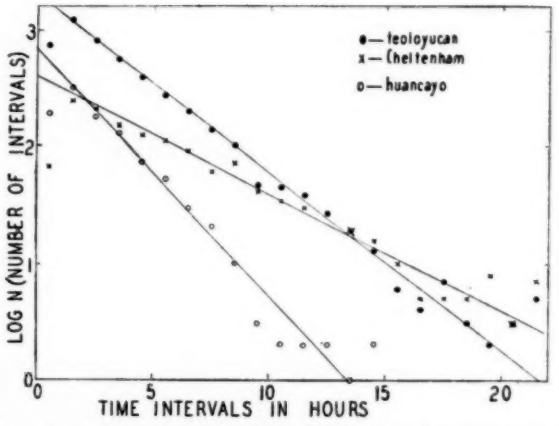

FIG. 4. Test for exponential distribution of intervals between successive bursts.

number of bursts registered, the agreement between theory and experiment is quite satisfactory. However, at Teoloyucan, the departures of experimental points from theory (broken curve) for all bursts is more pronounced, presumably for the reason mentioned above. Although the number of bursts greater than size 1 is much less, the agreement between theory (solid curves) and the experiment (circles) is quite close and within the probable error.

The method of Marsden and Barratt[5] was used as a further test of randomness. The time interval between each successive pair of bursts, to the nearest hour, was recorded, and the number of such intervals of a given length was counted. The results are shown in Fig. 4, where the ordinates represent logarithms of the number of intervals and the abscissae, time intervals in hours. For a very large number of bursts the curves should be straight lines. The experimental points are fairly represented by straight lines, except for very large time intervals where the number of intervals becomes very small. The number of intervals greater than t_1 and less than t_2 is given by

$$N_{t_1 \to t_2} = N(e^{-\mu t_1} - e^{-\mu t_2}) \sim N(t_2 - t_1)e^{-\mu t_1}$$

if $t_1 \gg (t_2 - t_1)$, where μ is the probable number of bursts per hour. The slopes of the lines, (0.35, 0.23, 0.49), should thus be equal to μ, the average number of bursts per hour, (0.35, 0.201 and 0.465, respectively, at Teoloyucan, Cheltenham, and Huancayo). Considering the small numbers of intervals, the agreement is satisfactory. So far as the results of this investigation are concerned, therefore, the bursts may be considered as a random series of events, the observed grouping being entirely statistical.

Inspection seemed to show that there was a greater probability that a small burst follows a large burst than that a large burst follows a small one. As a test for this, the intervals (Huancayo data) between successive bursts were classified as + and − in accordance with the alternative just mentioned. The time constant (μ) for each of these classes was determined separately. They were found to be practically equal, thus suggesting that the observation has no statistical basis.

These tests do not exclude the possibility of systematic diurnal variations of small amplitude; specific tests for such effects were applied to the data at Teoloyucan and Cheltenham. There was some indication of a systematic diurnal variation, but the data available do not extend over a sufficiently long period to make the conclusion certain. Further test for correlation of bursts at Teoloyucan with magnetic character-numbers showed no significant correlation.

In conclusion, the writer wishes to express his sincere thanks to Professor Carl Eckart for much helpful advice throughout the course of this investigation. The writer also wishes to thank Professor Arthur H. Compton for allowing him the use of the data.

[5] E. Marsden and T. Barratt, Proc. Phys. Soc. **23**, 367 (1911); **24**, 50 (1911).

Slow Mesons in the Cosmic Radiation

C. G. MONTGOMERY, W. E. RAMSEY, D. B. COWIE AND D. D. MONTGOMERY
Bartol Research Foundation of the Franklin Institute, Swarthmore, Pennsylvania

(Received August 9, 1939)

The following experiment was performed to measure the disintegration time of cosmic-ray mesons. Mesons falling on a lead plate were detected by a layer of counters above the plate. Some of these mesons presumably stopped within the plate and a short time later emitted a disintegration electron and a neutrino. The electron would, in a certain fraction of the cases, be detected by a second layer of counters placed below the plate. Those events were recorded in which a discharge of one of the upper counters was followed by a discharge in one of the lower counters after a time t_1 and before a time t_2. In the absence of the lead plate, no disintegration electrons were expected. However, a considerable number of counter discharges were recorded which must be interpreted as the result of an intrinsic time delay in the counter between the passage of the ionizing ray, and an appreciable change in potential of the counter wire. The number of disintegration electrons was measured by taking the difference in the counting rates with the lead plate present and absent. For t_1 equal to 1.5 microseconds, and t_2 equal to 20 microseconds, we expected 23 electrons per hour, assuming that the mean life of the mesotron is 2.7 microseconds. A series of observations results in the measured number of 1.4 ± 2.4 per hour, a value much smaller than expected. Possible explanations of this discrepancy are discussed, the most likely one perhaps being that most mesons are absorbed by some nuclear process before they come to rest.

INTRODUCTION

IT has been observed[1] that the absorption of the cosmic radiation in air depends not only upon the mass of air traversed but also upon the path length of the rays. An explanation of this anomaly was first suggested by Kulenkampff,[2] namely, that the mesons which comprise the hard component of the cosmic radiation are unstable, and decay spontaneously into electrons and neutrinos. The additional absorption resulting from this instability has been calculated by Euler and Heisenberg,[3] and harmony with the observations is realized if the mean life of a meson at rest is 2.7×10^{-6} second. Other observers[1] have determined values from 1.5 to more than 4 microseconds, the value deduced depending upon the assumptions made regarding the height of origin of the mesons and their rest masses.

Notwithstanding the short lifetime, some mesons should come to rest before disintegration, and it should be possible to determine, in a more direct manner, the time until decay. The rest-mass energy of a meson decaying at rest will be divided equally between the electron and the neutrino, and hence the electron will have considerable penetrating power.

EXPERIMENTAL METHOD

Over a plate of lead two centimeters thick and of 20×30 cm^2 area, was placed a set of twenty-one Geiger-Mueller counters, in parallel, each 1 cm in diameter and 15 cm long, filled with a mixture of 94 percent argon and 6 percent oxygen to a pressure of 9 cm of Hg.[4] The mesons falling upon the lead were detected by discharges of the counters. A certain fraction of these mesons presumably stopped in the lead plate, and a certain time later emitted electrons. Some of the electrons would impinge upon another layer of twenty-one counters below the lead plate. These lower counters were 1 cm in diameter and 20 cm long and filled to a pressure of 18 cm of Hg with the oxygen-argon mixture. The electrical recording circuits were so arranged as to record those cases in which a discharge of a counter in the top tray was followed by a discharge of a counter in the lower tray after a definite time interval t_1 and before a time t_2. Above the whole counter system were placed 12 cm of lead to absorb the soft component rays. The geometrical relations of the counters and the lead are shown to scale in Fig. 1.

[1] E.g., P. Ehrenfest, Jr., and A. Fréon, J. de phys. et rad. 9, 529 (1938); T. H. Johnson and M. A. Pomerantz, Phys. Rev. 55, 104 (1939).
[2] H. Kulenkampff, Verh. deut. phys. Ges., Breslau (1938).
[3] H. Euler and W. Heisenberg, Ergeb. exak. Naturwiss. 17, 1 (1938).
[4] G. L. Locher, Phys. Rev. 55, 675 (1939).

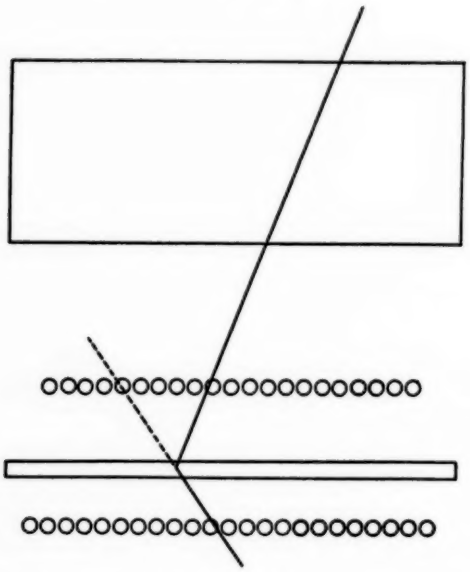

FIG. 1. Schematic diagram of the counter arrangement. A slow meson discharges one of the upper counters, stops in the thin lead plate, and some time later emits a neutrino and an electron which discharges one of the lower counters.

Figure 2 shows the diagram of the circuit for selecting the coincidences. A pulse from a counter in the top tray is delayed by the condenser across the plate resistance of the vacuum tube T_1 and is impressed on the grid of T_3 until the counter recovers. A pulse from a counter in the bottom tray is impressed on the grid of T_3, for only a short time, by the network in the plate circuit of T_2. If the bottom counter pulse occurs in the proper time interval, the resultant pulse on the grid of T_3 from the combination of top and bottom counter discharges is sufficient to overcome the bias to such an extent as to allow the delayed coincidence to be recorded. The time of delay could be adjusted by the bias on T_3 and the size of the condenser in the plate circuit of T_1. The three tubes were of the type RCA 6C6. The plate supply and the screen grid potentials were 45 volts, supplied from dry batteries, and the current for the heaters was supplied by a storage battery. The actual recording circuit is not shown in the diagram, since it consisted only of the conventional amplifier, with provision for lengthening the duration of the pulses, operating a watch recorder.

In order to determine the minimum time t_1, by which a lower counter discharge could follow a discharge of an upper counter and be recorded, it was necessary to employ a calibration circuit which would supply two pulses separated by a known time interval. Fig. 3 shows the schematic diagram of the circuit employed. A mercury switch (Sw) charges a condenser through a resistance. The switch makes contact in an extremely short time and the rise of potential of the condenser may be calculated with good accuracy. The potential rise of the condenser is impressed on the grids of two type 6C6 tubes, whose plate supply and screen grid potentials are 45 volts. One of these grids is biased to a large negative voltage and the other to a smaller one. Thus one tube begins to conduct before the other and we have two pulses produced, separated by a known time interval. The pulses are directly applied to the grids of T_1 and T_2 of the coincidence selector circuit, and values of t_1 are obtained as a function of the bias on T_3. A calibration curve obtained in this way is shown in Fig. 4. It may be thought of as representing the shape, but not the magnitude, of the voltage pulse which was impressed upon T_3 when a counter in the upper tray discharged.

An evaluation of t_1 in this manner is accurate only as long as the time taken for the vacuum tubes to be turned on or off is small compared to the times measured. Since the voltage range between a completely conducting and a completely nonconducting state of the tubes used under the conditions which obtained here is only about three volts, it is easy to see that the pulses from the calibrating circuit are sufficiently fast. The largest error in the lag determination is the error in the knowledge of the distributed capacity of the circuits, and this may be generously estimated at not more than 5 percent. The counter

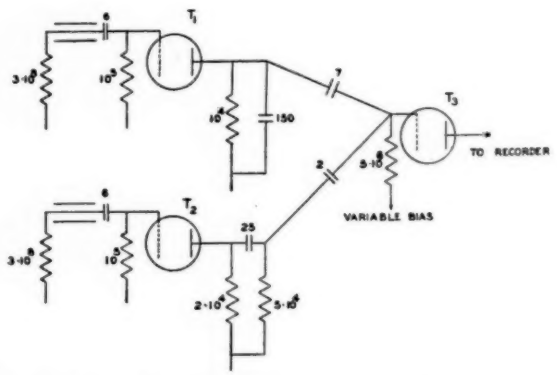

FIG. 2. Circuit for selecting the delayed coincidences.

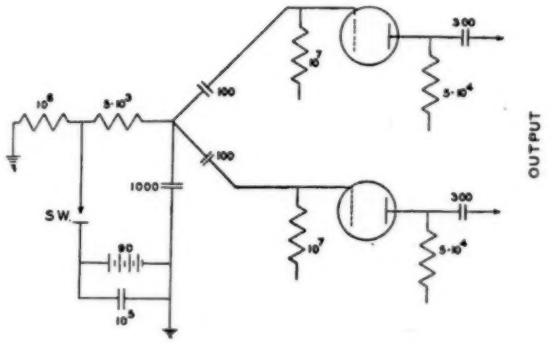

FIG. 3. Calibrating circuit for measuring the sensitive times of the coincidence selector circuit.

discharges must also be sufficiently fast for the calibration to be accurate. That this was the case was determined by two methods. First, if the size of a counter pulse be increased, and the speed remains the same, the time necessary for the counter wire to change in potential by a given amount will be proportionally lowered. By raising the high potential on the counters, the size of the pulse was increased by about 50 percent, but the number of counts recorded remained unchanged. This indicates that the counter breakdown time was small compared to the time of action of the circuit, and no correction need be applied. The second determination was made by one of us (W. E. Ramsey) by directly measuring the breakdown characteristics of the counters employed.[5] It was found that the time necessary for the tubes to be cut off was less than 2×10^{-7} sec., and therefore small enough to be neglected.

It is also necessary to determine the maximum time, t_2, for which a pulse from a lower counter could be delayed after an upper counter discharge, and still be recorded. Although this could have been determined in a manner similar to the determination of t_1, it was found more convenient to calculate t_2 from the number of accidental coincidences observed. The counter trays were placed side by side and the number of coincidences determined as a function of the individual counting rates of the trays. If this accidental rate is denoted by A, and the counting rates of the two trays by n_1 and n_2, then t_2 is given by A/n_1n_2. The small correction for showers and horizontal rays was shown to be negligible. The requisite accuracy in t_2 is small, since t_2 is much longer than the mean life of a meson.

Observations to detect delayed coincidences were made with the 2-cm plate of lead alternately present and absent. At the beginning and end of such a series, the calibration curve was determined to ensure that the circuit was operating properly and that the time lag did not change during the run. Actually a change of 5 to 10 percent took place during a twelve-hour observation period, because of the alterations of battery potentials. It was determined that this change varied linearly with time and the arithmetic mean value of the initial and final time lags was taken to apply to the whole run.

RESULTS

When observations were made with no lead present between the counters, it was found that, contrary to expectation, a considerable number of discharges were recorded, even for time lags up to five microseconds. By changing the number of counters and the relative position of the two trays, it was found that the counting rate with a lag in the circuit was proportional to the number of truly coincident discharges. It seems possible to explain the observations in only one way, namely: some of the counter discharges do not take place immediately after the passage of an ionizing ray through the counter, but the dis-

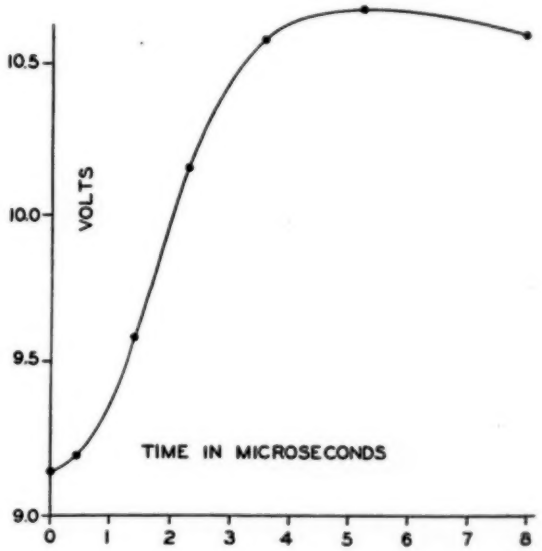

FIG. 4. Calibration curve of the selector circuit.

[5] A description of the method of measurement and the characteristics of several counters is in preparation for publication.

charge is delayed.[6] The circuit used measures the number of discharges in which the difference in time lag between the bottom counter and the top counter is more than the time, t_1, if t_2 is made long compared to t_1. Since, however, the percentage of the total number of rays which produce lagged discharges is small, the difference "bottom lag" minus "top lag" is equal to the bottom lag alone. Fig. 5 shows the observations which have been made. The results for the counters filled with 9 cm of gas were obtained by interchanging the upper and lower trays. The existence of this time lag sets a lower limit to the resolving power which is practical to use for coincidence work. For example, in a twofold coincidence unit employing counters such as the 9-cm ones used here, more than 10 percent of the coincidences would be lost, if the resolving time were made as small as two microseconds. Fortunately, this is small enough not to be serious in any experiments performed up to the present. This limit to practical resolving power is, of course, independent of the limit imposed by the finite breakdown time of some counters. A tentative explanation of this time lag may be the following: In a certain fraction of the cases, a cosmic ray traversing the counter will produce only one ion pair. If the electron collides with an oxygen molecule or other electro-negative impurity before it has time to initiate the discharge, there is a high probability that it will be captured and not released again until a short time later. Further experiments with different types of counters are at present under way.

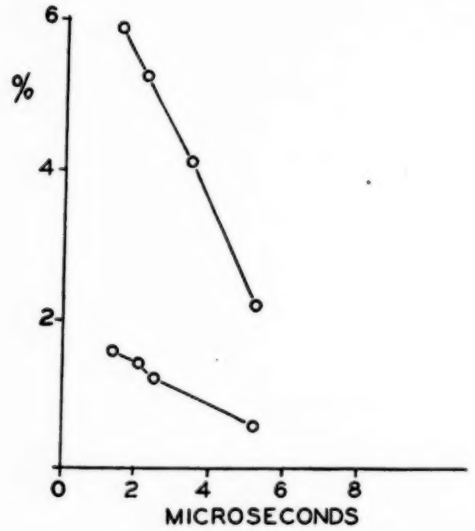

FIG. 5. The percentage of discharges of the counters (ordinate) which are delayed more than a certain time (abscissa) after the passage of the ray through the counter. Upper curve, 9 cm Hg pressure; lower curve, 18 cm Hg pressure.

[6] P. Auger, in a personal communication, informs us that similar time lags have been found in his laboratory.

The existence of intrinsic time lags in counters complicates the observation of the decay of mesons, but does not destroy the possibility. We must measure the difference in counting rates with the 2-cm lead plate present and absent. This difference represents the number of decay electrons from the lead. The observed difference must be corrected by a small amount (8 percent) because the absorption in the lead reduces the number of lagged counts. Observations were taken with several values of the times t_1 and t_2, but the most complete results were obtained for $t_1=1.5$ microseconds and $t_2=20$ microseconds. The number of mesons passing through the two sets of counters was about 7800 per hour. Since the absorption coefficient is about 0.01 cm^{-1} of lead, we should expect 156 per hour to be stopped in the 2-cm plate. The solid angle of the lower tray was such that only $\frac{1}{4}$, or 39 per hour, of the electrons from the decay of the mesons would be detected. If we assume a mean life of 2.7 microseconds, all but 23 per hour should have decayed before 1.5 microseconds, and practically all of them before 20 microseconds. This expected number is admittedly a rough estimate, but our lack of knowledge of the correct decay time makes it hardly worth while to make a more accurate calculation. When the lead plate was present, a series of runs which agreed well with one another gave 129 counts per hour. With the lead absent 140 counts per hour were observed. With the corrections applied, we observed 1.4 ± 2.4 decay electrons per hour, or no measurable effect, instead of the expected 23 per hour. The probable error is thus only about one-tenth of the expected value. The observations at other time lags also showed no effect.

DISCUSSION

The failure to observe the decay of mesons in the expected numbers may be explained in three ways. First, mesons may be stable and not decay

at all. If this be the case, some other explanation must be offered for the anomalous absorption of cosmic radiation in air. Second, the absorption experiments do not determine the mean life directly, but only the ratio of the mean life to the rest mass of the meson. Now if the mass of the cosmic-ray mesons is smaller than the mass of the mesons that have been observed in cloud chambers at the ends of their ranges, we could explain the absorption experiments by a lifetime which would be too small to have been observed in these experiments, but long enough to explain the absorption anomaly. If we could not have detected an effect twice as large as our probable error, then the lifetime could be as long as 0.7 microsecond. With this value, the cosmic-ray absorption experiments would then necessitate an upper limit to the meson mass of about 50 electron masses. This mass seems decidedly too small to give the correct range of nuclear forces, but it is possible that the mesons responsible for nuclear forces and cosmic-ray mesons are not identical. The recent work of Maier-Leibnitz[7] may be regarded as supporting this hypothesis in some degree, since she finds that the mesons that end their ranges in the cloud chamber occur too frequently to come from the stopping of cosmic rays, but seem to be produced as secondaries, presumably from nuclei. The mass determinations which result in values around 200 electron masses are presumably made with these nuclear mesons, and not with cosmic-ray mesons.

The third, and seemingly most likely, explanation is that mesons of low energy are strongly absorbed by atomic nuclei and do not come to rest. The rest-mass energy of the meson would be converted to some other form, possibly going into a shower. We can estimate the order of magnitude of the cross section for this absorption. The momentum distributions of cosmic-ray mesons observed in cloud chambers seem to indicate no large absorption except for small momenta, where there is a maximum in the distribution curve. The maximum varies from $pc=2\times10^8$ electron volts[8] where p is the momentum, up to almost 8×10^8 ev.[9] The maximum seems to be an instrumental one caused by the deflection of low energy rays away from the counters which control the expansion. However, an excess absorption of mesons would not be detected in this energy region, and we may assume that the mean range for absorption is less than the ranges of particles of this momentum. If we take 10^8 ev as the meson rest mass, the ranges of mesons of $pc=2$ or 8 times 10^8 ev are 5.7 and 52 cm of lead, respectively. If this is, say, twice the mean range of the particles for absorption, we would calculate a cross section of 5×10^{-26} cm^2 or 5×10^{-27} cm^2 per nuclear particle. Heitler[10] has estimated the cross section for meson absorption resulting in the emission of a gamma-ray and obtained 9×10^{-28} cm^2. Although this value seems definitely too low, the uncertainty of the present state of the theory may not allow the difference to be regarded as significant.

[7] H. Maier-Leibnitz, Zeits. f. Physik **112**, 569 (1939).

[8] P. M. S. Blackett, Proc. Roy. Soc. **A159**, 1 (1937).
[9] J. C. Street, J. Frank. Inst. **227**, 765 (1939).
[10] W. Heitler, Proc. Roy. Soc. **A166**, 529 (1938).

The Transition Effect for Large Bursts of Cosmic-Ray Ionization and the Number of Primary Electrons of Very High Energy

C. G. MONTGOMERY AND D. D. MONTGOMERY
Bartol Research Foundation of the Franklin Institute, Swarthmore, Pennsylvania

(Received August 10, 1939)

Bursts of cosmic-ray ionization were observed in the open air and under heavy roofs, with and without a one-cm lead plate over the ionization chamber. The increase in the number of bursts in the presence of the lead under heavy roofs is interpreted as an increase in the number of rays in the showers from the roof, while in the open air the bursts from the lead probably originate to a large extent from the action of electrons of high energy which are not members of cascade showers starting at the top of the atmosphere. If the bursts from the atmosphere with no lead present are to be accounted for by the assumption that they are parts of extensive cascade showers, it is possible to derive the number and energy distribution of the primary cosmic-ray electrons of energies of the order of 2×10^{15} electron volts.

UNTIL recently, one of the most annoying and least well-understood aspects of cosmic-ray showers was the number of showers that were recorded even when great care was taken to remove all shower-producing material from the vicinity of the apparatus. The recent work of Auger[1] and his collaborators has done much to clarify our picture of the occurrence of showers from the air, and the situation is becoming more satisfactory. In making observations of showers or bursts of cosmic-ray ionization at depths below sea level, the effect of material surrounding the apparatus becomes more acutely felt, since it is impossible to avoid the presence of large quantities of dense matter at short distances in the walls and ceiling of the laboratory. To investigate these effects, we have made some observations on large bursts both in the open air and under thick roofs.

The ionization chamber and photographically-recording vacuum-tube electrometer that were employed have been previously described.[2] The chamber had a diameter of 40 cm, and was constructed of magnesium with walls one cm thick. If we choose 60 ion pairs per centimeter as the specific ionization of a ray in nitrogen, we calculate, making a correction for lack of saturation, 60 rays per million ion pairs collected. Observations were made at three stations in the Bartol Research Foundation Laboratory. The first was in a room covered with about a meter of earth, or beneath a mass of earth and air equal to 13.6 meters of water; the second was in a room with only a heavy ceiling of concrete over it, the equivalent depth being 11.1 meters; and the third was in a light wooden building at a depth of 10.2 meters. The ionization chamber was located about 1.5 meters from the ceilings of the rooms and was twice or more this distance from the walls. Observations were taken with and without a lead plate, 1 cm in thickness and 41 cm square, over the chamber. In Table I are given the results of these observations. The size-frequency distribution curves are plotted in Fig. 1.

Perhaps one of the first points to meet the eye in connection with these observations is the large number of bursts observed in the basement room under 13.6 meters of material, a number comparable with that observed in the open air at a depth more than three meters less. These bursts originate to a large extent in the overlying layer of earth. When the 1-cm lead plate is present over the chamber, the size of the burst from the earth is increased by the lead. This occurs because the radiation of electrons and pair production by photons continue to be important processes down to regions of lower energy in lead than in earth. This increase in size of a burst results in the occurrence of an increased number of bursts of a given size. All sizes of bursts appear to be multiplied in the same proportion, as is evident from the parallelism of the two distribution

[1] P. Auger, R. Maze, P. Ehrenfest, Jr., and A. Fréon, J. de phys. et rad. **10**, 39 (1939).
[2] C. G. Montgomery and D. D. Montgomery, Phys. Rev. **47**, 429 (1935).

curves in Fig. 1, and we estimate this multiplication to be by about a factor of 1.7. The observed value of the multiplication may be compared with the value expected from the cascade theory. The average energy of a shower ray from a large thickness of earth is somewhat less than 10^8 electron volts. From the calculations of Arley,[3] we find, by interpolation, that an electron of 10^8 volts energy will be multiplied by a factor of 2.1 in a 1-cm lead plate. This is in sufficient agreement with the observed multiplication to assure us that the lead may be regarded as acting only to increase the number of rays in a burst, and is not acting as an appreciable source of additional showers.

If we try to interpret the observations made in the open air by the same picture, we encounter some difficulties. The frequency distributions with and without the lead are not parallel, but diverge considerably. If we interpret this as an increase in size of the bursts, we must conclude that the rays of a large burst have, on the average, a higher energy than those in a small burst. This is not in accord with the predictions of the cascade shower theory. We conclude, therefore, that at least two processes are taking place. First, a multiplication in the size of the air showers by the lead, just as in the case of the observations below ground, and second, the production of showers in the lead by some agency which differs from cascade electrons passing through the atmosphere. There is, however, another source of electrons which will produce large showers in the lead, namely, the electrons from the disintegration of cosmic-ray mesons. These electrons are not produced at the top of the atmosphere and are, therefore, not accompanied by a very large number of rays by the time that they reach sea level. Strictly speaking, this is also a process of multiplication of the number of electrons by the lead, and differs from the multiplication of showers from the earth only in the way the energy of the initial shower is distributed among the rays. We have shown elsewhere[4] that there is good agree-

[3] N. Arley, Proc. Roy. Soc. **A168**, 519 (1938).

[4] C. G. Montgomery and D. D. Montgomery, paper at the Chicago "Symposium on Cosmic Rays," June, 1939.

TABLE I. *The rate of occurrence of bursts of ionization per hour per 10^5 ion pairs, at three stations.*

Size in ion pairs $\times 10^{-6}$			1.1–1.2	1.2–1.3	1.3–1.5	1.5–2.0	2.0–2.5	2.5–3.0	3.0–4.0	4.0–6.0	≥6.0
10.2 m depth	no Pb	Number of bursts	66	52	30	31	7	7	4	6	2
		Rate	0.19	0.15	0.035	0.014	0.003	0.003	0.0009	0.0007	0.005
	1 cm Pb	Number of bursts	165	137	137	124	41	21	30	9	12
		Rate	0.77	0.64	0.32	0.12	0.038	0.020	0.014	0.002	0.06
11.1 m depth	no Pb	Number of bursts	267	195	175	116	33	20	14	13	5
		Rate	3.52	1.20	0.54	0.14	0.041	0.025	0.009	0.004	0.03
	1 cm Pb	Number of bursts	722	318	536	497	184	81	80	53	33
		Rate	5.67	1.86	1.56	0.58	0.21	0.095	0.047	0.015	0.19
13.6 m depth	no Pb	Number of bursts	43	28	29	38	21	11	4	3	11
		Rate	0.54	0.22	0.11	0.060	0.033	0.017	0.003	0.002	0.09
	1 cm Pb	Number of bursts	85	70	128	113	61	35	33	16	19
		Rate	0.93	0.52	0.47	0.17	0.090	0.052	0.024	0.006	0.14

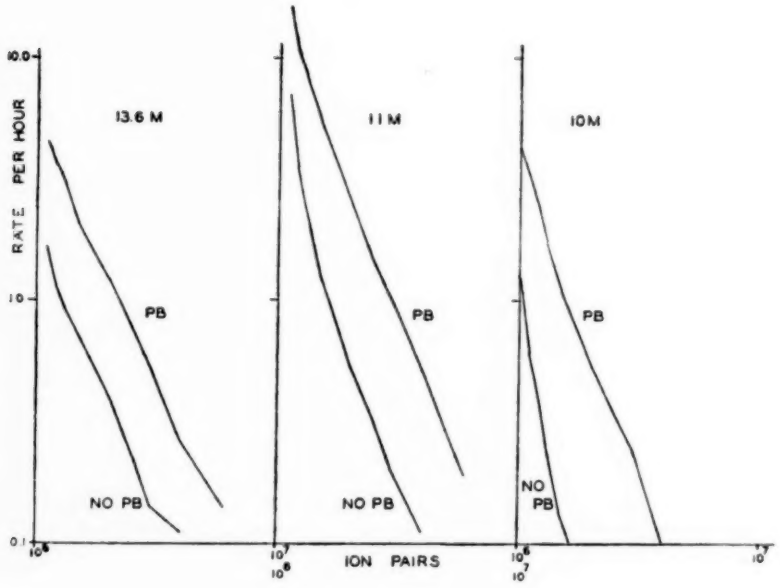

FIG. 1. The number of bursts of ionization greater than a given size, with and without a 1-cm lead plate over the chamber.

ment between the value of the mean life of a meson as calculated from the number of bursts observed and the values derived from absorption measurements of the cosmic radiation in air.

The set of observations made with the thick roof over the apparatus at a depth of 11.1 meters of water represents a case intermediate between the other two sets. We still have some divergence of the frequency distribution curves, but they are more nearly parallel than those taken in the open air.

We may draw some additional conclusions from the observations taken with no material over the chamber. If we suppose that the bursts observed are parts of showers of a great many rays which are spread over a large area, such as those observed by Auger,[1] and if we know the spreading to be expected, then we can calculate the number and distribution in energy of the primary electrons outside the earth's atmosphere which are responsible for these showers. The spreading to be expected has been estimated by Euler.[5] Let us suppose that a large shower of N rays at sea level has an axis passing through the point (r, φ) somewhere in the plane through the chamber perpendicular to the axis of the shower, not necessarily within the ionization chamber, supposed at the origin. Let $Np(r)$ be the average number of rays per unit area in the shower at the position of the chamber. Then if a is the area of the ionization chamber, the average number of rays in the chamber, n, is given by

$$n = aNp(r). \tag{1}$$

If this quantity is large, as in the case of these observations, we may neglect as a first approximation the fluctuations in it. If $j(E)dE$ be the number of primary electrons per square cm per second per unit solid angle having energies between E and $E+dE$, at the top of the atmosphere, then the number of showers coming from zenith angles between θ and $\theta+d\theta$, and having between N and $N+dN$ rays at sea level will be $j(E)\cdot(dE/dN)\cdot 2\pi \sin\theta dNd\theta$. The observed number of bursts, $O(n)$, having between n and $n+dn$ rays is

$$O(n)dn = \int_0^{\pi/2} d\theta \int_{\gamma=0}^{\infty} 2\pi r dr \cdot j \cdot 2\pi \sin\theta \left(\frac{dE}{dN}\right) dN, \tag{2}$$

in which E is given as a function of N and θ by the cascade shower theory, and N is given as a function of n and r by relation (1). Since the air above sea level may be considered a large thickness, we may use an approximate form of the results of the cascade theory as given by Euler and Heisenberg,[6]

$$N = (E/E_c)^{1.44} e^{-0.73h/\cos\theta - 3.2}, \tag{3}$$

[5] H. Euler and H. Wergeland, Naturwiss. **27**, 484 (1939).

[6] H. Euler and W. Heisenberg, Ergebn. exakt. Naturwiss. **17**, 1 (1938).

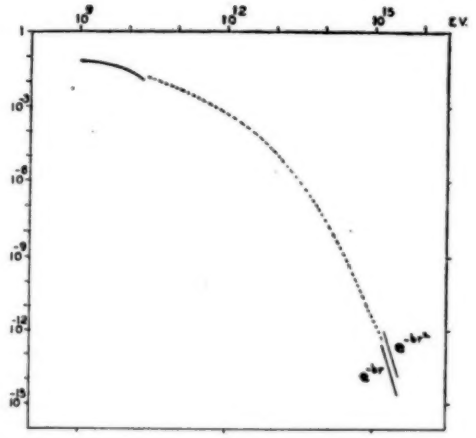

FIG. 2. The number of primary cosmic-ray electrons per square cm per second per unit solid angle having an energy greater than a given amount. The solid portion of the curve at low energies is derived from the latitude effect, the high energy portion is calculated from the burst observations in the open air.

where E_c is the critical energy for air, 1.5×10^8 electron volts, and h the atmospheric depth in meters of water. Let us assume that $j(E)$ may be expressed for the range of energies of interest to us by the empirical expression $j(E)=j_0/E^\lambda$, and we can evaluate the parameters j_0 and λ from the burst observations. The observations may be represented by an expression of the form $O(n)=A/n^s$. It is easy to show from (2) and (3) that $\lambda=1.44(s-1)+1$. s appears to be about 5.6, and therefore $\lambda=7.6$. From the number of bursts we can similarly evaluate j_0, if we know the function $p(r)$. Euler gives the function the form e^{-br}/r, where b is a constant. This form is evidently unsuited for application here on account of the infinity at the value r equals 0. We may, however, try similar functions of the types Ce^{-br} and Ce^{-br^2}, with the constants so determined that the functions are normalized and have the same "half-width" as Euler's function, the half-width being defined as the radius of the cylinder about the shower axis which contains one-half of the rays.* The results of these calculations may best be represented as in Fig. 2, where we have plotted on logarithmic scales the number of primary cosmic-ray electrons per square cm per second per unit solid angle having an energy greater than a given amount. The curve at the lower energies is determined by the latitude effect of the soft component of the radiation as calculated by Johnson.[7] The burst observations are concerned with the range of primary energies at about 2×10^{15} volts. Here, the two lines represent the two choices of the density distribution function. It is the uncertainty in the form of this function that limits the accuracy of the results of these calculations, but perhaps we can estimate from the figure the number of rays to better than an order of magnitude.

* *Note added in proof.*—The correct function, $p(r)$, to choose is, of course, the average value of Euler's function taken over the area of the chamber. This function will have no singularity at the origin. The expression for this average value is somewhat unmanageable and was not employed for this reason. The showers which contribute most to the observed bursts will have their axes outside the chamber, and here the factor $1/r$ in Euler's expression is not very effective. We should therefore expect that a more accurate calculation will yield results closer to those resulting from the chosen form Ce^{-br} than from Ce^{-br^2}, although the more accurate value will lie between the two. It is obvious that a more accurate calculation would not alter the main conclusions of this section.

[7] T. H. Johnson, Rev. Mod. Phys. **10**, 193 (1938).

Theory of the Diffuse Scattering of X-Rays by Crystals in the Region of the K Critical Absorption Wave-Length

G. E. M. JAUNCEY
Wayman Crow Hall of Physics, Washington University, St. Louis, Missouri

(Received July 24, 1939)

The scattering of x-rays according to the classical theory from a bound electron of natural frequency ν_q is first considered. Then Z electrons with various ν_q's are assembled into an atom and the scattering from the atom studied. The scattered rays are separated into coherent and incoherent parts by a study of the interference between the scattered rays from two similar atoms. From this S_{coh} and S_{incoh} are obtained for the atom. Kramers, Kallmann and Mark's idea of virtual oscillators is used so that S_{coh} and S_{incoh} are averaged for the distribution of oscillators. The λ^3 absorption law suggests either $2\nu_K^2\nu_q^{-3}d\nu_q$ or $4\lambda_K^{-4}\lambda_q^3 d\lambda_q$ as the fraction of oscillators with frequencies between ν_q and $\nu_q+d\nu_q$ or with wave-lengths between λ_q and $\lambda_q+d\lambda_q$. In determining the averages it makes a difference which distribution is used. The theory gives $S_{\text{coh}}=(f-\Delta f)^2\times(1-e^{-2M})/Z$, where Δf is the atomic structure factor decrement and e^{-2M} the Debye-Waller temperature factor. Also the theory gives $S_{\text{incoh}}=1-(1/Z)\Sigma E_r^2+Y$, where Y is negligible for $\lambda>\lambda_K$ but is quite large for $\lambda<\lambda_K$. Its size when $\lambda<\lambda_K$ suggests that Y is the classical analog of the energy which goes into the K fluorescent rays. Since these rays are removed by absorption in aluminum in experiments on diffuse scattering, Y is omitted in S_{incoh}. Finally $S=S_{\text{coh}}+S_{\text{incoh}}/\{1+(h/mc)\text{ vers }\phi\}^3$. Hönl's theoretical value of $\Delta f=2.3$ is compared with McNatt's experimental value 2.5 for Cu $K\alpha$ x-rays scattered by zinc.

1. INTRODUCTION

UNTIL recently all of the experimental work on the diffuse scattering of x-rays by crystals has been done in this laboratory with wave-lengths much shorter than the K critical absorption wave-length of the crystal being examined. Recently, however, McNatt[1] has been investigating the diffuse scattering of Cu $K\alpha$ ($\lambda=1.54$A) and Zn $K\alpha$ ($\lambda=1.433$A) x-rays from single crystals of zinc ($\lambda_K=1.28$A). In these cases λ/λ_K is somewhat greater than unity and the theory of diffuse scattering must be extended to the region of anomalous dispersion.

The early papers by Debye,[2] Faxen,[3] and Laue[4] on the theory of diffuse scattering by single crystals took account only of what is now called the coherent part of the scattered rays. The early experiments of Jauncey[5] and Jauncey and May[6] immediately showed the inadequacy of the then existent theory to describe the experimental results. After the discovery of the Compton effect, Compton[7] suggested that the incoherent part of the scattered rays should be taken into account. Both theory and experiments on diffuse scattering then languished until 1931 when Jauncey,[8] Jauncey and Harvey,[9] and, independently, Woo[10] extended the theory so as to include the incoherently scattered rays. There was some discussion between Woo and Jauncey as to the correct separation of the coherent and incoherent rays, but finally in 1932 these two writers[11, 12] came to an agreement on the formulas

$$S=S_{\text{coh}}+S_{\text{incoh}}/\{1+(h/mc)\text{ vers }\phi\}^3,$$
$$S_{\text{coh}}=(f^2/Z)(1-e^{-2M}), \qquad (1)$$
$$S_{\text{incoh}}=1-(1/Z)\sum E_r^2,$$

where f is the true atomic structure factor, E_r is the electronic structure factor for the rth (K, L, etc.) type of electron, and e^{-M} is the Debye-Waller[2, 13] temperature factor. Further extension of the theory was made in 1933 by Harvey, Williams and Jauncey[14] to take account of the Pauli exclusion principle; but, since this leads to a small change in S_{incoh} which is negligible except in crystals consisting of light atoms (such as NaF)

[1] E. M. McNatt, Phys. Rev. **56**, 406 (1939).
[2] P. Debye, Ann. d. Physik **43**, 49 (1914).
[3] H. Faxen, Ann. d. Physik **54**, 615 (1917).
[4] M. v. Laue, Ann. d. Physik **81**, 877 (1926).
[5] G. E. M. Jauncey, Phys. Rev. **20**, 405 (1922). Note: Figs. 2 and 6 in this article should be interchanged.
[6] G. E. M. Jauncey and H. L. May, Phys. Rev. **23**, 128 (1924).
[7] A. H. Compton, *X-Rays and Electrons* (Van Nostrand, New York, 1926), p. 170.
[8] G. E. M. Jauncey, Phys. Rev. **37**, 1193 (1931).
[9] G. E. M. Jauncey and G. G. Harvey, Phys. Rev. **37**, 1203 (1931).
[10] Y. H. Woo, Phys. Rev. **38**, 6 (1931).
[11] Y. H. Woo, Phys. Rev. **41**, 21 (1932).
[12] G. E. M. Jauncey, Phys. Rev. **42**, 453 (1932).
[13] I. Waller, Zeits. f. Physik **17**, 398 (1923).
[14] G. G. Harvey, P. S. Williams and G. E. M. Jauncey, Phys. Rev. **46**, 365 (1934).

we shall not consider this further development in this paper.

2. Theory

We shall use the symbol CA to refer to Compton and Allison's[15] book on x-rays—thus CA (4.30) refers to Eq. (4.30) in this book.

(a) Scattering from a bound electron

The classical theory of the forced, damped oscillations of an electron is described according to CA (4.30) by the differential equation

$$\frac{d^2x}{dt^2}-(2e^2/3mc^3)\frac{d^3x}{dt^3}+\omega_q^2x=-E_0(e/m)\sin\omega t, \quad (2)$$

where x is the displacement of the electron from its "rest" position—that is, the position it would have occupied if no radiation were falling on the electron. The frequency of the incident rays is $\omega/2\pi$ and the natural frequency of the q-type of electron is $\omega_q/2\pi$. The impressed electric field is zero when $t=0$. The negative sign on the right of (2) is caused by the negative charge on the electron, since e represents the charge on the electron in magnitude only.

The steady-state solution of (2) is

$$x=A\sin(\omega t+\psi), \quad (3)$$

where

$$A^2=E_0^2(e^2/m^2)/\{(\omega^2-\omega_q^2)^2+4r_e^2\omega^6/9c^2\}, \quad (4)$$

$$\tan\psi=2r_e\omega^3/3c(\omega^2-\omega_q^2), \quad (5)$$

and $r_e=e^2/mc^2=2.82\times10^{-13}$ cm. The acceleration of the electron is

$$a=\frac{d^2x}{dt^2}=-A\omega^2\sin(\omega t+\psi). \quad (6)$$

According to CA (2.01) and (2.05), the field strength of the electric wave arriving at time t at a distance R from the accelerated electron and in a direction θ_E with the electric vector of the incident polarized rays is

$$E=E_{\theta_E}\sin\{\omega(t-R/c)+\psi\}, \quad (7)$$

where

$$E_{\theta_E}=Ae\omega^2\sin\theta_E/Rc^2. \quad (8)$$

Also, similar to CA (3.01), we have

$$\frac{I_{\theta_E}}{I_0}=\frac{E_{\theta_E}^2}{E_0^2}=\frac{e^4\sin^2\theta_E}{R^2m^2c^4}\cdot\frac{\omega^4}{(\omega^2-\omega_q^2)^2+4r_e^2\omega^6/9c^2}. \quad (9)$$

Finally, for unpolarized rays scattered across unit area in a direction ϕ with the primary beam we arrive at

$$I_\phi=B^2I_e, \quad (10)$$

where

$$B=\omega^2\{(\omega^2-\omega_q^2)^2+4r_e^2\omega^6/9c^2\}^{-\frac{1}{2}} \quad (11)$$

and

$$I_e=I_0(e^4/R^2m^2c^4)\cdot(1+\cos^2\phi)/2, \quad (12)$$

the Thomson formula for scattering from a single free electron.

For ordinary x-rays and for ω_q not exceedingly close to ω the term $4r_e^2\omega^6/9c^2$ under the braces in (11) is negligible with respect to $(\omega^2-\omega_q^2)^2$ and we may write

$$B=\omega^2/(\omega^2-\omega_q^2). \quad (13)$$

Unless ω is exceedingly close to ω_q, $\tan\psi$ is either a small negative or a small positive number. From (5) and (13), we may say that B retains the positive value

$$B=|\omega^2/(\omega^2-\omega_q^2)|=|\nu^2/(\nu^2-\nu_q^2)| \quad (14)$$

and that the phase changes suddenly by 180° as ω decreases through ω_q. For a "free" electron $\omega_q/\omega\to0$, so that $B=1$ and there is no change of phase on scattering.

(b) Scattering from a single atom

We shall proceed along the lines of Jauncey's paper of 1931. We introduce the reference line OZ which bisects the angle between the forward direction OB of the scattered rays and the backward direction OA of the primary rays. Perpendicular to this reference line, we draw the reference plane through the center, or nucleus, of the atom. Then at a given instant of time the rth electron of the electron cloud surrounding the nucleus is at P at a distance z_r from the plane. Draw a plane BD perpendicular to OB at a large distance R from O in Fig. 1. The phase of the scattered wave arriving at BD from a "free" electron on the reference plane is independent of the position of the electron in the reference plane and we shall assume for convenience that the phase of such a wave is zero. The phase of a

[15] A. H. Compton and S. K. Allison, *X-Rays in Theory and Experiment* (Van Nostrand, New York, 1935.)

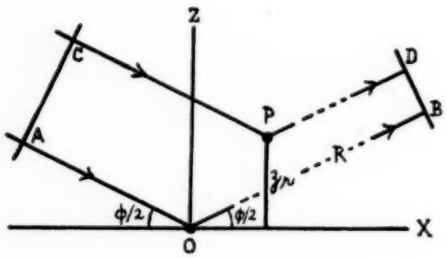

FIG. 1. Interference of x-rays scattered by a cloud of electrons.

scattered wave at BD from the rth electron at z_r is $kz_r+\psi_r$, where

$$k=(4\pi \sin \tfrac{1}{2}\phi)/\lambda \qquad (15)$$

and ψ_r is the change of phase on scattering. The amplitudes of the waves scattered by all the Z electrons of the atom are added vectorially to obtain the resultant amplitude of the scattered waves arriving at the plane BD. Hence the scattered intensity per unit area on BD is

$$(I_\phi/I_e)_{\text{inst}}=\{\sum_{r=1}^{Z} B_r \cos(kz_r+\psi_r)\}^2 + \{\sum_{r=1}^{Z} B_r \sin(kz_r+\psi_r)\}^2$$

$$=\sum_{r=1}^{Z} B_r^2+\sum_{r=1}^{Z}{}' \sum_{s=1}^{Z}{}' B_rB_s \times \cos\{k(z_r-z_s)+\psi_r-\psi_s\}, \qquad (16)$$

where B_r is the value of B as given by (11) or (14) for the rth electron and the symbol $\Sigma'\Sigma'$ indicates that in the double summation $r\neq s$. If for all electrons $\omega_r/\omega\to 0$, $B=1$ and $\psi_r-\psi_s=0$, so that (16) reduces to

$$I_\phi=I_e\{Z+\sum_{r=1}^{Z}{}' \sum_{s=1}^{Z}{}' \cos k(z_r-z_s)\}, \qquad (17)$$

the formula given in Jauncey's paper[8] of 1931. We shall now simplify the problem by assuming that we are interested in the region $\lambda\approx\lambda_K$ and that therefore $B_r=B_K$ for the two K electrons and $B_r=1$ for the other electrons. Consequently, also $\psi_r-\psi_s=\pm\psi_K$ when r or s represents a K electron and $\psi_r-\psi_s=0$ when r and s represent either the two K electrons or two of the non-K electrons. Applying these assumptions to (16), we obtain

$$(I_\phi/I_e)_{\text{inst}}=Z-2(1-B_K^2) +\sum_{r=3}^{Z}{}' \sum_{s=3}^{Z}{}' \cos k(z_r-z_s)+2B_K^2\cos k(z_1-z_2) +2B_K\sum_{r=3}^{Z} \sum_{s=1}^{2} \cos\{k(z_r-z_s)-\psi_K\}, \qquad (18)$$

where the subscripts 1 and 2 refer to the K electrons and the subscripts 3, $4\cdots Z$ refer to the non-K electrons.

The intensity given by (18) is an instantaneous intensity resulting from an instantaneous configuration of the electrons in the atom. The probability of this intensity occurring is that of the configuration occurring. We shall represent this latter by $p(z_1, z_2, z_3, \cdots z_Z)dz_1dz_2\cdots dz_Z$. No further progress can be made unless further assumptions are made concerning this probability. These further assumptions are: (1) *the probability distribution function for the rth electron is independent of that of the sth electron*, so that we may write

$$p(z_1, z_2, \cdots z_Z)=p_1(z_1)\cdot p_2(z_2)\cdots p_Z(z_Z), \qquad (19)$$

and (2) *the rth electron is just as likely to be above the reference plane as below it*, so that

$$p_r(z_r)=p_r(-z_r). \qquad (20)$$

In other words $p_r(z_r)$ is an even function of z_r. The average scattered intensity is then given by

$$(I_\phi/I_e)_{Av}=\int_{-\infty}^{\infty}(I_\phi/I_e)_{\text{inst}} \prod_{r=1}^{Z} p_r dz_r, \qquad (21)$$

where p_r is written for $p_r(z_r)$. Remembering that the integral of an odd function from $-\infty$ to $+\infty$ is zero and that the sine is an odd function and also that

$$\int_{-\infty}^{\infty} p_r dz_r=1, \qquad (22)$$

since the rth electron must be somewhere, we obtain

$$(I_\phi/I_e)_{Av}=Z-2+2B_K^2(1+E_K^2) +4B_KE_K\cos\psi_K\sum_{r=3}^{Z} E_r+\sum_{r=3}^{Z}{}' \sum_{s=3}^{Z}{}' E_rE_s, \qquad (23)$$

where

$$E_r=\int_{-\infty}^{\infty}\rho_r\cos kz_r dz_r, \tag{24}$$

the "electronic structure factor" for the rth electron. Now put

$$\sum_{r=1}^{Z}E_r=f,$$

so that

$$\sum_{r=3}^{Z}E_r=f-2E_K \tag{25}$$

and

$$\sum_{r=3}^{Z}{}'\sum_{s=3}^{Z}{}'E_rE_s=(f-2E_K)^2-(\sum_{r=1}^{Z}E_r^2-2E_K^2). \tag{26}$$

Eq. (23) now becomes

$$(I\phi/I_e)_M=Z-\sum_{1}^{Z}E_r^2-2(1-B_K^2)$$
$$+2E_K^2\{1-B_K^2(2\cos^2\psi_K-1\}$$
$$+\{f-2E_K(1-B_K\cos\psi_K)\}^2. \tag{27}$$

When $\omega_K/\omega\to 0$, this reduces to

$$(I_\phi/I_e)_M=Z-\sum_{1}^{Z}E_r^2+f^2, \tag{28}$$

which Raman[16] and Compton[17] have obtained for this case.

(c) Separation of the coherent rays

If a large number n of atoms which individually scatter according to (28) are assembled into a three-dimensional lattice or crystal, Jauncey, Harvey and Woo[8, 9, 11, 12] have shown that the intensity of the rays scattered by the lattice is given by

$$(I_\phi/I_e)=n(Z-\sum_{1}^{Z}E_r^2)+f^2(n+Xe^{-2M}), \tag{28a}$$

where X is a triple trigonometrical summation and e^{-2M} is introduced to take account of the thermal vibrations of the atoms in the lattice. The value of X is $-n$ excepting for the directions of the Laue-Bragg reflections when X takes on the value of $+n^2-n$. If the thermal vibrations are reduced to zero, then, except in the Laue-Bragg directions, the factor of f^2 in (28a) is $(n+X)=0$. This means that the destructive interference except in the Laue-Bragg directions is complete. Following the ideas of Raman[16] the part of (28) which is reduced to zero by multiplication by $(n+X)$ in (28a) is the coherent part of (28). Hence f^2 represents the coherent part of (28), while the remainder, $Z-\Sigma E_r^2$, represents the incoherent part. This second part exists whether or not the atoms are assembled into a lattice.

As a simplification of this method of separating out the coherent scattered rays, the n atoms need only be assembled into a line of equally spaced atoms. In this case

$$X=2\sum_{r=1}^{n-1}(n-r)\cos rka, \tag{28b}$$

where a is the projection of the separation of two adjacent atoms on the z axis or reference line of Fig. 1. A graph of X/n against ka is shown in Fig. 2 for $n=8$. It is seen that, even for a small number like 8, X/n is close to -1 or X to $-n$ except in directions near to those where $ka=2m\pi$, m being zero or an integer. These exceptional directions are those included in the cones shown in CA Fig. V-14 and they correspond to the Laue-Bragg directions in the case of a three-dimensional lattice.

For the purpose of separating the coherent rays we may reduce the linear lattice to two atoms. In this case we have two atoms at A and B, Fig. 3. In this case $(n+X)$ reduces to $2(1+\cos ka)$. Let the reference plane pass through the center of the atom at A, we then

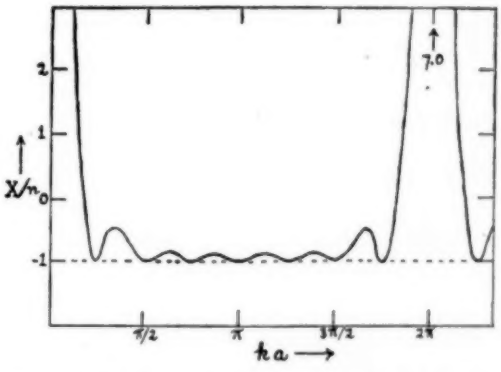

FIG. 2. Graph of X/n against ka for a line lattice.

[16] C. V. Raman, Ind. J. Phys. **3**, 357 (1928).
[17] A. H. Compton, Phys. Rev. **35**, 925 (1930).

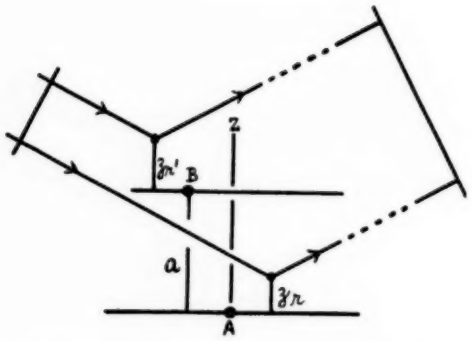

FIG. 3. Interference of x-rays scattered by the electrons in two atoms.

represent the z of an electron in atom A as z_r and the z of an electron in atom B as $z_{r'}+a$. The subscripts r and s refer to electrons in atom A and r' and s' to electrons in atom B. Eq. (16) now becomes

$$(I_\phi/I_e)_{\text{inst}}=\sum_{r=1}^{Z} B_r^2+\sum_{r'=1}^{Z} B_{r'}^2$$
$$+\sum_{r=1}^{Z}{}'\sum_{s=1}^{Z}{}' B_r B_s \cos\{k(z_r-z_s)+\psi_r-\psi_s\}$$
$$\sum_{r'=1}^{Z}{}'\sum_{s'=1}^{Z}{}' B_{r'}B_{s'} \cos\{k(z_{r'}-z_{s'})+\psi_{r'}-\psi_{s'}\}$$
$$+2\sum_{r=1}^{Z}\sum_{s'=1}^{Z} B_r B_{s'} \cos\{k(z_r-z_{s'}+a)+\psi_r-\psi_{s'}\}. \quad (29)$$

Introducing the probability distribution functions, p_r, as before and assuming that the p_r for the rth electron in atom A (or B) is not affected by the presence of atom B (or A), we find after tedious computation that

$$(I_\phi/I_e)_{\text{Au}}=2(1+\cos ka)$$
$$\times[\{f-2E_K(1-B_K\cos\psi_K)\}^2$$
$$+4E_K^2B_K^2\sin^2\psi_K]$$
$$+2[Z-\sum_{r=1}^{Z} E_r^2-2(1-B_K^2)(1-E_K^2)]. \quad (30)$$

The factor of $2(1+\cos ka)$ in (30) is the coherent part of (27). The remainder of the right side of (27) is the incoherent part.

We now introduce the symbol

$$S\equiv(1/nZ)\cdot(I_\phi/I_e)_{\text{Au}}, \quad (31)$$

where n is the number of atoms participating in the production of the scattered intensity I_ϕ, n being small enough, however, so that no correction for absorption need be made. After introducing the effect of the Compton change of wavelength on the incoherent portion of (27), we write (27) in the form

$$S_{\text{atom}}=S_{\text{coh}}+S_{\text{incoh}}/\{1+(h/mc)\text{ vers }\phi\},^3 \quad (32)$$

where

$$S_{\text{coh}}=\frac{1}{Z}[\{f-2E_K(1-B_K\cos\psi_K)\}^2$$
$$+4E_K^2B_K^2\sin^2\psi_K], \quad (33)$$

$$S_{\text{incoh}}=1-\frac{1}{Z}\sum_{r=1}^{Z} E_r^2+Y \quad (34)$$

and

$$Y=-2(1-B_K^2)(1-E_K^2)/Z. \quad (34a)$$

(d) Frequency of the orbital motion of the electrons

In the previous subsections (b) and (c), it has been tacitly assumed that an electron did not on account of its orbital motion appreciably change its position in the atom during a complete cycle of the incident x-rays. In other words, it was assumed that

$$\frac{\text{orbital frequency}}{\text{x-ray frequency}}\ll 1. \quad (35)$$

For the nth Bohr orbit of a hydrogenic atom this ratio is $(Z^2/2\pi n^3)\cdot(\lambda/137\ a_{\text{H}})$ where a_{H} is the radius of the first Bohr orbit in hydrogen. For Cu $K\alpha$ rays scattered from the L electrons of zinc the effective Z is about 25 and the ratio is 0.266. Although this is not very small compared to unity we shall as an approximation assume that (35) is fulfilled for the L electrons. For the K electrons the effective Z is about 29.5 and the ratio is 2.94. For this case the condition of (35) is not fulfilled and E_K for the K electrons is not given by (24).

In McNatt's experiments[1] the largest value of $(\sin\frac{1}{2}\phi)/\lambda$ is 0.6, for which, according to James and Brindley's tables,[18] E_K for zinc is 0.990. This departure from unity is due to the probability

[18] R. W. James and G. W. Brindley, Phil. Mag. **12**, 81 (1931).

distribution function $p_K(z_K)$ in (24) being small but appreciable for values of z_K greater than zero. However, if during a cycle of the incident wave the electron makes something like three revolutions about the nucleus, then no matter what the value of z_K at the beginning of the cycle z_K passes through the value zero and cos kz_K passes through the value unity. It is plausible to expect that the average of cos kz_K is closer to unity than the value given by (24). Hence we may expect E_K to be closer to unity than 0.990. To be on the safe side we shall use James and Brindley's values of E_K. Then in (34) we have, from (14) and for Zn $K\alpha$ rays ($\lambda/\lambda_K=1.12$) scattered from zinc, $Y=0.02$. The value of Y for Cu $K\alpha$ rays ($\lambda/\lambda_K=1.20$) is 0.005 and its value for $\lambda/\lambda_K=1.06$ is 0.1. Since S values have not been measured under the best conditions with an error less than about 0.1, we are justified in neglecting the quantity Y in the region λ greater than but not too close to λ_K. In this region

$$S_{\text{incoh}}=1-\frac{1}{Z}\sum_{r=1}^{z}E_r^2. \tag{36}$$

Also for Zn $K\alpha$ rays on zinc, the term

$$(4E_K^2B_K^2\sin^2\psi_K^2)/Z$$

in (33) is from (5) and (14) of the order 10^{-7} and is completely negligible and we replace (33) by

$$S_{\text{coh}}=\{f-2E_K(1-B_K\cos\psi_K)\}^2/Z. \tag{37}$$

(e) Atomic structure factor decrement

In the theory of refraction and absorption of x-rays, Kramers, Kallmann and Mark[19] introduced the idea of virtual oscillators. Instead of the K electrons of all atoms at all times having a natural frequency $\omega_K/2\pi$, they introduced virtual oscillators having natural frequencies $\nu_q=\omega_q/2\pi$ all the way from $\omega_K/2\pi$ to infinity. In an assembly of atoms let the probability of a K electron having a frequency ν_q in the range $d\nu_q$ be $P(\nu_q)d\nu_q$. Applying the method of Kramers, Kallmann and Mark, we then calculate an average S_{atom} for all the virtual oscillators. But now comes the question of the distribution or averaging fraction $P(\nu_q)d\nu_q$. Kramers, Kallmann and Mark obtain this from the experimental absorption law which states that the mass absorption coefficient varies as $1/\nu^3$ or as λ^3 so long as $\nu=c/\lambda>\nu_K$. If we think of the frequency aspect of the law, we are inclined to adopt

$$2\nu_K^2d\nu_q/\nu_q^3 \tag{38}$$

for the averaging fraction, while, if we think of the wave-length aspect, we are inclined to adopt

$$4\lambda_q^3d\lambda_q/\lambda_K^4 \tag{39}$$

for the averaging fraction. The averaging fraction (38) was used by Kramers, Kallmann and Mark. Either of these is suggested by the absorption law. It should be noted that (38) does not transform into (39) when we put $\nu=c/\lambda$ but into $2\lambda_qd\lambda_q/\lambda_K^2$ which implies a λ instead of λ^3 law of absorption! The averaging fraction is thus arbitrary even for a given absorption law.

Because of the distribution of oscillators from ν_K to ∞ (λ_K to 0), we can no longer neglect the quantities Y and $(4E_K^2B_K^2\sin^2\psi_q)/Z$ when $\lambda<\lambda_K$. We must therefore recognize two cases: $\lambda>\lambda_K$ and $\lambda<\lambda_K$.

Case I. $\lambda>\lambda_K$.—In this case it is only S_{coh} which according to (32), (36) and (37) is a function of ν_q/ν or λ_q/λ and hence we need only average this portion of S_{atom}. Since the coherent part of the radiation comes from the addition of amplitudes we find $(\langle S_{\text{coh}}{}^{\frac{1}{2}}\rangle_{Av})^2$. For this, from (37), we need $\langle B_q\cos\psi_q\rangle_{Av}$. Using the averaging fraction (38), we obtain[20] from (5) and (14)

$$\langle B_q\cos\psi_q\rangle_{Av}=-\{1+w_K^2\log(1-w_K^{-2})\}, \tag{40}$$

since $\cos\psi_q\approx-1$. We shall in this paper define Δf by

$$\Delta f=f-Z^{\frac{1}{2}}\langle S_{\text{coh}}{}^{\frac{1}{2}}\rangle_{Av}, \tag{41}$$

whence, in virtue of (37) and (40),

$$\Delta f=-2w_K^2\log(1-w_K^{-2}), \tag{42}$$

since $E_K\approx1$. Δf is called the atomic structure factor decrement. On the other hand, if we use the averaging fraction (39), we obtain

$$\langle B_q\cos\psi_q\rangle_{Av}=-\{1+2w_K^2+2w_K^4\log(1-w_K^{-2})\} \tag{43}$$

and

$$\Delta f=-4w_K^2\{1+w_K^2\log(1-w_K^{-2})\}. \tag{44}$$

[19] H. Kallmann and H. Mark, Ann. d. Physik **82**, 585 (1927). See also CA, p. 292.

[20] B. O. Peirce, *A Short Table of Integrals*, pp. 10, 11 and 26.

We see therefore that the calculation of Δf is somewhat arbitrary. Others have encountered the same difficulty in working out the theoretical formula for the intensity of the Bragg reflection of x-rays from crystals. We shall not attempt any further in this paper to calculate Δf but shall use the theoretical value of Δf as found by others. So far the most satisfactory theoretical formula for Δf has been found independently by Hönl[21] and Williams.[22] Bruce[23] using Hönl's theory has obtained a simple formula for calculating Δf.

Case II. $\lambda<\lambda_K$.—It is now no longer possible to neglect the quantities we have previously mentioned, nor can we substitute (14) for (11)since in the range of integration ω_q (or ν_q) passes through the value ω (or ν) and B_q according to (14) goes to infinity. However, if we include the radiation damping term $4r_r^2\omega^6/9c^6$ which occurs in formula (11) for B_q, the integrand in the integral for determining $\langle B_q\cos\psi_q\rangle_{Av}$ no longer goes to infinity when ω_q passes through ω. It turns out that $\langle B_q\cos\psi_q\rangle_{Av}$, if the averaging fraction (38) is used, is given by the right side of (40) plus a term with $2r_e\omega/3c$ as a factor. The order of magnitude of this factor is 10^{-4} and so the added term may be neglected. However, in virtue of (33) and (34), $B_q\cos\psi_q$ does not determine Δf as it does when $\lambda>\lambda_K$. We leave the calculation of Δf to others.

The quantity Y is of interest because it occurs in the incoherent part of the scattered rays. We shall attempt to find the magnitude of Y. We first determine $\langle B_q^2\rangle_{Av}$ rather than $(\langle B_q\rangle_{Av})^2$ since the incoherent part comes from the addition of intensities. Applying the averaging fraction (38) to the square of (11), we obtain[20]

$$B_q^2=(1+D^2)^{-1}+w_K^2(1+D^2)^{-2}\times\log\{(1-w_K^{-2})^2+D^2w_K^{-4}\}+\{(1-D^2)/D(1+D^2)\}\times\tan^{-1}\{D/(w_K^2-1)\},\quad(45)$$

where $D=2r_e\omega/3c=1.17\times10^{-4}/\lambda$ when λ is in angstroms. Since D is small (45) reduces to

$$\langle B_q^2\rangle_{Av}=1+2w_K^2\log(1-w_K^{-2})+(w_K^2/D)\tan^{-1}\{D/(w_K^2-1)\}.\quad(46)$$

In this $\tan^{-1}\{D/(w_K^2-1)\}$ approaches π or $D/(w_K^2-1)$ according as $\lambda<$ or $>\lambda_K$. In the latter case $\langle B_q^2\rangle_{Av}\to0$ when $w_K\gg1$, while in the former case the term containing D becomes by far the most important term on the right of (46) and we write

$$\langle B_q^2\rangle_{Av}=w_K^2\pi/D,\quad(47)$$

when $\lambda<\lambda_K$.

Since the Schroedinger probability distribution function for a K electron of an element like zinc is very nearly that of an electron in a hydrogenic atom with a nuclear charge $+Ze$, we may write as an approximation

$$1-E_K^2=(Z^2\alpha^2\lambda_K^2/\lambda^2)\sin^2\tfrac{1}{2}\phi,\quad(48)$$

where $\alpha=2\pi e^2/hc=1/137$. We now have

$$\langle Y\rangle_{Av}=(3Z\alpha^2/2r_e)\lambda\sin^2\tfrac{1}{2}\phi,\quad(49)$$

since we may replace $1-\langle B_q^2\rangle_{Av}$ by $-\langle B_q^2\rangle_{Av}$.

Instead of applying the averaging fraction (38), we might have applied (39). In this case, after making approximations, (47) is replaced by

$$\langle B_q^2\rangle_{Av}=2w_K^4\pi/D\quad(50)$$

and (49) by

$$\langle Y\rangle_{Av}=(3Z\alpha^2/r_e)\cdot(\lambda^3/\lambda_K^2)\cdot\sin^2\tfrac{1}{2}\phi.\quad(51)$$

The numerical values of $\langle Y\rangle_{Av}$ are 30 from (49) and 18.5 from (51) when zinc is irradiated by Mo $K\alpha$ rays ($\lambda=0.71$A) and the secondary rays are measured at $\phi=90°$. At this place we shall drop the average sign from Y and from now on use Y to represent its average. The greatest value of $S=S_{\text{coh}}+S_{\text{incoh}}$ for zinc measured in this laboratory is about 6 while the value of S_{incoh} is always less than unity when Y is neglected or omitted. So if Y is considered as a correction term it is much greater than the quantities which are being corrected.

It is known that when x-rays fall upon a substance both scattered rays and much more intense K fluorescent rays are produced provided that $\lambda<\lambda_K$. These fluorescent rays are incoherent with the primary rays. The magnitude of Y suggests that Y represents the classical analog of the energy which appears as fluorescent rays when a substance is irradiated by x-rays whose $\lambda<\lambda_K$. In experiments on diffuse scattering it is usual when $\lambda<\lambda_K$ to place absorbing material

[21] H. Hönl, Zeits. f. Physik **84**, 1 (1933).
[22] E. J. Williams, Proc. Roy. Soc. **143**, 358 (1933).
[23] W. A. Bruce, Phys. Rev. **53**, 802 (1938).

such as aluminum in the scattered beam so as to cut out the more absorbable fluorescent component of the beam. Consequently the quantity Y does not enter into what is ordinarily called "diffuse scattering." This is a paper on diffuse scattering and the writer feels that further consideration of Y should be deferred to a later paper.

(f) Diffuse scattering from a crystal

Jauncey[12] and Woo[11] have shown that if atoms whose S values are known are assembled into a crystal lattice, the S values for the diffuse scattering from the crystal are obtained by subtracting e^{-2M} times the coherent part of S for the atom from the S_{atom} values. Thus, using (32), (36) and (41), we obtain the very good approximation

$$S_{\text{crystal}}=(f-\Delta f)^2(1-e^{-2M})/Z + \{1-(1/Z)\Sigma E_r^2\}/\{1+(h/mc)\ \text{vers}\ \phi\}^3 \quad (52)$$

for the region $\lambda>\lambda_K$ and also for the region $\lambda<\lambda_K$ if in the latter case care is taken to remove or to correct for the fluorescent rays.

3. Conclusion

The formula for the diffuse scattering of x-rays from a crystal in the region λ/λ_K close but not exceedingly close to unity differs only from the formula previously worked out for the region $\lambda/\lambda_K \ll 1$ in that f in the formula for S is replaced by $f-\Delta f$.

Table I. *Values of Δf for zinc.*

λ/λ_K	McNatt (exp.)	Eq. (42) (theory)	Hönl (theory)
1.12	3.65	4.0	2.8
1.20	2.5	3.4	2.3

McNatt's experimental values of Δf for zinc are shown in Table I. These are the only experimental values of Δf so far obtained by diffuse scattering. Theoretical values are shown in the table. The agreement of experiment with Hönl's theory is little better than with (42) of this paper. However, on account of the relatively low intensity of the Zn $K\alpha$ rays in McNatt's experiments, the writer believes that McNatt's value for Δf is more reliable for the stronger Cu $K\alpha$ rays ($\lambda/\lambda_K=1.20$). Here the agreement of McNatt's and Hönl's values is as good as can at present be expected. On account of the arbitrariness in averaging $B_q \cos \psi_q$ the writer holds no particular brief for the values shown in the third column of Table I.

Finally the writer wishes to point out that Δf as given by (42) or (44) for $\lambda>\lambda_K$ leads to the value 2 when $\lambda/\lambda_K \gg 1$. This implies that the K electrons are inoperative in the scattering process in this region. Similarly the L electrons become inoperative when $\lambda/\lambda_L \gg 1$. In the case of ordinary light irradiating a substance like zinc, the K, L and some or all of the M electrons are inoperative as far as scattering is concerned.

Evidence of a Periodic Deviation from the Schottky Line. I

R. L. E. SEIFERT* AND T. E. PHIPPS
Department of Chemistry, University of Illinois, Urbana, Illinois

(Received June 19, 1939)

A periodic deviation from the Schottky line has been observed for tungsten and for tantalum. For fields less than 4×10^4 volts cm^{-1} the deviations are of the order of the experimental error. For fields greater than this the sign and magnitude of the peak deviations may be seen from the following series, the first number in each case being the value of $E^{\frac{1}{2}}$ in volt$^{\frac{1}{2}}$ cm$^{-\frac{1}{2}}$, and the second being the percent deviation from a least-squares reference line: 200, $+0.03(\pm0.01)$; 265, $-0.07(\pm0.01)$; 365, $+0.12(\pm0.01)$; 501, $-0.11(\pm0.01)$. The data refer to a 1-mil tungsten wire at 1610°K. There is no appreciable effect of temperature upon the positions of the peaks along the $E^{\frac{1}{2}}$ axis. The magnitude of the deviations decreases with increasing temperature. The results with tantalum agree within experimental error with those for tungsten.

INTRODUCTION

SINCE the formulation by Schottky[1] of a theory to account for the increase in the electron current from a hot metal with increase in the accelerating electric field at its surface, numerous investigations[2–11] of thermionic emission have been made to test this theory,[12] which predicts that for all metals

$$\frac{d\log_{10} i}{dE^{\frac{1}{2}}}=\frac{\epsilon^{\frac{1}{2}}}{2.3026k}\frac{1}{T},$$

in which i is the specific electronic current at T°K; E is the accelerating field; ϵ is the electronic charge; and k is Boltzmann's constant. If the unit of E is int. volt cm^{-1}, and if ϵ and k are taken, respectively, as 4.774×10^{-10} e.s. unit and 1.3709×10^{-16} erg deg.$^{-1}$, the coefficient of $1/T$ is 1.908. The results of the earlier investigations deviated from this theoretical slope by as much as 25 to 100 percent. These deviations were attributed in part to uncertainty in the determination of the effective field at the surface of the emitting metal. The more recent investigations by de Bruyne,[7] by Pforte,[9] and by Nottingham[11] have yielded emission curves having slopes which agree within one percent with the theoretical value.

Schottky lines obtained in this laboratory by Phipps and Clemans,[13] with accelerating fields up to 5×10^4 volts cm^{-1}, showed close agreement with the expected Schottky slope, but indicated a perceptible curvature of the line in the sense of a slight decrease in slope with increasing field. This deviation was reproducible and beyond experimental error. The present work sought to increase the accuracy of the measurements and to follow the course of the deviation to higher fields.

EXPERIMENTAL

In order to obtain accurate measurements of the thermionic emission from metals, it is essential that the geometry of the emission tube be known with exactness; that the temperature of the emitting metal be known and kept constant for each isotherm; that the various voltages applied to the collector be accurately known; that the resulting emission currents be accurately measured; and that all the measurements be made in a vacuum sufficiently high that the surface of the metal remain clean and the emission be reproducible during the course of a series of measurements.

* Present address: Alma College, Alma, Michigan.

[1] W. Schottky, Physik. Zeits. **15**, 872 (1914); Ann. d. Physik **44**, 1011 (1914).

[2] W. Schottky, Physik. Zeits. **20**, 220 (1919); Zeits. f. Physik **14**, 63 (1923).

[3] S. Dushman *et al.*, Phys. Rev. **25**, 338 (1925).

[4] J. Becker and D. Mueller, Phys. Rev. **31**, 431 (1928).

[5] C. C. Lauritsen and S. S. Mackeown, Phys. Rev. **32**, 326 (1928).

[6] L. A. Dubridge, Phys. Rev. **32**, 961 (1928).

[7] N. A. de Bruyne, Proc. Roy. Soc. **A120**, 423 (1928).

[8] R. S. Bartlett, Proc. Roy. Soc. **A121**, 456 (1928).

[9] W. S. Pforte, Zeits. f. Physik **49**, 46 (1928).

[10] N. B. Reynolds, Phys. Rev. **35**, 158 (1930).

[11] W. B. Nottingham, Phys. Rev. **47**, 806 (1935); **49**, 78 (1936).

[12] For full discussions of this theory see K. T. Compton and I. Langmuir, Rev. Mod. Phys. **2**, 123 (1930); J. A. Becker, *ibid.* **7**, 95 (1935).

[13] T. E. Phipps and J. E. Clemens, unpublished data, 1935.

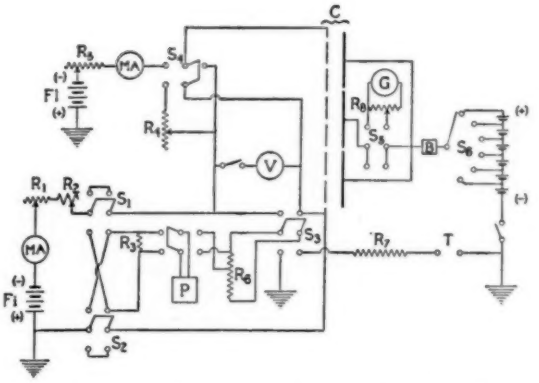

FIG. 1. Electrical circuit. *B*, relay circuit breaker; *C*, thermionic tube; *G*, galvanometer; *MA*, milliammeter; *P*, type *K L* and *N* potentiometer; *T*, terminals for calibration of voltage taps on S_6; *V*, voltmeter.

The thermionic tube

Each of the thermionic tubes, shown diagrammatically in Fig. 1, was constructed as described by Clemens and Phipps.[14] The collecting plates of some of the tubes were formed by the evaporation of platinum onto the walls of the tube, those of others by the evaporation of tungsten. The length (2 to 3 cm) and the diameter (3 cm) of the plates were measured within 0.03 percent at room temperature and corrected to liquid-air temperature. The space between the plate and the guard rings, which never exceeded 0.015 cm, was measured within one percent. One-half the width of each of these two spaces was added to the length of the plate. A straight tungsten filament was mounted coaxial with the plate and guard rings, well within 0.05 cm of the exact center. Filaments, 2 mils, 1 mil, and 0.5 mil in diameter, of high purity, cleaned tungsten wire, No. 218, obtained from the Incandescent Lamp Department of the General Electric Company, were used.* The exact diameters of the filaments were obtained by determining the length and weight of one-meter samples taken from each end of the sections which were used for filaments. Each length was measured with an accuracy of 0.01 percent and each weight with an accuracy of 0.05 percent.† The diameter of each sample was then calculated from the relation given by Jones and Langmuir,[15] and the average value for each pair of samples was taken as the diameter of the section from which the samples were obtained. The uniformity of the filament diameter appears to have varied between the different filament sizes, though in no case did the calculated diameters of the two individual samples vary by more than 0.2, 0.08 and 0.06 percent, respectively, for the 2-mil, 1-mil and 0.5-mil filaments. These filament diameters, calculated at room temperature, were corrected to the operating filament temperatures by use of the thermal expansion data given by Jones and Langmuir.[16]

Filament temperature

The temperature of the filament was determined from the current-diameter-temperature data given by Jones and Langmuir.[15] In the calculations presented herein the temperatures given in the table of Jones and Langmuir have been assumed to be correct.[17] The filament current was determined by measuring the potential drop across the one-ohm standard resistance* R_3 (Fig. 1) with the potentiometer *P*. The standard resistance was calibrated within 0.01 percent, and the potentiometer was calibrated by the method of Young and Hartouch[18] to 0.01 millivolt. The standard cell used with the potentiometer was calibrated to six significant figures by the National Bureau of Standards. The resulting accuracy with which the potential drop across the standard resistance was determined at the lowest filament temperature for the 2-mil, 1-mil and 0.5-mil filaments was 0.01, 0.03 and 0.006 percent, respectively. Therefore, the maximum possible error of the filament

[14] J. E. Clemens and T. E. Phipps, Rev. Sci. Inst. **8**, 133 (1937).

* Tungsten wire of still higher purity has recently been furnished us by the Incandescent Lamp Department of the General Electric Company, through the courtesy of Mr. B. L. Benbow. The data in the present paper, however, refer only to the No. 218 wire.

† Mr. C. W. Beazley weighed these samples on a microbalance, using weights calibrated by the National Bureau of Standards.

[15] H. A. Jones and I. Langmuir, Gen. Elec. Rev. **30**, 310 (1927).

[16] H. A. Jones and I. Langmuir, Gen. Elec. Rev. **30**, 354 (1927).

[17] The accuracy of this temperature scale has been questioned by W. H. Brattain and J. A. Becker, Phys. Rev. **43**, 428 (1933); by W. B. Nottingham, *ibid.* **49**, 78 (1936); and by H. B. Wahlin and L. V. Whitney, *ibid.* **50**, 735 (1936).

* A calibrated ten-ohm standard resistance was used with the 0.5-mil filaments.

[18] T. F. Young and P. J. Hartouch, private communication.

temperature resulting from the experimental measurements here involved was less than 0.2 percent even in the most unfavorable case. By the use of a galvanometer of high voltage sensitivity in the potentiometer circuit, it was possible to keep the filament current constant well within 0.003 percent by hand regulation of resistance R_2 (Fig. 1). In order to facilitate keeping the filament current constant to this degree, switch S_4 and resistance R_4 were introduced so that the filament could be flashed by batteries *Fl* without appreciably disturbing the current flowing from the filament batteries *Fi*. The switches S_1 and S_2 made it possible to introduce the standard resistance at either end of the filament, so that it was possible to keep either the input or output of the filament current constant at the value corresponding to the setting of the potentiometer *P*. For filament temperatures lower than 2000°K the electron emission was the same with the standard resistance in either position. Therefore, at these temperatures no measurable gradient of the heating current along the filament was produced by the emission current.

Plate potentials

The plate potentials, which were applied by means of the mercury switch S_6 (Fig. 1), were obtained from a bank of Burgess Heavy Duty "B" Batteries, the maximum voltage of which was about 2400 volts in the earlier measurements and about 4700 for the later work. In order to avoid drawing currents sufficiently large to produce a noticeable polarization, the batteries were calibrated in steps of less than 140 volts, before and after each series of emission measurements, by means of the potentiometer *P* and the volt box arrangement R_6 and R_7. The total potential of each of the available taps on switch S_6, as obtained by the summation of the constituent steps, varied less than 0.1 percent over a period of several months, when corrected for the temperature coefficient of the battery potential. It was therefore assumed that the e.m.f. of the battery remained constant throughout a series of emission measurements, and that values at the different taps were those given by a recent calibration, except for correction to the existing battery temperature. These applied battery potentials had to be corrected, however, for the voltage drop down the filament; for the drop across the standard resistance, if the latter were on the grounded side of the filament; for the voltage drop across the high resistance protective relay *B* (Fig. 1); and finally for the contact potential between the filament and the plate. The voltage drop down the filament from ground to the center of the plate was easily determined within 0.01 volt from the determination of the filament voltage with the volt box R_6 and the measurement of the corresponding filament sections. The emission current was so small that the voltage drop across the relay *B* was negligible except at the higher filament temperatures. At these temperatures it was calculated from the resistance of the relay and the measurement of the total emission current to plate and guard rings. The contact potential was determined to within 0.1 volt by the method described by Becker.[12]

Measurement of emission current

The emission current was measured by means of a current-sensitive G-M galvanometer, which had been equipped in this laboratory with a quartz fiber suspension of approximately 18μ (0.0018 cm) diameter, in order to produce a better zero return of the galvanometer coil than that obtainable with metal ribbon suspensions. With quartz fiber suspension, even after a full scale deflection of 80 cm at 5 meters' scale distance, the coil consistently returned to within 0.1 mm of the initial zero reading. Calibration proved the galvanometer deflection to be linear with current over the entire scale length, within the possible 0.1 mm error in the reading of the deflection. For each filament temperature the galvanometer sensitivity was adjusted by setting the shunt resistance R_8 (Fig. 1) so that a full scale deflection resulted upon the application of the highest plate voltage. This shunt setting was then used for all measurements at that temperature. Consequently the relative emission currents for each isotherm were given by the galvanometer deflections and were independent of the galvanometer sensitivity determinations. However, the possible error in each galvanometer reading being 0.1 mm, the percent error in the deflections was larger for the lower applied voltages than for the higher, since in the former

case the galvanometer deflections were smaller. In order to obtain the absolute values of the emission currents, the galvanometer was calibrated by means of a White potentiometer. Over a period of several weeks the galvanometer sensitivity thus determined varied within 0.15 percent of the mean value, though the possible experimental error of each calibration was considerably less than this. The galvanometer was introduced into the plate circuit by means of the mercury cup switch S_5 (Fig. 1), which was so constructed that the galvanometer could be introduced without interrupting the plate current. Thus the surge of current from the plate produced by the application of high plate potentials did not pass through the galvanometer to cause a sudden excessive deflection and vitiate the excellent zero return of the coil. The entire plate circuit was so well insulated that no measurable current passed through the galvanometer when the highest plate potential was applied with the filament cold.

Procedure

For the duration of each series of measurements the thermionic tube remained sealed to the vacuum line while the mercury pumps operated continually. Initially the tube and vacuum line back to the first diffusion pump were baked out at 480–500°C for at least 48 hours. Thereafter liquid air was kept constantly about a trap between the tube and the pumps. The thermionic tube was immersed in liquid air during the time that the filament was being aged and emission measurements made. The filament was aged according to the schedule given by Taylor and Langmuir.[19] After the filament was flashed five or six times to give a total of one minute at 2900°K, the emission, contrary to expectation, continued to increase slightly upon further flashing at that temperature. However, calculations, based upon the evaporation data given by Jones and Langmuir,[15] showed that this increase in emission could be accounted for entirely by a rise in filament temperature resulting from the passage of the same current through the filament now slightly thinned by evaporation. After aging the filament, the tube and vacuum line were again baked out as before.

After testing the tube to insure that both guard rings were functioning and that there was adequate insulation between them and the plate, emission measurements were made by maintaining a constant filament temperature and applying to the plate in succession the voltages available on the mercury switch S_6 (Fig. 1). At frequent intervals measurements were repeated at previously employed voltage taps in order to test the reproducibility of the emission. Only occasionally (usually following the application of high voltages) did the galvanometer deflection fail to check within one or two tenths of a millimeter a former reading at the same tap. This was thought to be due to the release of an oxidizing gas from the plate under electron bombardment, and a consequent coating of the filament; for, after flashing the filament to 2400 or 2600°K, it was again possible to check former deflections. Since continued flashing at 2400–2600°K did not change the emission, and since the emission would normally remain constant for more than an hour without further flashing of the filament, it was concluded that the surface of the tungsten was clean and that the residual gases in the vacuum were not influencing the emission.

Discussion of Results

Choice of reference line

Many emission isotherms ($\log_{10} i$ *versus* $E^{\frac{1}{2}}$) were obtained for 2-mil, 1-mil, and 0.5-mil tungsten filaments and for a 2-mil tantalum filament, in a number of different experimental tubes. As has been briefly reported previously,[20] these curves were all similar in that the experimental points deviate in a regular manner from a straight line. In order to show this fluctuation more clearly than is possible on a curve of $\log_{10} i$ against $E^{\frac{1}{2}}$, the deviation of the experimental points from a reference line was plotted against $E^{\frac{1}{2}}$. In each case the reference line was obtained by calculating the most probable straight line through the experimental points by the method of least squares. This procedure for selecting a reference line was quite arbitrary,

[19] J. B. Taylor and I. Langmuir, Phys. Rev. **44**, 430 (1933).

[20] R. L. E. Seifert and T. E. Phipps, Phys. Rev. **53**, 493 (1938).

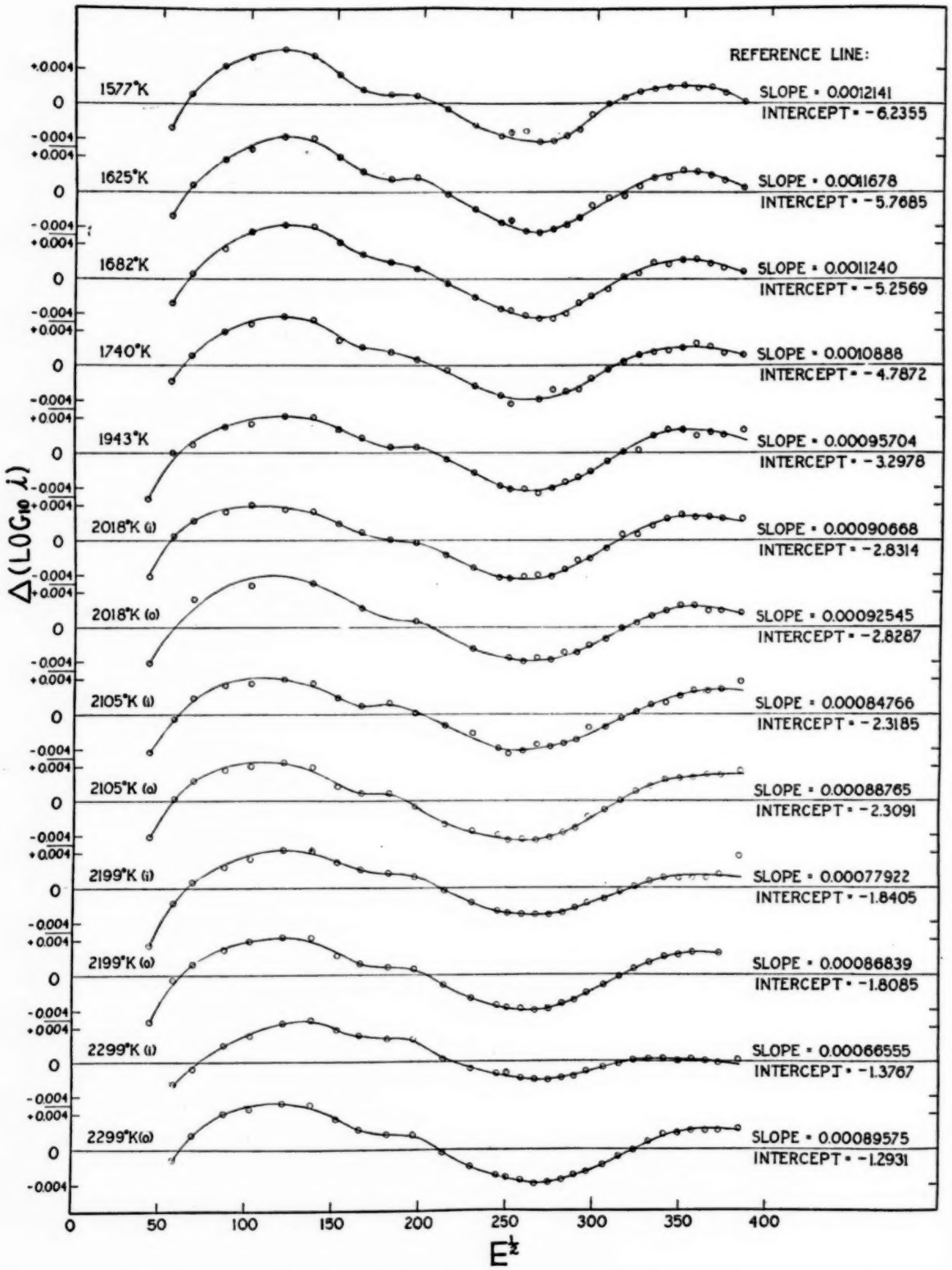

FIG. 2. Δ ($\log_{10} i$), the deviation of the logarithm of the isothermal specific emission current from the reference line indicated, as a function of $E^{\frac{1}{2}}$, the square root of the field (volt$^{\frac{1}{2}}$ cm$^{-\frac{1}{2}}$) at the surface of the emitting tungsten. Data obtained with 2-mil tungsten filament, in thermionic tube 1-D with platinum plates and spiral-spring mounting of filament. The notation T°K(i) indicates that the current input was kept constant at the value calculated for T°K; similarly, T°K(o) designates constant output at the value calculated for T°K. (Only for filament temperatures above 2000°K was the electron emission less for constant input than for constant output.)

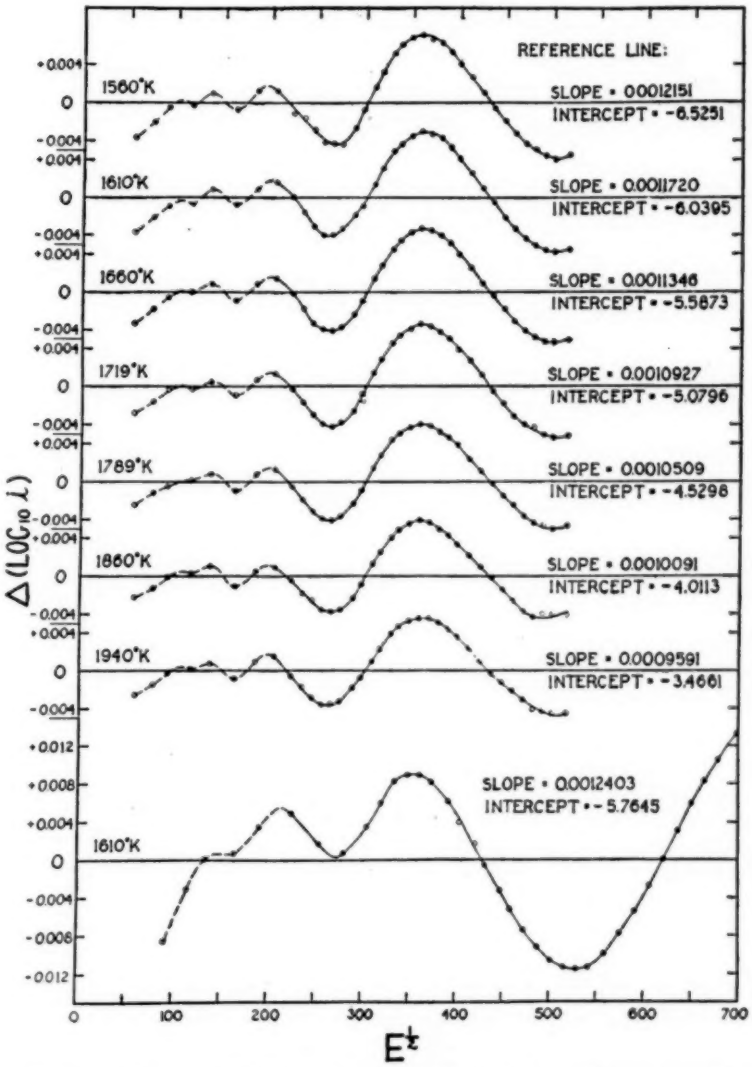

FIG. 3. $\Delta(\log_{10} i)$, deviation of the logarithm of the isothermal specific emission current from the reference line indicated, as a function of $E^{\frac{1}{2}}$, the square root of the field (volt$^{\frac{1}{2}}$ cm$^{-\frac{1}{2}}$) at the surface of the emitting tungsten. The upper seven curves are for a 1-mil tungsten filament. The lowest curve is for an incompletely aged 0.5-mil tungsten filament. Data were obtained with thermionic tube 2-C, with tungsten plates, and with spiral-spring mounting of filaments.

since any curve obtained by a least-squares calculation has significance only if the displacement of points from the resulting curve arises from random errors. In this case, even a casual inspection of a large-scale plot of $\log_{10} i$ against $E^{\frac{1}{2}}$ revealed that the deviation from a straight line was not random but regular and periodic. Nevertheless a least-squares reference line was employed since its intercept on the axis of ordinate is directly comparable with the "zero field" values of $\log_{10} i$ of earlier experimenters, whose usual practice was to extrapolate a least-squares line to zero field.

The resulting deviation curves for some of the filaments are shown in Figs. 2, 3, 4 and 5, in which the deviation is given in the same units as $\log_{10} i$. The values of slope and intercept given to the right of each curve are those calculated by the method of least squares for the reference line that was used in obtaining the deviation curve. It is seen that the heights of the maxima and minima for a given filament decrease slightly

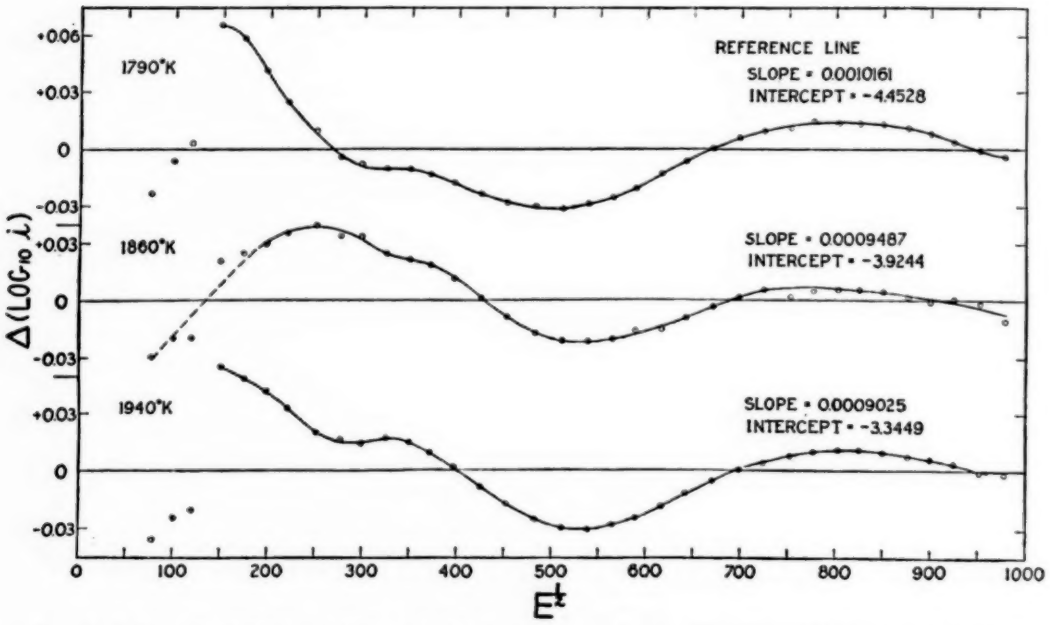

FIG. 4. Δ ($\log_{10} i$), deviation of the logarithm of the isothermal specific emission current from the reference line indicated, as a function of $E^{\frac{1}{2}}$, the square root of the field (volt$^{\frac{1}{2}}$ cm$^{-\frac{1}{2}}$) at the surface of the emitting tungsten. Data obtained with a 0.5-mil tungsten filament, in thermionic tube 3-A, with platinum plates, and with loop-spring mounting of filament.

with increasing temperature, as is best shown by the 1-mil data, Fig. 3, which were obtained with tungsten plates. The steadiness of emission and the reproducibility of the data were even better in this case than with the other filaments.

Experience with 0.5-mil wire

The sets of curves shown for the 2-mil (Fig. 2), 1-mil (Fig. 3), and 0.5-mil (Fig. 4) tungsten have been chosen because each set represents a series of isotherms obtained with the same filament and tube. The tungsten plates which were used for obtaining emission data with 1-mil filaments permitted even better vacuum conditions than had been obtained with the platinum plates used with the 2-mil filaments. It was observed, however, that the tungsten plates pitted badly under high voltage electron bombardment. Since a higher range of plate voltages was available at the time when the 0.5-mil data were obtained, platinum plates were again used.

The 0.5-mil filaments, when mounted with spiral springs, invariably burned out before the aging had been completed. The 0.5-mil curve which is included in Fig. 3 was accordingly taken after only a partial aging, namely, after 3 hours at 2400°K. In this case the emission at representative voltage taps was then observed after short intervals of further aging. The following behavior was observed. An additional 7 hours aging at 2400°K decreased the emission to 97.5 percent of the value observed after 3 hours. One hour at 2600°K increased the emission to approximately 100 percent, and also increased the effect of applied voltage upon emission above that which was observed after the initial aging. Thus, after the one hour of aging at 2600°K the emission current at the lowest plate voltage was 0.4 percent less and at the highest plate voltage 0.6 percent greater than it had been after the initial three hours of aging at 2400°K. Despite these confusing results of aging which shifted the position of the emission curve along the $\log_{10} i$ axis, the positions and magnitudes of the deviations from a straight line did not change. The 0.5-mil data shown in Fig. 4 were obtained when using a semi-circular loop spring to mount the filament. This permitted complete aging of the filament without its burning out.

Variation of experimental conditions

In addition to using different plate material in a number of tubes, the following variations were also made. During the course of the work two

different electrical circuits were used, which were mounted in different positions in the laboratory. In these two circuits the instruments were placed in different relative positions, the wiring diagram remaining essentially the same. The "*B*" batteries were wired in a different order in the two circuits, and voltage taps of different value were used as the total available voltage was increased. The same galvanometer was used in each case; however, the respective scale distances were approximately 8 meters and 5 meters, so that the angular deflection of the galvanometer coil to produce a given reading was different in the two cases. Different sections of the scale were used for making emission measurements over the same range of applied voltages, in order to insure against errors due to non-uniformity of the scale or to its position. These variations in the experimental conditions had no effect upon the deviation curves. This was taken to indicate that the periodic deviations do not arise from experimental defect, but are to be regarded as a property of the emitting surface. Since the deviation curves for aged tantalum (Fig. 5) and for incompletely aged tungsten (bottom curve, Fig. 3) are identical with those of aged tungsten in respect both to position of the deviations along the E axis and to their magnitude, it follows that the effect is independent of both the state and the nature of the metal surface, as is the Schottky effect itself. At considerably higher fields, for which the "characteristic distance" of the Schottky theory is of the order of a few angstrom units only, it cannot be assumed that the periodic deviations will continue to be independent of the nature of the surface.

Variation in the shape of the deviation curves

Similarity between the deviation curves obtained for the different sizes of filaments is obscured somewhat by the fact that the method of least squares is not applicable for obtaining comparable reference lines, since both the slope and the intercept of such lines depend upon the range of field values used and upon the distribution of the experimental points along the $E^{\frac{1}{2}}$ axis. This comes from the fact, already mentioned, that the experimental points do not deviate from a straight line in accordance with a statistical distribution of error, but rather in accordance with the small, though definite, periodic deviation here revealed. The fact that the deviation curves for the 1-mil filaments (Fig. 3) appear to lie fairly symmetrically about the calculated reference line is considered to be the result of a fortuitous termination of the experimental curve at a point which favored symmetry about the least-squares line. Whether or not it is desirable to choose a line of symmetry as reference line will depend upon the theoretical significance to be given to the deviation. A line with the Schottky slope and an empirically adjusted intercept has been employed on

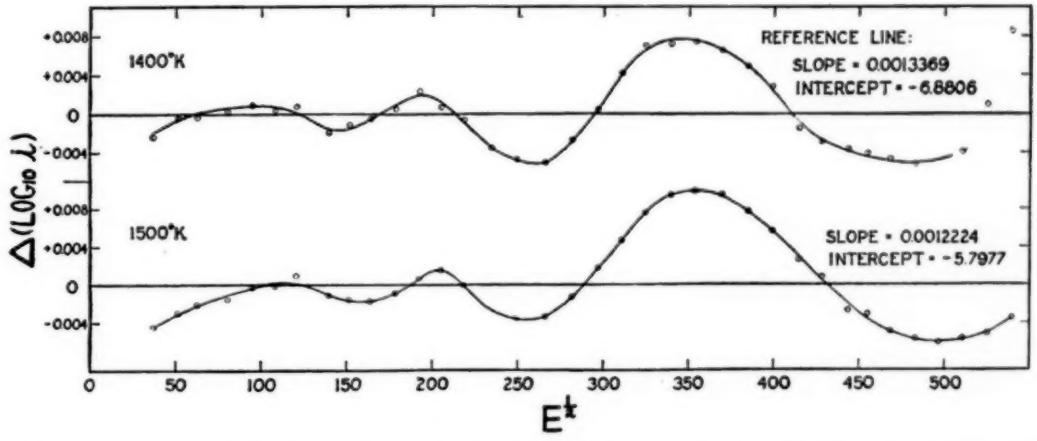

FIG. 5. Δ ($\log_{10} i$), deviation of the logarithm of the isothermal specific emission current from the reference line indicated, as a function of $E^{\frac{1}{2}}$, the square root of the field (volt$^{\frac{1}{2}}$ cm$^{-\frac{1}{2}}$), at the surface of the emitting tantalum. Data were obtained with a 2-mil tantalum filament, in thermionic tube 3-A, with platinum plates, and with spiral-spring mounting of filament.

occasion as a reference line. The deviation curves with respect to such a line were very similar to those in the figures except that the deviations were negative, with the result that the deviation curve showed a downward trend from the horizontal reference line with increasing field. A Schottky line may nevertheless be a line of symmetry, since an ill-chosen value for the electronic charge or an error in temperature inherent in the temperature scale adopted (or both causes together) may have led to an incorrect value for the Schottky slope and consequently to a deviation curve unsymmetrical with respect to a line of that slope.

The calculation of work function

In determining the work function of a metal at zero applied field, use has frequently been made of the emission at zero field as obtained by a linear extrapolation of the $\log_{10} i - E^{\frac{1}{2}}$ line to the axis of ordinate. Since deviations from exact linearity do exist and since these deviations increase in magnitude with increasing field, the resulting value at zero field will depend upon the experimental range of applied field from which the extrapolation is made, as well as upon the distribution of the experimental points within the range of field under consideration. Thus, for example, if the work function, ϕ, of tungsten is calculated from the Richardson equation, $i_0 = AT^2 \exp[-\varphi\epsilon/kT]$, using the values of zero field emission found by linear extrapolation of a least-squares line involving all points of the isotherms shown in Fig. 2, the resulting value of ϕ is different from that obtained if only a portion of the experimental data is used in the calculation of $\log_{10} i$. Table I gives the slope and intercept of each of the least-squares straight lines obtained for the entire 1577°K isotherm and for two segments of it. The values of ϕ given in Table I

TABLE I. *Thermionic emission data for tungsten.*

Range of field, volt cm^{-1}	2500 to 150,000	70,000 to 115,000	115,000 to 150,000
Slope of isotherm, 1577°K	0.0012141	0.0013201	0.0011609
Intercept of 1577°K isotherm	−6.2355	−6.2702	−6.2161
Work function, electron volt	4.556	4.567	4.539

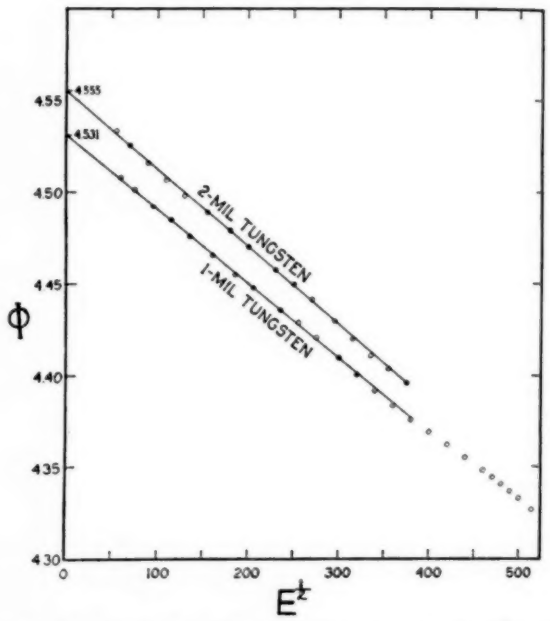

FIG. 6. The work function ϕ (electron volt) of tungsten as a function of $E^{\frac{1}{2}}$, the square root of the field (volt$^{\frac{1}{2}}$ cm$^{-\frac{1}{2}}$) at the surface of the tungsten.

are calculated* from the values of i_0 obtained by extrapolation of the other isotherms in Fig. 2 over the same ranges of applied field. If ϕ is calculated from data taken throughout a still higher range of applied fields, the results may be expected to vary by even a larger amount owing to the larger deviations from the Schottky line at higher fields.

Discussion of errors

From the smoothed deviation curves it is possible to calculate the actual emission at the same applied field for all filament temperatures, and therefrom to obtain the values of ϕ and A at that applied field for the filament under consideration. The resulting values of ϕ and A as a function of $E^{\frac{1}{2}}$ are shown in Figs. 6 and 7 for the 2-mil and 1-mil data of Figs. 2 and 3. These values of ϕ and A for each value of $E^{\frac{1}{2}}$ were calculated from the slope and intercept of the least-squares straight line through the points on a Richardson plot for that value of $E^{\frac{1}{2}}$. From the residuals of the ordinates it was possible to

* In the calculation of the values of ϕ given in this paper the charge on the electron was taken as 4.774×10^{-10} e.s.u. For filament temperatures above 2000°K use was made of the average value of $\log_{10} i$ as obtained from the two curves, one for constant filament input and the other for constant output. (See legend under Fig. 2.)

calculate the probable error in each of the values of ϕ and A. The maximum values found for the probable errors of ϕ and A, considering all values of $E^{\frac{1}{2}}$, were 0.0029 e.v. and 1.01 amp. cm^{-2} $deg.^{-2}$, respectively. The probable errors calculated for most of the points shown were considerably less than this. These calculated probable errors take account of experimental errors in the determination of the galvanometer sensitivity at each shunt value, and also of experimental errors in the determination of the "Jones-Langmuir temperature"; but they do not take account of inherent errors in the determination of the absolute magnitude of either quantity. For this reason the actual uncertainty in the values of ϕ and A is much greater than would be indicated by the small probable errors, though this additional error is the same for all the values of ϕ and A.

In addition to the errors just mentioned there is another source of error in the determination of the filament temperature; namely, that the filament is mounted at the center of a reflecting metallic plate held at the temperature of liquid air, whereas the current-diameter-temperature function[15] was determined with the filament surrounded by clear glass walls at room temperature. To determine the order of magnitude of the error thus introduced, measurements were made of the potential drop across the central 2-cm section of a 12-cm length of 2-mil tungsten filament, both when mounted at the center of a tungstenized glass tube and when mounted at the center of a clear glass tube, the filament current being maintained at the same set of values in each case. These measurements were made at seven different filament temperatures in the range 1600–1940°K. When mounted at the center of the tungstenized tube the resistance of the filament was found in each case to be 0.6 ($\pm$0.02) percent greater than when mounted in a clear glass tube. The possible effects of different plates, different sizes of filament, and exact positions of mounting were not determined. This constant error in T would give rise to the same percent error in ϕ and to twice as great a percent error in A. This "plate reflectivity" error in temperature may account for the discrepancy of 0.51 percent in the work function (shown in Fig. 6) between results obtained with platinum and with tungsten plates. Such a constant error in T is not as serious as a variable error would be; for the latter may lead to relatively large errors in ϕ and in A, particularly if the temperature range is short, and the number of filament temperatures employed is small.

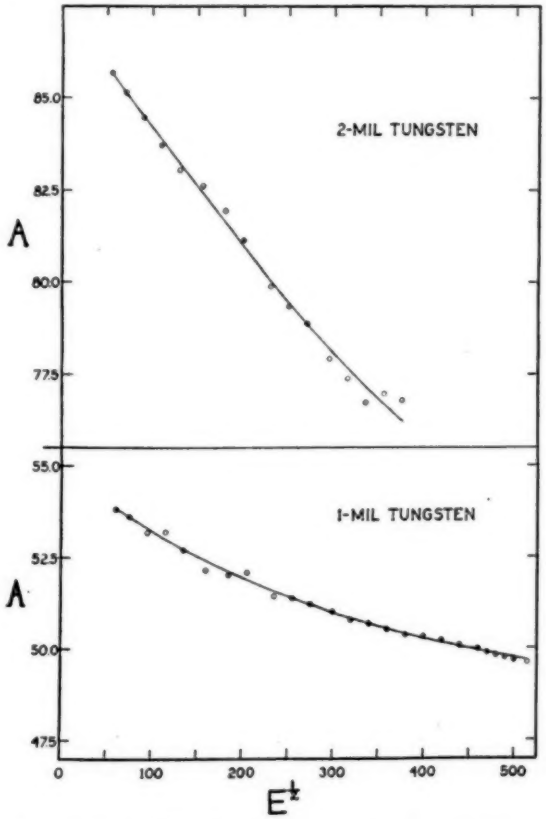

FIG. 7. The Richardson constant A for tungsten as a function of $E^{\frac{1}{2}}$, the square root of the field (volt$^{\frac{1}{2}}$ $cm^{-\frac{1}{2}}$) at the surface of the tungsten.

The effect of field upon work function

While the absolute values of ϕ here calculated are in error due to the causes mentioned above, the percent error is constant in all the values of ϕ on a ϕ *versus* $E^{\frac{1}{2}}$ plot, such as the two shown in Fig. 6. In these curves, then, we may observe the effect of the applied field upon the Richardson work function, ϕ. In Fig. 6 "zero field" work functions have been found by extrapolating the least-squares straight line calculated for the experimental points in the range of $E^{\frac{1}{2}}$ from 60 to 380 volt$^{\frac{1}{2}}$ $cm^{-\frac{1}{2}}$. (In spite of the small scale of the plot in Fig. 6 the periodic deviations from these lines can be observed; these deviations are magnified in Fig. 8.) The slope of the line, ϕ

versus $E^{\frac{1}{2}}$, should be, according to the Schottky theory, $-(299.9\epsilon)^{\frac{1}{2}}$ for the units employed here. The experimental values of the slopes determined from the 2-mil and the 1-mil data, respectively, are -4.246×10^{-4} and -4.073×10^{-4} volt$^{\frac{1}{2}}$ electron cm$^{\frac{1}{2}}$. Even if the recently suggested[21] larger value of ϵ, 4.8029×10^{-10} e.s.u. were used in all the calculations, the theoretical Schottky slope would be only 3.795×10^{-4} volt$^{\frac{1}{2}}$ electron cm$^{\frac{1}{2}}$, which is 10 percent less than the experimental value would be for the 2-mil data and 6 percent less than that from the 1-mil data. This discrepancy may rise from two obvious sources (other than that which comes from uncertainty in the value of ϵ); namely, from error in the factor converting applied plate voltage to effective field at the surface of the emitter, and from a constant percent error in the absolute values of ϕ.

Deviation curves for ϕ and A

In order to show more clearly the deviations of ϕ from a linear function of $E^{\frac{1}{2}}$, the line in Fig. 6 for the 1-mil filament was extrapolated to the higher fields and the deviations of ϕ from this line were calculated. The resulting deviation curve is shown in Fig. 8. At low fields, because of the increased percent error in $E^{\frac{1}{2}}$, and because of proximity to "space-charge" conditions, the measurements are less accurate than at high fields. Consequently it cannot be said with certainty whether the deviations in this range are nonexistent or are only being masked by the large errors. In this connection it should be pointed out that the deviation curve is sensitive to errors in $E^{\frac{1}{2}}$, since an error in this quantity shifts a point on the deviation curve both horizontally and vertically from its correct position. Since the values of ϕ and A were calculated from the emission as given by the smoothed deviation curves (Figs. 2 and 3), errors in the position of these deviation curves at low fields resulted in errors in both ϕ and A at the same values of $E^{\frac{1}{2}}$.

It can be seen in Fig. 7 that the experimental values of A lie consistently on a smooth curve[22] only at high values of $E^{\frac{1}{2}}$. In order to obtain a magnified deviation curve it is desirable to have as reference line a simple curve which lies near the experimental points. In order to obtain such a deviation curve for the 1-mil data shown in Fig. 7, the equation $A=54.800-0.01700E^{\frac{1}{2}}+1.400\times10^{-5}E$ was used as a reference curve. The resulting deviation curve (Fig. 8) gives slight evidence that the values of A tend to exhibit maxima and minima at the same values of E at which maxima and minima appear in the emission ($\log_{10} i$ *versus* $E^{\frac{1}{2}}$) curves. However, the

[21] R. T. Birge, Nature **137**, 187 (1936).

[22] The slope of the A *versus* $E^{\frac{1}{2}}$ curve, according to the Schottky theory, is zero.

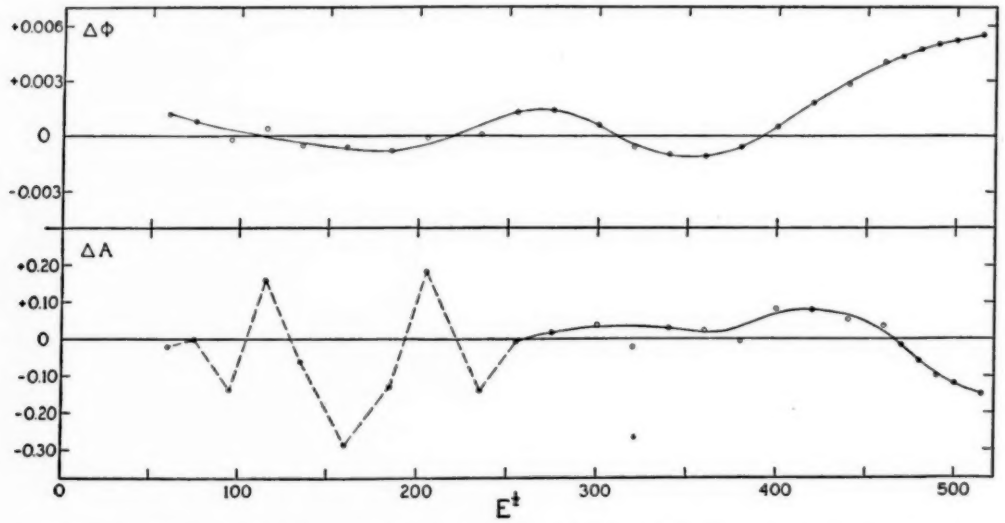

FIG. 8. Top curve: Deviation in electron-volts of ϕ for the 1-mil tungsten (Fig. 6) from the reference line, $\phi=4.531-4.073\times10^{-4}E^{\frac{1}{2}}$. Bottom curve: Deviation in amp. cm^{-2} deg.$^{-2}$ of A for the 1-mil tungsten (Fig. 7) from the reference curve $A=54.800-0.01700E^{\frac{1}{2}}+1.400\times10^{-5}E$.

existence of maxima and minima in the A curve is not as pronounced as in the ϕ curve. The ϕ values show definite maxima and minima at values of $E^{\frac{1}{2}}$ corresponding, respectively, to minima and maxima in the emission curves (compare Figs. 8 and 3). It appears then that the Richardson work function, ϕ, is a periodic function of $E^{\frac{1}{2}}$, which exhibits an increasing amplitude with increasing field. The deviation from a least-squares line is small; the maximum value up to applied fields of the order 250,000 volts cm^{-1} is about 0.1 percent of the value of ϕ. The fact that the Richardson A as well as the Richardson ϕ may be a periodic function of $E^{\frac{1}{2}}$ could be due to the form of the Richardson equation; for, if the work function is not constant, but varies linearly with the temperature, the coefficient of T appears in the experimental constant A.

The periodic deviations from the Schottky line reported above are given theoretical consideration by Dr. H. M. Mott-Smith in an accompanying paper.

OCTOBER 1, 1939 PHYSICAL REVIEW VOLUME 56

Evidence of a Periodic Deviation from the Schottky Line. II

D. TURNBULL AND T. E. PHIPPS
Noyes Chemical Laboratory, University of Illinois, Urbana, Illinois

(Received June 19, 1939)

The periodic deviation from the Schottky line observed by Seifert and Phipps was studied in greater detail for tungsten up to fields of 6.5×10^5 volts cm^{-1}. The deviation continued with increasing period and amplitude up to the highest fields investigated. The characteristic Schottky distance from the surface, x_0, was calculated for all values of the field at which maximal and minimal values of the deviation occurred. The difference between successive x_0 values was of the order 24A between $E^{\frac{1}{2}}=160$ and $E^{\frac{1}{2}}=266$; of the order 17A between $E^{\frac{1}{2}}=266$ and $E^{\frac{1}{2}}=505$; and of the order 12A between $E^{\frac{1}{2}}=505$ and $E^{\frac{1}{2}}=752$. The temperature coefficient of the position of these maximal and minimal values along the $E^{\frac{1}{2}}$ axis, $dE_m^{\frac{1}{2}}/(E_m^{\frac{1}{2}}dT)$, if it exists at all, is less than 5.9×10^{-5} deg.$^{-1}$.

INTRODUCTION

RECENTLY Phipps and Seifert[1] measured the electron emission from clean tungsten as a function of the applied electrical field and found that the Schottky equation,

$$i=i_0 \exp\left[(e^{\frac{1}{2}}E^{\frac{1}{2}})/(kT)\right],$$

in which i_0 is the specific electron current at zero field and E is the electrical field, is valid only as a first approximation. By plotting $\Delta \log_{10} i$, which is the deviation from a reference line calculated by the method of least squares, against $E^{\frac{1}{2}}$ a periodic curve was obtained, whose period and amplitude increased with increasing field. That investigation was extended to fields of 2.6×10^5 volts cm^{-1}. Later work by the same authors[2] indicated that for clean tungsten the periodic behavior continued to fields as high as 9×10^5 volts cm^{-1}, and that the electron current from clean tantalum deviated in the same manner as tungsten, to the highest field investigated, namely, to 2.6×10^5 volts cm^{-1}. The purpose of the present investigation was to determine more accurately the values of $E^{\frac{1}{2}}$ at which the maximal and minimal values of the deviation occur and to make a more careful study of the phenomenon above fields of 2.6×10^5 volts cm^{-1}.

EXPERIMENTAL

The electrical circuit for measuring the electron current and for controlling the temperature of the filament was the same as described by Seifert and Phipps.[2] The Jones-Langmuir[3] temperature scale for tungsten was employed in the previous work.[2] In the present investigation a correction was made for the fact, observed by Seifert and

[1] T. E. Phipps and R. L. E. Seifert, Phys. Rev. **53**, 493 (1938).
[2] R. L. E. Seifert and T. E. Phipps, Phys. Rev., preceding paper.
[3] H. A. Jones and I. Langmuir, Gen. Elec. Rev. **30**, 310 (1927).

Phipps, that the resistance of the filament was 0.6 percent higher when it was mounted at the center of a reflecting metallic plate than when it was mounted in a clear glass tube. At 1700°K this correction was of the order 10°K.

The thermionic tube used in this work has been described by Clemens and Phipps.[4] Tension was supplied to the filament by means of a loop spring previously described.[2] For part of the investigation a tungsten filament (General Electric, Lot No. 218) 0.002534 cm in diameter was used. For the rest of the work tungsten of very high purity, 0.001288 cm in diameter, was used. This wire was furnished by the Incandescent Lamp Department of the General Electric Company, Cleveland Wire Works Division, through the courtesy of Messers B. L. Benbow and A. Poritsky. It was stated[5] that this sample contains 0.008 percent molybdenum and possibly also impurities of low work function in spectroscopic amounts. The method of determining the diameter has been described.[2]

Results

The deviation $\Delta \log_{10} i$ from a straight line was calculated by Seifert and Phipps[2] by using a reference line of which the slope and intercept were calculated by the method of least squares. The slopes so obtained depended, however, upon the values of $E^{\frac{1}{2}}$ at which the series was terminated and for this reason it was difficult to compare different sets of data which were terminated at different values of $E^{\frac{1}{2}}$. In the present investigation $\Delta \log_{10} i$ was calculated from the equation,

$$\Delta \log_{10} i = \log_{10} i - \log_{10} i_0 - ME^{\frac{1}{2}}.$$

The slope of the reference line, M, was the Schottky slope, calculated from the equation,

$$M = e^{\frac{1}{2}}/(kT).$$

Since varying the intercept of the Schottky line, $\log_{10} i_0$, resulted only in raising or lowering the Schottky line parallel to itself, arbitrary intercepts were used throughout this investigation. The characteristic Schottky distance, x_0, at which the maximal and minimal values of the deviation occur was calculated from the Schottky theory by the equation,

$$x_0 = e^{\frac{1}{2}}/(2E^{\frac{1}{2}}).$$

With the substitutions, $e = 4.8029 \times 10^{-10}$ e.s.u.,[6]

TABLE I. *The positions along the $E^{\frac{1}{2}}$ axis at which maximal and minimal values of the deviation from the Schottky line occur, with the corresponding Schottky distance, x_0, from the surface.*

	$E^{1/2}$	δ	x_0	Δx_0	$x_0^{3/4}$	$\Delta(x_0^{3/4})$
min.	110±2		172.5±3.0		47.6±0.8	
		0.01±0.01		26.5±5.2		5.6±1.4
max.	130±2		146.0±2.2		42.0±0.6	
		0.09±0.02		27.4±3.6		6.1±1.0
min.	160±2		118.6±1.4		35.9±0.4	
		0.15±0.03		23.7±2.3		4.8±0.7
max.	200±2		94.9±0.9		31.1±0.3	
		0.18±0.04		23.5±1.5		6.5±0.5
min.	266±1.5		71.4±0.6		24.6±0.2	
		0.23±0.03		16.9±1.0		4.6±0.4
max.	348±3		54.5±0.4		20.0±0.2	
		0.48±0.02		16.9±0.7		4.8±0.3
min.	505±4		37.6±0.3		15.2±0.1	
		0.77±0.02		12.4±0.5		4.0±0.2
max.	752±6		25.2±0.2		11.2±0.1	

[4] J. E. Clemens and T. E. Phipps, Rev. Sci. Inst. **8**, 133 (1937).

[5] Private communication from Mr. A. Poritsky to T. E. Phipps.

[6] R. T. Birge, Nature **137**, 187 (1936).

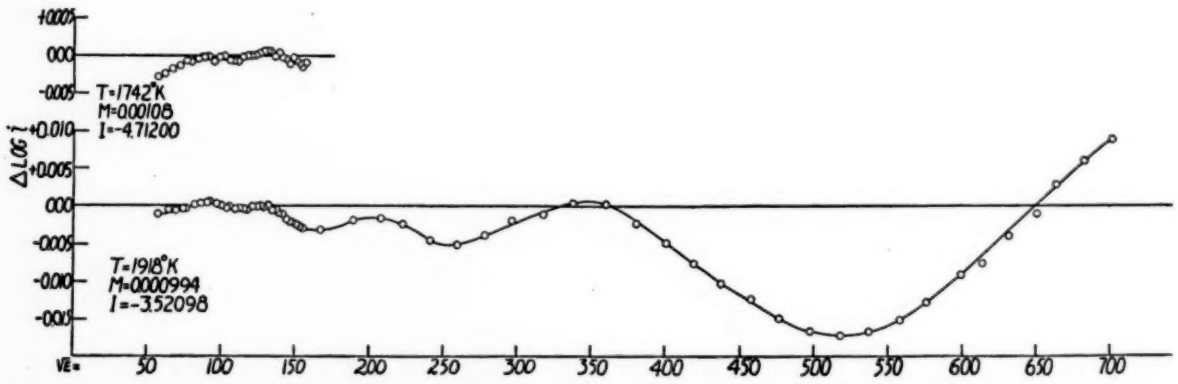

FIG. 1. Data for tungsten of diameter 0.002534 cm, showing detail at fields below $E^{\frac{1}{2}} = 155$ volts$^{\frac{1}{2}}$ cm$^{-\frac{1}{2}}$ for two temperatures. Ordinate: deviation of the logarithm of the specific emission from a line having the Schottky slope M and an arbitrary intercept I, as indicated. Abscissa: square root of the field at the surface of the emitter.

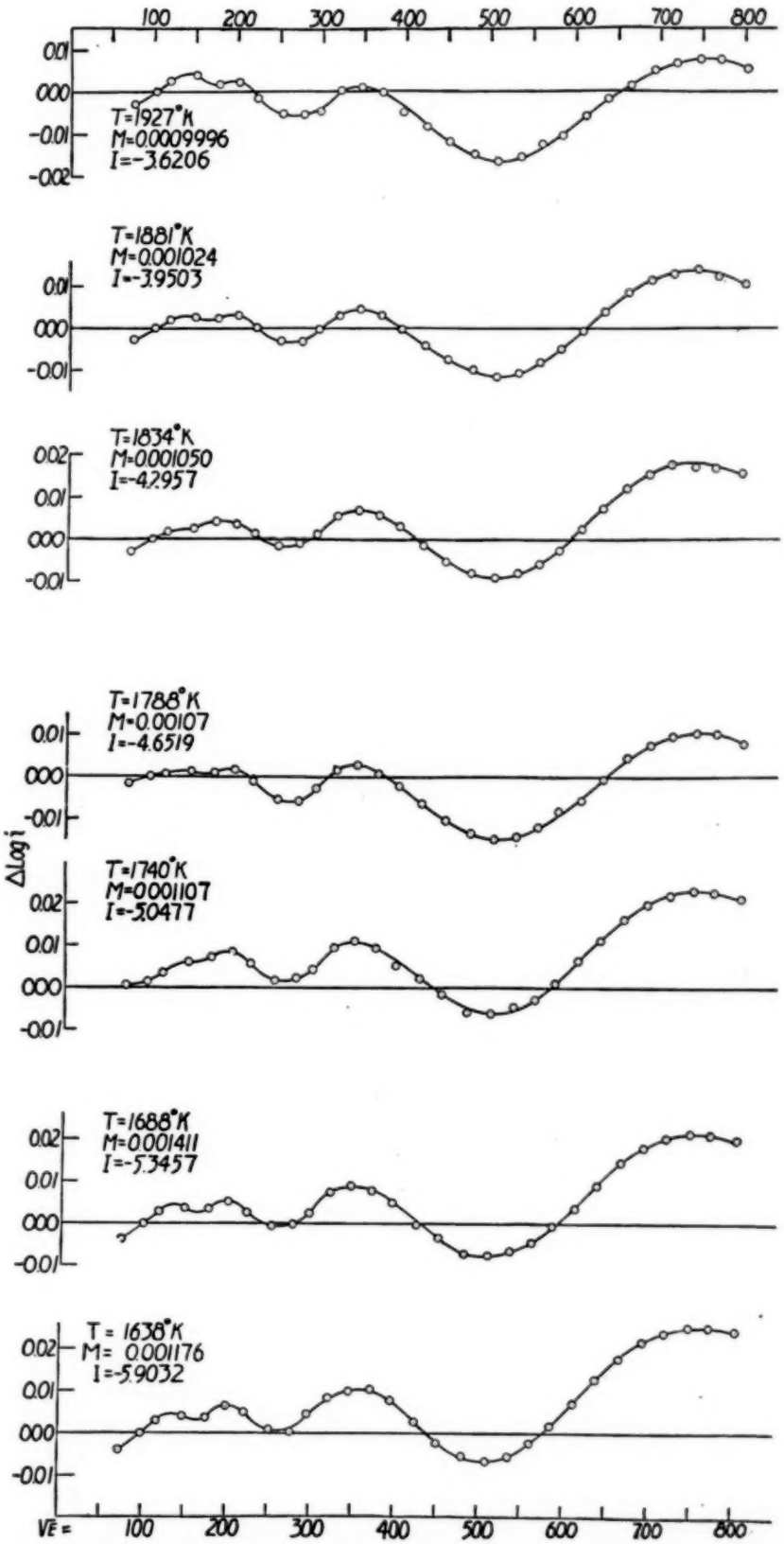

FIG. 2. Data for tungsten of diameter 0.001288 cm, up to fields of 6.5×10^5 volts cm^{-1} at seven temperatures. Ordinate: deviation of the logarithm of the specific emission from a line having the Schottky slope M and an arbitrary intercept I, as indicated. Abscissa: square root of the field at the surface of the emitter.

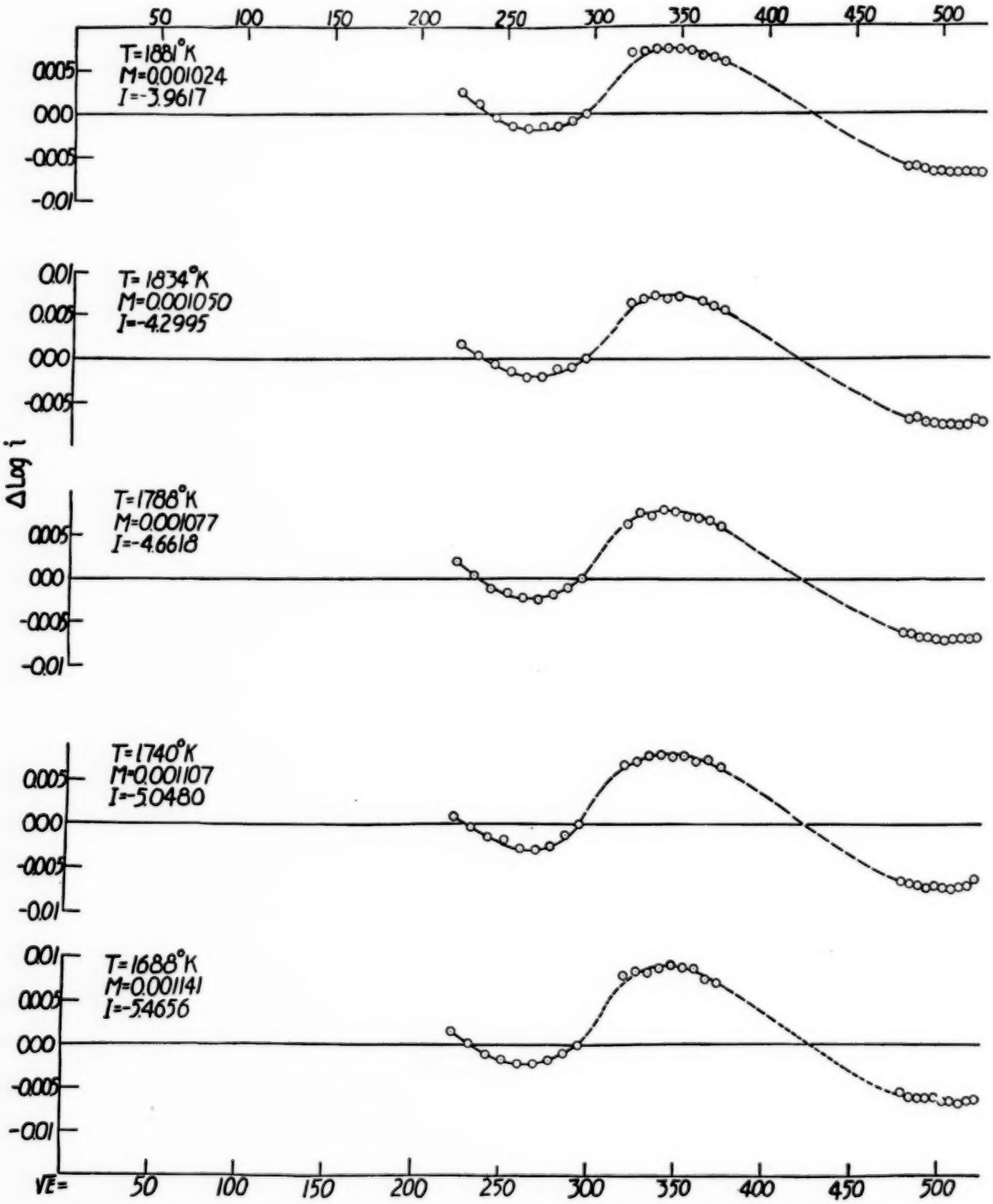

FIG. 3. Data for tungsten of diameter 0.001288 cm, showing greater detail in the region of the maximal and minimal values of the deviation, at five temperatures. Ordinate: deviation of the logarithm of the specific emission from a line having the Schottky slope M and an arbitrary intercept I, as indicated. Abscissa: square root of the field at the surface of the emitter.

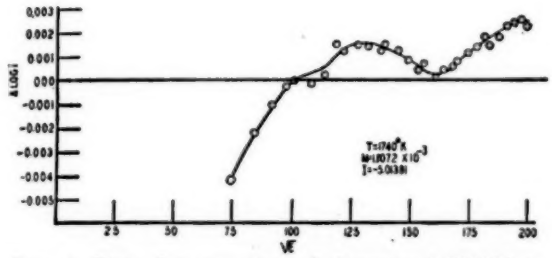

FIG. 4. Data for tungsten of diameter 0.001288 cm, showing greater details below $E^{\frac{1}{2}}=200$ volts$^{\frac{1}{2}}$ cm$^{-\frac{1}{2}}$ for one temperature. Ordinate: deviation of the logarithm of the specific emission from a line having the Schottky slope M and an arbitrary intercept I, as indicated. Abscissa: square root of the field at the surface of the emitter.

299.9 int. volt = 1 e.s.v., and 10^8A = 1 cm, x_0 is found in Angstrom units from the equation,

$$x_0=(1.898\times10^4)/E^{\frac{1}{2}},$$

in which E is given in int. volt cm^{-1}. The percent deviation from the Schottky line, δ (Table I, column 3), is defined as the absolute value of the quantity obtained by subtracting the percent deviation at a given maximum or minimum from the percent deviation of the minimum or maximum immediately preceding it. The error in δ (Table I, column 3), $d\delta$, was calculated from the formula,

$$d\delta=\pm\partial\log_{10}D_g\pm(Mq\partial V)/(2E^{\frac{1}{2}}),$$

in which D_g is the galvanometer deflection, q is the conversion factor from applied voltage to field at the surface of the emitter, and V is the applied voltage. There are errors in the determination of q and M, but since these quantities remain constant throughout the course of a given experiment their errors will not change the relative positions of the points on the deviation curve. In calculating $d\delta$, it was assumed that ∂V was ±0.0005 V and $\partial D_g=\pm0.2$ mm.

The results are shown graphically in Figs. 1, 2, 3 and 4 in which $\Delta\log_{10}i$ was plotted against $E^{\frac{1}{2}}$ and in which $\log_{10}i_0$ was replaced by the symbol I. Fig. 1 shows the results for tungsten 0.002534 cm in diameter, to fields of 5×10^5 volts cm^{-1}. The points are grouped very closely below $E^{\frac{1}{2}}=155$ in order to determine the detail of the curve more accurately than had been done previously in this region, where the deviation is small. Fig. 2 shows the results for tungsten wire of very high purity, 0.001288 cm in diameter, up to fields of 6.5×10^5 volts cm^{-1}, for seven temperatures between 1638°K and 1927°K. Fig. 3 shows the results for the same tungsten wire with the points grouped very closely in the region of the maximal and minimal values of the deviation, in order to determine more accurately the values of $E^{\frac{1}{2}}$ at which they occur. Fig. 4 shows the results for this wire with the points grouped closely below $E^{\frac{1}{2}}=200$.

Table I, column 2, shows the most probable values of $E^{\frac{1}{2}}$ at which the maximal and minimal values of the deviation occur, together with the probable errors in their determination. These values were obtained by assuming that there was no temperature dependence of the positions of the maximal and minimal values along the $E^{\frac{1}{2}}$ axis and by giving weight to the determinations in which the greatest number of experimental points were grouped in the region about the minimum or maximum value. The Δx_0 values (Table I, column 5) were found by subtracting from a given x_0 value the one just preceding it in the table. The significance of the Δx_0 values and $\Delta(x_0^{\frac{1}{2}})$ values are discussed in an accompanying note by H. M. Mott-Smith.[7] The percent deviation, δ (Table I, column 3), for $E^{\frac{1}{2}}\leqq160$ was calculated from data taken at 1918°K (Fig. 1); for $E^{\frac{1}{2}}\geqq200$ it was calculated from data taken at 1881°K (Fig. 2). These data show that the amplitude of the deviation and its period increase with increasing field up to 5.65×10^5 volts cm^{-1}. The difference between successive x_0 values are of the order of 24A between $E^{\frac{1}{2}}=160$ and $E^{\frac{1}{2}}=266$; of the order of 17A between $E^{\frac{1}{2}}=266$ and $E^{\frac{1}{2}}=505$; and of the order of 12A between $E^{\frac{1}{2}}=505$ and $E^{\frac{1}{2}}=752$. No marked difference was observed in the thermionic behavior of well-aged commercial tungsten wire and tungsten wire of very high purity.

The magnitude of the percent deviation, δ, increases with temperature. At 1638°K, the lowest temperature employed, the value of δ between $E^{\frac{1}{2}}_{\min}=505$ and $E^{\frac{1}{2}}_{\max}=752$ is 0.63 ± 0.02 percent; and at 1927°K, the highest temperature employed, it is 0.81 ± 0.02 percent. The position of the minimum occurring at $E^{\frac{1}{2}}=266$ was reproduced within ±1.5 volts$^{\frac{1}{2}}$ cm$^{-\frac{1}{2}}$ for temperatures from 1688°K to 1881°K. From this we may conclude that the temperature coefficient of the position of the maximum or minimum along the $E^{\frac{1}{2}}$ axis, defined as $dE_m^{\frac{1}{2}}/(E_m^{\frac{1}{2}}dT)$, is equal to or less than 6×10^{-5} deg.$^{-1}$.

[7] H. M. Mott-Smith, Phys. Rev., this issue.

The Periodic Deviation from the Schottky Line

H. M. MOTT-SMITH
Department of Physics, University of Illinois, Urbana, Illinois

(Received June 19, 1939)

The width of the potential hump traversed by thermions moving between parallel plates depends upon the strength E of the external field at the cathode. Partial reflection at this hump, analogous to the partial reflection of light passing through a thin plate, may account for the small deviations from the Schottky line, depending in a periodic manner on $\sqrt{E}$, observed by Phipps, Seifert and Turnbull. A calculation based on this analogy shows rough agreement between the theory and the data. An approximate solution of the wave equation yields a small term of suitable period, but to start the theory, one needs a really accurate solution probably best obtained by mechanical integration.

THE explanation which suggests itself for the results described in the preceding papers is partial reflection of the emitted electrons at the potential barrier formed by the combination of the Schottky image force with the external field. This potential $V(x)=-e^2/4x-eEx$ (E=field strength at cathode surface, x=distance from this surface) has a maximum at $x=x_0=(e/4E)^{\frac{1}{2}}$, and the parameter x_0 also fixes the scale of length for the potential distribution; so that, e.g., the distance between two points where the potential is V_0 less than the maximum varies as $x_0^{\frac{1}{2}}$ when V_0 is small. Considering the optical analogy we see that for electrons tunneling through the barrier the transmission coefficient D varies monotonically with electron energy and some arbitrarily defined width of the barrier, which will depend on E. But for electrons passing over the peak, D may be a fluctuating function of the energy and of E, because of interference between the partial waves scattered from the two sides of the barrier. For instance, if we compare the barrier with a uniform plate of thickness, t, D will pass from a maximum to a minimum or vice versa when t changes by a quarter wave-length. The thickness t must depend on the parameter x_0 because x_0 determines the scale of lengths, and for simplicity we may begin by assuming $t=x_0$. On this picture the maxima and minima in the curve of deviations from the Schottky line should correspond to values of x_0 equally spaced by the amount $\lambda/4$ where λ is some average wave-length for electrons with a Maxwellian velocity distribution with the temperature T of the cathode. From column 4, Table I of the preceding paper[1] one can see that the differences Δx_0 actually are roughly constant, though there is a decided trend to lower values as x_0 itself decreases. There is some indication that the equivalent plate thickness t varies approximately as $x_0^{3/4}$. This is shown by columns 6 and 7 of the same table.

Dr. D. Turnbull has kindly prepared the following table for me based on the combined results of his own experimental work and that of Seifert and Phipps.[2] It is seen to be substantially in agreement with the table mentioned above. Taking λ to correspond to the electron energy kT, the range of λ was from 42 to 47A for the different temperatures used. In agreement with the above theory, Seifert and Phipps[2] found that the positions of the maxima and minima were the same for a tantalum cathode as for tungsten. There was no observable dependence upon cathode temperature, but this may be due to the relatively small temperature range of the experiments.

When x_0 is several times λ there will be several maxima of D in that part of the Maxwellian distribution that makes an appreciable contribution to the current, and consequently the fluctuations of the average of D over the Maxwellian distribution will be less than those of D itself. We should get the greatest fluctuations when x_0 is of the order of λ, so that the amplitude of the fluctuations should increase from right to left in Table I. This is the case, the increase in amplitude being very marked.

[1] D. Turnbull and T. E. Phipps, Phys. Rev., this issue.
[2] R. L. E. Seifert and T. E. Phipps, Phys. Rev., this issue.

TABLE I. *Values of x_0 and Δx_0. The maxima are set in bold face type. The probable errors of the values in the first row range from ±0.3 at the left to ±3 A at the right.*

x_0 (A)	**25.5**	38	**54**	72.5	**95.5**	117.5	**139**	164
Δx_0	12.5	16	18.5	23	22	21.5	25	
$x_0^{2/3}$	11.5	15.2	19.9	24.7	30.5	35.6	40.4	45.8
$\Delta(x_0^{2/3})$	3.7	4.7	4.8	5.8	5.1	4.8	5.4	

To formulate the theory quantitatively it is necessary to obtain an accurate solution of the wave equation. The W.B.K. first approximation will not serve, since it is just the one which starts by neglecting diffraction effects, and so always gives a nonfluctuating D. To begin with we may replace $V(x)$ by a parabolic potential function. The exact solution can then be obtained in terms of the parabolic-cylinder function but it turns out that in this case D has no fluctuations even for positive electron kinetic energies. It is interesting that here the W.B.K. method gives exactly the same result. This is the counterpart of the fact that for a harmonic oscillator the W.B.K. approximation gives the correct energy levels. As a better approximation we may try using a combination of a parabola with a straight line of slope $-eE$. D is then expressible in a series of which one small term is periodic in $2x_0/\lambda$, indicating that the above x_0 differences should be $\lambda/2$, which is seen to be roughly verified by the table. However, the neglected terms may cancel this result. To settle the question as to whether D really does have fluctuations it would probably be necessary to resort to a numerical or mechanical solution of the wave equation.

OCTOBER 1, 1939 PHYSICAL REVIEW VOLUME 56

Zeeman Effect in the Hyperfine Structure of Iodine. II

ARTHUR S. FRY* AND RUSSELL A. FISHER
Northwestern University, Evanston, Illinois

(Received August 14, 1939)

Observations of the Zeeman effect in the hyperfine structure of iodine II lines at fields of 4000 to 16,000 gauss provide an independent confirmation of the value $2\frac{1}{2}$ units as the spin of the iodine nucleus. The patterns observed in intermediate fields have been interpreted with the help of the theory of Goudsmit and Bacher. Evidence of a nuclear quadrupole interaction is detected in some Zeeman patterns.

THE hyperfine structure of iodine I and II has been investigated exhaustively by Tolansky,[1,4] Tolansky and Forrester,[2] and Murakawa.[3] However, these extensive measurements do not yield directly a conclusive value for the nuclear spin because the interval rule is not obeyed. The departures from the interval rule are only in part attributable to ordinary perturbations. By introducing a nuclear quadrupole and finally octopole moment, Tolansky and Forrester[2] and Tolansky[4] have been able to interpret observed intervals as arising from a spin of $2\frac{1}{2}$ units.

As an alternative approach to determination of the nuclear spin we have studied the Zeeman effect in the hyperfine structure of certain lines of iodine II. Since the magnetic fields attainable in our work were insufficient to produce the Back-Goudsmit effect in the wider hypermultiplets of iodine II we have had to deal with the more complex situation of hyperfine Zeeman effect in intermediate fields. The theory of hyperfine Zeeman effect in intermediate fields as developed by Goudsmit and Bacher[5] has been applied in

* Now with Research Laboratories Division, General Motors Corporation, Detroit, Michigan.

[1] S. Tolansky, Nature **127**, 855 (1931); Proc. Roy. Soc. **136**, 585 (1932); **A149**, 269 (1935); **A152**, 663 (1935); Proc. Phys. Soc. London **48**, 49 (1936).

[2] S. Tolansky and G. O. Forrester, Proc. Roy. Soc. **A168**, 78 (1938).

[3] K. Murakawa, Inst. Phys. and Chem. Res., Tokyo **420**, 285 (1933); Zeits. f. Physik **109**, 162 (1938).

[4] S. Tolansky, Proc. Roy. Soc. **A170**, 205 (1939).

[5] S. Goudsmit and R. F. Bacher, Zeits. f. Physik **66**, 13 (1930).

analysis of the patterns observed and incidentally subjected to a rather extensive experimental test.

The light source employed, which is a modified form of Schüler's metal hollow cathode discharge tube is described in detail elsewhere.[6] In this work on iodine it was necessary to use a cathode of tungsten and anode of molybdenum in order to avoid the formation of troublesome iodine compounds. Helium at approximately 6 mm pressure was used as the exciting gas. The iodine was introduced simply by placing a few crystals inside the anode cylinder. No measures for purifying the gas were necessary in this work because the iodine itself when excited in the discharge served as a most effective getter, the discharge becoming perfectly clean after one minute's operation. Discharge currents of less than 100 milliamperes were ordinarily employed.

A water-cooled Weiss electromagnet having 576 turns and fitted with truncated conical pole pieces produced fields up to 16,100 gauss with a maximum exciting current of 65 amperes and pole separation of 17 mm. Field strengths were measured from the simple Zeeman triplet of the iodine line λ4986.9 whose hyperfine structure is so narrow as to be practically negligible.

The patterns were resolved by means of a ruled Fabry-Perot interferometer[7] having a resolving power of approximately 25 times the order crossed with a glass prism spectrograph. A Rochon prism was used to separate the π from the σ components in the patterns. Since the pattern of π components is always simpler and more readily resolved in these structures, only the π components were carefully studied and measured.

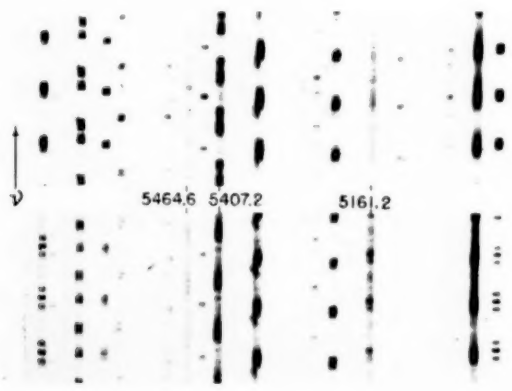

FIG. 1. Enlarged reproductions of spectrograms taken with 5.3 mm interferometer spacer showing π components in hyperfine Zeeman patterns of iodine; above at 4900 gauss, below at 9200 gauss.

[6] R. A. Fisher and A. S. Fry, following paper.
[7] R. C. Machler and R. A. Fisher, J. Opt. Soc. Am. **25**, 315 (1935).

Spectrograms were taken at a number of fields ranging from about 4000 to 16,000 gauss. Interferometer spacers of from 3.7 to 10 mm were used depending upon the field and the width of the pattern to be resolved. Fig. 1 is a reproduction of typical spectrograms taken at 4900 and 9200 gauss with a spacer of 5.3 mm.

Lines in a spectrum exhibiting high multiplicities, such as that of iodine, must have certain favorable properties if the hyperfine Zeeman patterns in intermediate fields are to be other than a hopeless confusion. Our study has been confined primarily to the behavior in magnetic fields of three lines of iodine II. These lines are suitable, first because the differences between interval factors of the states involved in each transition are large, thus producing widely spread hyperfine components in the Back-Goudsmit type of pattern. Second, for each of these lines the g values of the states are large, allowing more rapid approach to the Back-Goudsmit condition. Third, the differences between g values are small so that the complete Zeeman patterns are narrow enough to be studied with a Fabry-Perot interferometer. Two lines, λ5464.6 and λ5407.25, have the further simplifying property that the value of J does not change in the transition. These patterns were measured at several field strengths. The third line, λ5161.2, was observed in an interesting and simple pattern only at one particular field.

In seeking an interpretation of the Zeeman patterns observed at the various fields it was necessary for us to make at the outset assumptions concerning the value of I for the iodine nucleus and then to determine which of these values is qualitatively in accord with the observations. By proceeding in this manner we find that the only value for I which is consistent with the observed patterns is $2\frac{1}{2}$, the value assigned by Murakawa and by Tolansky. Adopting this value for I we have available the values determined by Tolansky and Forrester for the hyperfine interval factors. The g values for the states of interest to us are available either

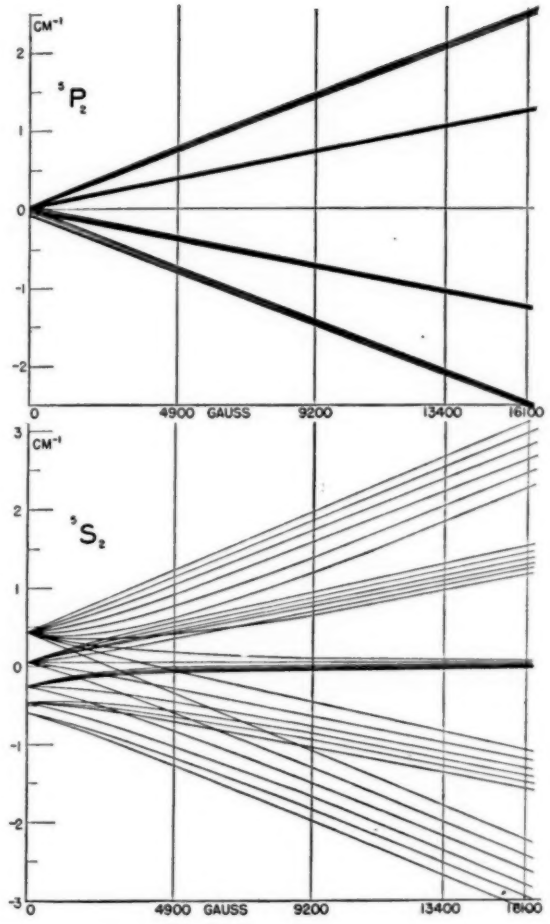

FIG. 2. Theoretical behavior of sublevels of $5s^25p^36s\ ^5S_2$ and $5s^25p^36p\ ^5P_2$ states of iodine II as function of magnetic field strength. Level separations are given in cm^{-1}.

through the work of Lacroute[8] or from the new measurements. Introducing these numerical values, we are able to calculate positions of the energy levels at any desired field by the method of Goudsmit and Bacher. Finally the line pattern at each field may be predicted with the aid of the intensity equations and compared with that observed. Detailed discussion of this comparison with reference to each line follows.

λ5464.6

The states and constants of the states from which the line λ5464.6 originates are:

$5s^25p^36s\ ^5S_2$	—	$5s^25p^36p\ ^5P_2$
$g=1.78$		$g=1.67$
$A=0.0874\ cm^{-1}$		$A=0.0075\ cm^{-1}$.

[8] P. Lacroute, Ann. d. Physik **3**, 5 (1935).

The numerical values of the interval factors A are from Tolansky and Forrester's analysis. The value $g=1.78$ is from Lacroute's observations, while the second g was determined in the present analysis through an assumption of the correctness of the first g. The $^5P_2$ state is already approaching the Back-Goudsmit condition at 2000 gauss. Thus Goudsmit and Bacher's first approximation equations are adequate for treating the behavior of the sublevels of this state at the fields with which we are concerned. The $^5S_2$ state, having wide hyperfine structure, only begins to approach the Back-Goudsmit condition at 16,000 gauss. The general equations of Goudsmit and Bacher must here be used in computing the positions of the energy levels. These computations, which involve the numerical solution of a set of ten algebraic equations ranging from the first to the fifth degree, have been carried out for fields of

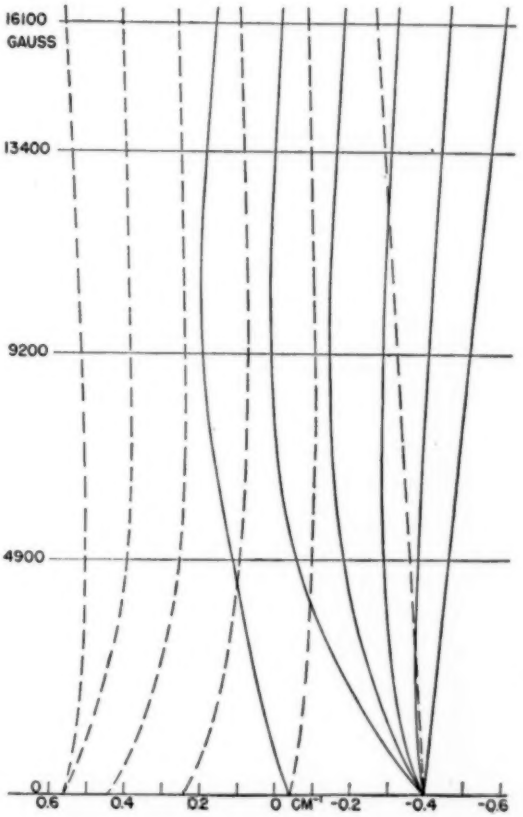

FIG. 3. Theoretical behavior of pattern of strong π components of λ5464.6, iodine II with varying magnetic field. Line distribution is plotted horizontally against field strength in gauss. Dotted components originate in the transition $M_J=-2\rightarrow M_J=-2$, solid components in the transition $M_J=2\rightarrow M_J=2$. These components have comparable intensities at fields above 4000 gauss.

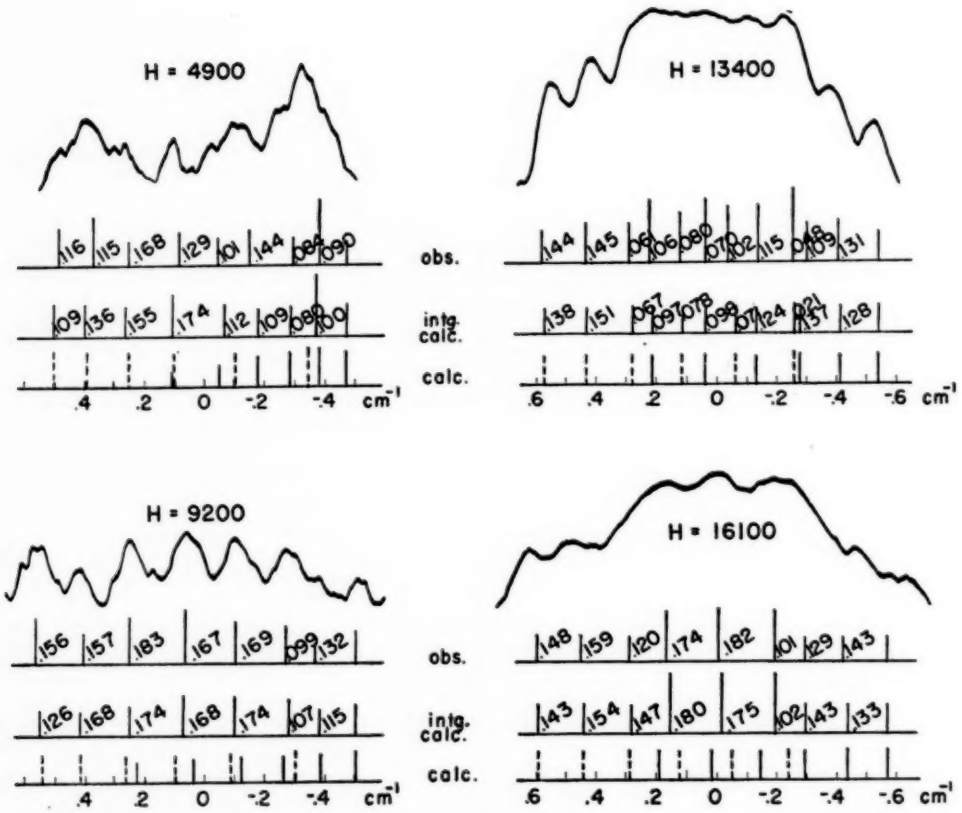

FIG. 4. Graphical comparison of calculated and observed π Zeeman patterns of λ5464.57 at four different fields. Integrated calculated patterns are obtained by representing as a single component close groups of components not expected to be resolved. Lengths of lines are proportional to intensities. Above each set of graphs is a microphotometer trace of a corresponding observed interferometer pattern.

4900, 9200, 13,400 and 16,100 gauss. These fields were chosen because experimental observations there proved particularly satisfactory. The theoretical behavior of the sublevels of the $^5P_2$ and $^5S_2$ states as functions of the magnetic field up to 16,100 gauss is shown graphically in Fig. 2.

The character of the line pattern resulting from the transitions between these two sets of levels may be determined for each field when the relative intensities of the numerous individual components have been found from Goudsmit and Bacher's intensity equations. Confining ourselves to the π components, we find that only 28 have intensities different from zero. Of these components 4 have intensities of less than one percent of that of the strongest at fields above 4900 gauss and 12 more have intensities of less than 20 percent of that of the strongest. The remaining 12, originating in the transitions $M_J=2\rightarrow M_J=2$ and $M_J=-2\rightarrow M_J=-2$, are strong and have comparable intensities which approach equality at the higher fields. This relative simplicity is a consequence of the fact that J does not change in the transition. Fig. 3 shows graphically the behavior of the line pattern made up of these 12 strong π components with varying field. The 6 components originating in the transition between levels having $M_J=-2$ are distinguished from the other set by dashed lines in the figure.

Figure 4 shows a graphical comparison of the observed and theoretically calculated patterns of π components of λ5464.6 at four different fields. The heights of the vertical lines representing components are proportional to their intensities. Intervals between components in cm^{-1} are indicated. The lower pattern for each field shows the calculated positions and intensities of the 12 strong π components. The two groups of components are distinguished in this pattern as in

Fig. 3. The middle pattern marked "intg. calc." is the integrated calculated pattern obtained when neighboring components not expected to be resolved are shown as a single component. The upper pattern shows the measured positions of observed components. Above each group of graphical patterns is an unretouched microphotometer trace of the corresponding observed interferometer pattern reduced to approximately the scale of the graphs. In comparing the microphotometer trace with the graphs it is to be remembered that the correspondence cannot be exact since the interferometer does not give a normal dispersion. However, to improve the apparent correspondence we have chosen orders rather far from the center of the interference pattern but have sacrificed something in resolution thereby. The reported positions of components in the observed pattern are the result of comparator measurements upon several orders of the interferometer pattern.

The comparison represented in Fig. 4 shows, we believe, a satisfactory qualitative agreement in that the general structure and number of components observed at each field corresponds with that expected. Our neglect of the weak components in the predicted patterns will introduce some distortion, but the quantitative agreement also seems satisfactory upon the whole.

λ5407.25

The line λ5407.25 is very similar in character to λ5464.6. It originates in the transition between two states described as follows:

$5s^25p^36s\ ^3D_2$	—	$5s^25p^36p\ ^3D_2$
$g=1.26$		$g=1.19$
$A=0.0584\ \text{cm}^{-1}$		$A=0.0068\ \text{cm}^{-1}$.

The value $g=1.19$ was determined in the present analysis by accepting the other g value of 1.26 as found by Lacroute. The A values are again from Tolansky and Forrester. Calculation of the pattern for this line at the four different fields has also been carried out. Fig. 5 shows the comparison between the calculated and observed patterns. The qualitative agreement seems again satisfactory. The quantitative agreement is, however, less complete than for λ5464.6. It is to be noted that the middle portion of the observed pattern is shifted toward the right relative to the predicted pattern in each case.

λ5161.2

A comparatively simple pattern was observed for the line λ5161.2 only at fields near 4900 gauss. The states involved are:

$5s^25p^36s\ ^5S_2$	—	$5s^25p^36p\ ^5P_3$
$g=1.78$		$g=1.55$
$A=0.0874\ \text{cm}^{-1}$		$A=0.0009\ \text{cm}^{-1}$.

The value $g=1.55$ was determined in the present analysis. Because this is a transition of the type $J\rightarrow J+1$ there are 30 components in the π pattern of comparable intensity and all must be included in the calculated pattern. The comparison between calculated and observed patterns for this line is shown in Fig. 6.

Discussion

Nuclear spin

Any change in the value for I introduced into the computations alters radically the predicted pattern both in regard to the number and the arrangement of components. The agreement between the theoretically calculated and the observed Zeeman patterns discussed above constitutes, we believe, a demonstration of the correctness of the value $I=2\frac{1}{2}$ for the iodine nucleus.

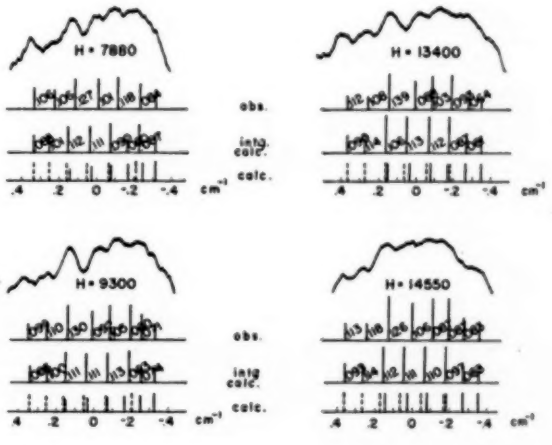

Fig. 5. Graphical comparison of calculated and observed π Zeeman patterns of λ5407.25 at four different fields.

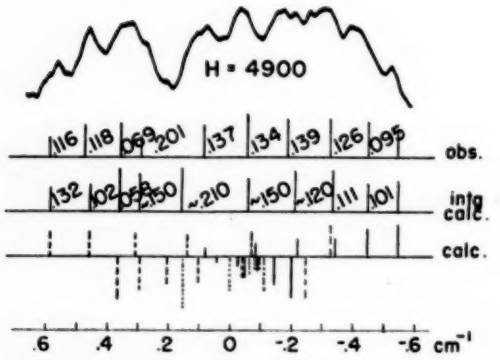

FIG. 6. Graphical comparison of calculated and observed π Zeeman patterns of λ5161.18 at 4900 gauss.

Theory of hyperfine Zeeman effect

In applying the theory of Goudsmit and Bacher to prediction of the Zeeman patterns of iodine II in a wide range of fields we have subjected the theory to a severe test. The agreement between prediction and experiment indicates that the theory is adequate in such highly complex cases.

Nuclear quadrupole effects

It has been pointed out that the experimental patterns of λ5407.2 were apparently distorted as compared with the predicted patterns. This affect we believe is to be attributed to the influence of a nuclear quadrupole moment. The appearance of this interaction in the Zeeman effect has been predicted by Schmidt.[9] He obtains the following approximate expression for the quadrupole interaction energy in the Back-Goudsmit condition:

$$Eq = b[\tfrac{3}{8}I(I+1)J(J+1)+6M_I^2M_J^2 - 2M_J^2I(I+1)-2M_I^2J(J+1)],$$

where b is the quadrupole coupling constant. This term introduces an unsymmetrical shift of the hyperfine Zeeman levels although the total width of a group associated with a particular value of M_J is unchanged, as is that of the entire Zeeman pattern. A numerical value for b of the $5s^25p^36s\ ^3D_2$ state has been determined by Tolansky and Forrester from their hyperfine structure analysis. Their value is -0.00028 cm^{-1}.[10] Using this value we obtain the following corrections to be applied to the positions of the respective components of each M_J group in the line pattern, beginning at the high frequency side of the group: $+0.013$, $+0.007$, 0, 0, -0.007, -0.013 cm^{-1}. The result is a shift toward lower frequencies of the central components of the combined pattern. This is precisely the type of distortion observed in λ5407.2 and the quantitative agreement is satisfactory. We conclude, therefore, that the quadrupole interaction is observed in these Zeeman patterns.

[9] T. Schmidt, Zeits. f. Physik **111**, 332 (1938).

[10] We employ the coefficient obtained by Tolansky and Forrester when only a quadrupole interaction was assumed. The coefficient obtained later by Tolansky when an octopole interaction was introduced seems less satisfactory.

A Hollow Cathode Source for the Zeeman Effect

RUSSELL A. FISHER AND ARTHUR S. FRY*
Northwestern University, Evanston, Illinois

(Received August 14, 1939)

A modification of the Schüler type of hollow cathode discharge tube adapts it for use in magnetic fields. Details of the design and operating characteristics of the tube are discussed.

EXPERIMENTS to determine under what conditions a hollow cathode discharge could be maintained in a magnetic field were made in this laboratory two years ago by J. R. Platt and one of us[1] (R. A. F.). As a result of these experiments and other tests more recently performed a design has been worked out for a hollow cathode discharge tube which operates satisfactorily in the highest fields attainable with our present apparatus (nearly 17,000 gauss). Because the sharpness of emitted spectral lines characteristic of the Schüler type[2] of discharge tube is largely retained in this source it is well adapted for observation of the Zeeman effect in hyperfine structure.[3] It is also applicable to observation of ordinary Zeeman effects in weaker fields since the sharpness of the lines makes wide separation of the patterns unnecessary.

The glow in an ordinary hollow cathode is much weakened by a magnetic field of a few hundred gauss applied perpendicular to the axis of the discharge and soon entirely extinguished. If the pressure of the gas in the tube is reduced slightly below that for normal operation the appearance of the discharge in a weak magnetic field is somewhat improved. If an abnormally small cathode cavity is introduced the maximum field in which a discharge can be maintained is found to be increased. These two observations may be understood as a consequence of the influence of the field in reducing the *effective* mean free path of electrons in the discharge by causing them to traverse curved paths. Günther-Schulze[4] has shown that a necessary condition for the maintenance of a glow in a cathode cavity is that the electron mean free path approximate the width of the cavity. An indicated modification in adapting the Schüler tube to operation in higher magnetic fields is thus a reduction in the dimension of the hollow cathode.

* Now with Research Laboratories Division, General Motors Corporation, Detroit, Michigan.

[1] See J. R. Platt, Master's thesis, Northwestern University, 1937. Also R. A. Fisher, A. S. Fry and J. R. Platt, Phys. Rev. **53**, 934(A) (1938).

[2] H. Schüler, Zeits. f. Physik **35**, 323 (1926); **59**, 149 (1930).

[3] See observations on the Zeeman effect in the hyperfine structure of iodine reported by us in the preceding paper.

[4] A. Günther-Schulze, Zeits. f. Physik **19**, 313 (1923). See also R. A. Sawyer, Phys. Rev. **36**, 44 (1930).

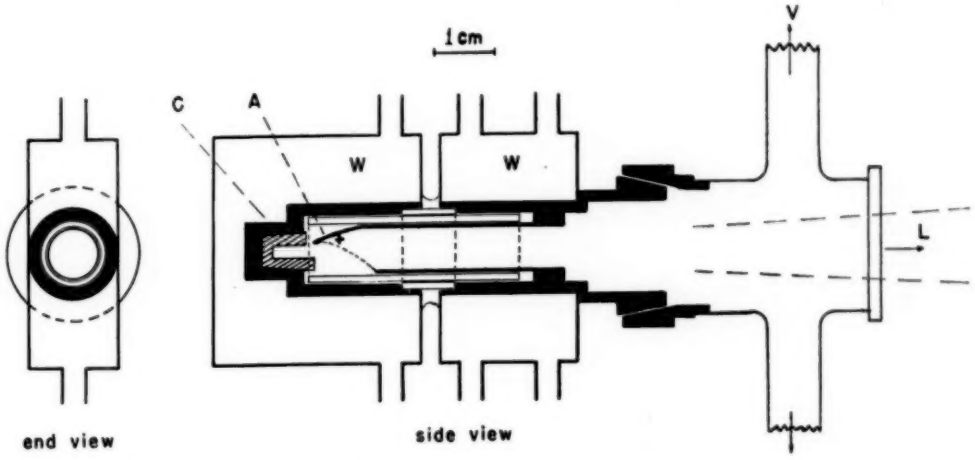

FIG. 1. Detail drawing of hollow cathode discharge tube.

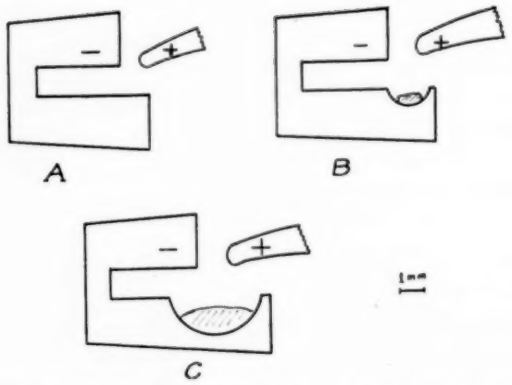

FIG. 2. Relation of anode to cathode in different forms of cathode.

A second effect of the field is a deviation and redistribution of the current in the discharge column extending from the cathode cavity. This effect is so great at higher fields that the anode and cathode must be placed in extreme proximity in order for a discharge to be maintained. The unsymmetrical character of the discharge may be compensated by an unsymmetrical arrangement of the anode relative to the cathode.

GENERAL DESIGN OF THE TUBE

After extensive tests involving cathode cavities of various shapes and sizes and various geometrical arrangements of anode relative to cathode a discharge tube was constructed as drawn to scale in Fig. 1. This tube is mounted with its axis horizontal and perpendicular to the magnetic field. It thus permits only observation of the transverse Zeeman effect through the window L at the right. The discharge is carried, as usual, by a properly purified inert gas. The dimensions are such that the tube may be placed between pole pieces 16 mm apart.

The walls of the tube are formed by a brass cylinder 55 mm long having an outer diameter of 15 mm and an inner diameter of 12 mm. This cylinder is divided into two parts which are separated and insulated from one another by a short glass ring having the same inner diameter as the brass. The two parts of the tube and the glass ring are joined by Picein wax. Inside the brass wall is a glass sleeve extending nearly the length of the tube and fitting loosely enough to be withdrawn. At one end of the cylinder is located the hollow cathode (C in the figure). It is a removable plug of some nonferromagnetic metal fitting snugly into a tapered hole at the closed end of the brass cylinder. Extending through the tube inside the glass sleeve is the anode cylinder which is also removable and held in place by friction. At one end of this anode cylinder is a brass ring which fits against the outer wall of the tube. The other end is a tapered prong (A in the figure) resembling somewhat the point of a pen, but with a rounded tip, which extends to a position just above the cathode cavity.

The water-cooling jackets, W, of the two halves of the tube are flat, as shown in the end view, to avoid unnecessary separation of the pole pieces. The metal at the end of the tube surrounding the cathode is machined away to provide more effective cooling. The tube as a whole is connected to the vacuum system through the ground joint shown, which permits convenient access to the removable anode and cathode.

THE CATHODE AND ANODE

The cathode cavity is in a removable plug because action of the discharge in the magnetic field causes a groove to be cut rather rapidly into the metal directly below the cavity. Thus after a few hours of operation the cavity is so deformed that the cathode must be removed and machined or replaced by a new one. Aluminum as cathode material is more resistant to this erosion than other metals which we have used. However, if aluminum is attacked chemically by the substance present in the discharge, as it is by iodine, some other metal must be substituted. Tungsten is satisfactory although it is more difficult to machine and more rapidly eroded.

A cylindrical cavity between 1 and $1\frac{1}{2}$ mm in diameter seems to be most satisfactory for

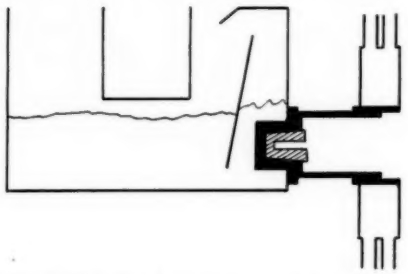

FIG. 3. Detail of liquid-air-cooled cathode.

(*a*) (*b*) (*c*)

FIG. 4. Zeeman patterns resolved by Fabry-Perot interferometer. *a*, λ4810 of zinc at 9900 gauss, π components only, 5.2-mm interferometer spacer; *b*, λ5719 of bismuth at 9500 gauss, 2.4-mm spacer; *c*, λ5350 of thallium at fields of 8000, 9000 and 10,000 gauss, 5.2-mm spacer.

operation in fields greater than 10,000 gauss. At lower fields the diameter may be greater. The depth of the cavity is immaterial so long as it is more than twice the diameter. A small shelf extending out from the cathode on the side of the cavity opposite the anode, as shown in Fig. 2, *A*, seems to prolong the life of the cathode.

Substances which are readily vaporized may be introduced into the discharge by being placed inside the anode cylinder. Others, such as the common metals, having low vapor pressures, must be introduced more directly into the cavity. Fig. 2, *B*, illustrates a cathode suitable for exciting such substances. A piece of the substance is placed in a depression in the shelf before the cavity where it receives vigorous bombardment by the discharge. If the substance is melted by the bombardment it may be placed in a larger well as shown in Fig. 2, *C*.

Aluminum is the most satisfactory material for the anode, although molybdenum or tungsten will serve. The tip of the anode should be about 1 mm in front of the cathode face and 1 mm above the opening as shown in Fig. 2. The direction of the magnetic field must be such as to deviate the discharge column issuing from the cavity *downward* and *away* from the anode. If the field is reversed an arc is apt to result.

Chemical attack upon the brass wall of the tube near the cathode may be eliminated by shrinking the end of the glass sleeve until it fits closely around the cathode plug.

A modification of the cathode portion of the tube permitting cooling of the cathode by liquid air has been constructed as shown in Fig. 3. The attached liquid-air chamber is of brass and is covered with thin sheets of cork. The baffles shown prevent the liquid air from being thrown out by the boiling at the cathode.

Operating Characteristics

The pressure of the rare gas in the tube for optimum operation depends rather critically upon the field strength and the discharge current and must be readily adjustable. When argon is used the pressure ranges between 5 mm at high fields and 12 mm at low fields. With helium it is somewhat higher.

The potential difference between anode and cathode increases with increasing field, varying from 400 to 800 volts at a current of 100 milliamperes.

The discharge current for stable operation may have any value between 15 and 100 milliamperes. If the higher value is exceeded there is a tendency toward arcing.

When the pressure is properly adjusted relative to the field strength the source operates with perfect stability for hours without attention. The highest field attained by our magnet evidently does not represent a limit in operation of the tube since the discharge seems only to become more intense as the field increases. The hollow cathode glow resembles that in the ordinary Schüler tube except that it is considerably more brilliant. The tube operates satisfactorily in zero field but at an elevated gas pressure.

The sharpness of emitted lines is comparable, although perhaps not quite equal to that attained with the water-cooled Schüler tube. We have resolved Zeeman components whose separation is as little as 0.040 cm^{-1} in the indium spectrum using the water-cooled source. Fig. 4 gives examples of Zeeman patterns observed with this source by means of a Fabry-Perot interferometer. Tests with the liquid-air-cooled cathode have not been extensive enough to determine whether there is a significant gain in line sharpness compared with the water-cooled tube. It may only be said that the liquid-air cooling does not impair the discharge. It is, however, necessary to place the material directly in the cathode in order to obtain any excitation at the low temperature.

Interferometer Wave-Lengths of Certain Lines in the Secondary Spectrum of Hydrogen

LEWIS S. COMBES, ROYAL M. FRYE AND NORTON A. KENT
Boston University, Boston, Massachusetts

(Received August 2, 1939)

Interferometer determinations have been made of the wave-lengths of twenty-four lines of the molecular spectrum of hydrogen in the region λ4900 to λ5900, with an etalon crossed with a Littrow spectrograph. A least-squares method is described for calculating the wave-lengths.

THE apparatus used in this work was essentially the same as that employed by Kent and Lacount[1] in measuring the wave-lengths of D_2 and HD except that the speculum grating was replaced by an aluminum instrument (ruled by R. W. Wood) having 15,000 lines per inch, with most of the light thrown into the first order on one side.

The Littrow spectrograph, etalon and most of the optical apparatus rested on a vibrationless, thermostated mounting in the research laboratory at Boston University.[2]

The water-cooled discharge tube contained hydrogen at a pressure of about 0.3 mm of mercury, and was run at a current density of about 600 ma per cm². A Pfund arc, used to obtain iron standards on each plate, was exposed at the beginning and end of each run and at one hour intervals between. Six plates (Eastman Spectroscopic I–D) were taken.

Eleven iron lines recommended as standards by the International Astronomical Union[3] and twenty-four hydrogen lines were measured. The diameters of four or five interference rings of each line were measured on a Gaertner comparator.

The wave-lengths were calculated by a least-squares method using the following familiar relations developed from the theory of the etalon.

$$p\lambda = 2t, \tag{1}$$

$$p = P + E, \tag{2}$$

$$n + E = KD_n^2, \tag{3}$$

$$K\lambda = \text{the plate constant}, \tag{4}$$

where t is the distance between reflecting surfaces of etalon; λ the wave-length; p the order of interference at the center of the ring system; P the integral order of interference; E the fractional order of interference; n the number of the ring (0, 1, 2, 3, etc.); D_n the diameter of the nth ring; K the constant for a single wave-length.

Referring to Eq. (3), if D_n^2 be plotted against n for any one wave-length a straight line is obtained (as in Fig. 1) the slope of which is $1/K$. Then if any value of D_n^2 be multiplied by the reciprocal of the slope (K), E may be evaluated.

The slope of this line for each iron standard was obtained by the method of least squares, and $K\lambda$ calculated. The mean value of $K\lambda$ for the eleven iron standards was used as the plate constant.

A corrected K for each iron standard was obtained by dividing the plate constant by λ. Then E was obtained by multiplying D_2^2 by K. This value of D_2^2 is a corrected value obtained

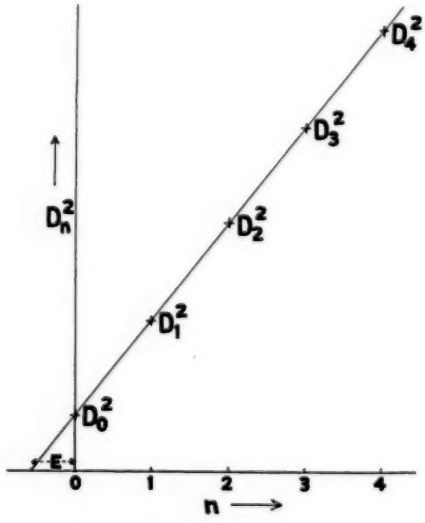

FIG. 1. Graph of $KD_n^2 = n + E$.

[1] Norton A. Kent and Reginald G. Lacount, Phys. Rev. **51**, 241 (1937).
[2] Norton A. Kent and Reginald G. Lacount, "A Spring Suspended and Thermostated Littrow Spectrograph," J. Opt. Soc. Am. **28**, 266 (1938).
[3] Trans. Int. Astronom. Union **3**, 86 (1928).

TABLE I. *Correlation of results.*

PLATE No. 12	No. 13	No. 14	No. 16	No. 17	No. 18	MEAN	SPREAD $\times 10^3$	A.D. $\times 10^3$	P.E. $\times 10^3$	I	MEAN WAVE-LENGTH
0.2417	0.2408	0.2416	0.2402	0.2395	0.2410	0.2408	2.2	0.6	0.2	2	4934.241
.3124	.3121	.3131	.3128	.3149	.3135	.3131	2.8	.7	.2	0	4973.313
.0325	.0330	.0330	.0312	.0331	.0318	.0324	1.9	.6	.2	1	5013.032
.3652	.3658	.3672	.3650	.3666	.3668	.3661	2.2	.8	.3	0	5030.366
.8293	.8298	.8281	.8287	.8290	.8285	.8289	1.7	.5	.2	0	5039.829
.0936	.0936	.0939	.0947	.0944	.0944	.0941	1.1	.4	.1	0	5055.094
.1280	.1263	.1266	.1268	.1267	.1279	.1271	1.7	.6	.2	0	5113.127
.3387	.3381	.3392	.3385	.3382	.3377	.3384	1.5	.4	.1	0_2	5146.338
.3717	.3720	.3713	.3698	.3709	.3711	.3711	2.2	.5	.2	0_1	5196.371
.6111	.6114	.6115	.6112	.6120	.6124	.6116	1.3	.4	.1	0_1	5256.612
.9126	.9133	.9112	.9116	.9114	.9137	.9123	2.4	.9	.3	0_1	5355.912
.1604	.1611	.1615	.1629	.1609	.1606	.1612	2.5	.6	.2	1	5388.161
.8905	.8908	.8918	.8923	.8907	.8925	.8914	2.0	.8	.3	2	5419.891
.0800	.0794	.0803	.0799	.0798	.0806	.0800	1.2	.3	.1	0	5481.080
.5112	.5116	.5123	.5091	.5106	.5113	.5110	3.2	.8	.3	0	5505.511
.4615	.4603	.4605	.4605	.4608	.4617	.4609	1.4	.5	.2	2	5537.461
.6347	.6362	.6367	.6344	.6361	.6368	.6358	2.4	.8	.3	0	5597.636
.5461	.5459	.5450	.5429	.5446	.5439	.5447	3.2	.9	.3	0	5612.545
.7456	.7472	.7460	.7473	.7478	.7464	.7467	2.2	.7	.2	0	5655.747
.5458	.5460	.5475	.5459	.5446	.5473	.5462	2.9	.8	.3	2	5728.546
.0424	.0418	.0435	.0439	.0420	.0421	.0426	1.7	.7	.2	3	5775.043
.0938	.0954	.0961	.0955	.0966	.0947	.0954	2.8	.7	.2	2	5806.095
.7592	.7584	.7594	.7595	.7568	.7578	.7585	2.7	.8	.3	2	5822.759
.3117	.3127	.3129		.3113	.3124	.3122	1.6	.6	.2	1	5849.312
						Mean	2.1	.6	.2		

by least-squares calculation and is not the square of the measured value of D_2. D_2^2 was used because it was considered that the probable error in calculating it was less than for any other value of D_n^2. P was obtained for each iron standard by dividing an approximate value of $2t$ by λ. Then $p=P+E$ and a corrected value of $2t$ was obtained by using Eq. (1). The mean value of $2t$ obtained for the eleven iron standards was calculated. This was the value of $2t$ used later in calculating the corrected wave-lengths of the hydrogen lines.

A corrected K was obtained for each hydrogen line by dividing the plate constant by an approximate value of λ. These approximate wave-lengths were obtained from the measurements of Gale, Monk and Lee.[4] E for each hydrogen line was evaluated as for the iron standards. Then $P=2t/\lambda$ (approx.), $p=P+E$ and a corrected value of λ was obtained from Eq. (1).

The results obtained on all six plates are shown in Table I. Only the decimal part of the wave-length is given in the first seven columns. A line of average intensity, I, is designated by 0, 0_4 indicating the weakest and 5 the strongest lines on the plate.

The spread, average deviation and probable error are shown in the table. The maximum spread was 0.0032A and the mean spread was 0.0021A. About one-half the mean spread would seem to be a conservative estimate of the actual probability of error: that is the values are probably correct to $\pm$0.001A. This is much larger than the calculated mean probable error which is 0.0002A but other factors must be considered. For example there seems to be some doubt as to the accuracy of some of the iron standards recommended by the International Astronomical Union.[3] For certain iron standards the calculated value of $2t$ was always lower than the average. If four iron standards which consistently gave low values for $2t$ were omitted and the calculations based on the other standards alone, the results would be increased by about 0.00002 percent. This would mean an increase of 0.001A for each wave-length. Hence the probable error of $\pm$0.001A seems reasonable.

Acknowledgment is made to the members of the staff and graduate students who assisted in this work, particularly to Dr. Reginald G. Lacount and Mr. Royal C. Bryant. The expense was met largely by a grant to Dr. Kent by the Committee of the Permanent Science Fund of the American Academy of Arts and Sciences. This aid is most gratefully acknowledged.

[4] H. G. Gale, G. S. Monk and K. D. Lee, Astrophys. J. 67, 89 (1928).

Note on Coriolis Coupling Terms in Polyatomic Molecules

H. A. JAHN
Davy-Faraday Laboratory, Royal Institution, London, England
(Received May 4, 1939)

A method is given by which, knowing the displacement vectors of the normal modes of vibration of any polyatomic molecule, we can determine at once which normal modes are coupled by Coriolis forces when the molecule rotates. The water, formaldehyde, ethylene and carbon dioxide molecules are taken as examples to illustrate the method.

IN this journal Nielsen[1] has recently investigated the Coriolis coupling of different modes of vibration of an asymmetrical top molecule. The terms he investigates are of the same nature as those which couple the twofold and threefold degenerate modes of the methane molecule. These terms were first discussed by the writer in his Leipzig thesis in 1935[2] and the resulting Coriolis perturbation has since been subject to detailed calculation.[3] It is the purpose of the present note to derive a simple and general method of obtaining for any given molecule which Coriolis terms occur in the Hamiltonian and hence which normal modes may be subject to Coriolis perturbations. A classification of the matrix elements of these coupling terms in an asymmetrical top molecule has been given by E. Bright Wilson[4] but he did not give a classification of the coupling terms themselves as is given here and has been outlined elsewhere.[5] It is easy to extend Wilson's calculation of the matrix elements of the Coriolis terms to symmetrical top and spherical top molecules and one can then in principle calculate the energy levels and optical spectra. It is not however the purpose of the present note to make such calculations (as have been made already by the writer for methane and by Nielsen for formaldehyde) but rather to show how from general symmetry considerations alone, without detailed calculation, we can predict which absorption bands of a given polyatomic molecule are likely to be subject to Coriolis perturbations.

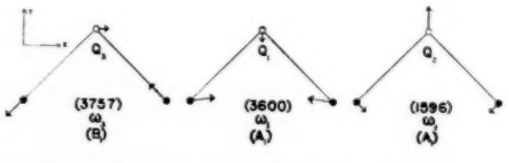

FIG. 1. Normal modes of the water molecule.

Let us consider for instance the water molecule which has the three normal modes of vibration shown in Fig. 1. (The symbols A_1, B_1 describe the symmetry types (see below).)

Consider the first mode (Q_3). If the molecule is not rotating then this is a normal mode of vibration of the molecule. Each atom executes simple harmonic motion with the frequency ω_3. We may put

$$x_0=a_0 \sin \omega_3 t,\quad x_1=-a_1 \sin \omega_3 t,\quad x_2=-a_1 \sin \omega_3 t,$$
$$y_0=0,\qquad y_1=-b_1 \sin \omega_3 t,\quad y_2=b_1 \sin \omega_3 t,$$

where a_0, a_1 and b_1 determine the amplitudes. The velocities of the atoms are then

$$\dot{x}_0=a_0\omega_3 \cos \omega_3 t,\quad \dot{x}_1=-a_1\omega_3 \cos \omega_3 t,$$
$$\dot{y}_0=0,\qquad \dot{y}_1=-b_1\omega_3 \cos \omega_3 t,$$
$$\dot{x}_2=-a_1\omega_3 \cos \omega_3 t,$$
$$\dot{y}_2=b_1\omega_3 \cos \omega_3 t.$$

The atoms all pass through their equilibrium positions together at $t=0$ and their velocities are then

$$\dot{x}_0=a_0\omega_3,\quad \dot{x}_1=-a_1\omega_3,\quad \dot{x}_2=-a_1\omega_3,$$
$$\dot{y}_0=0,\qquad \dot{y}_1=-b_1\omega_3,\quad \dot{y}_2=b_1\omega_3.$$

Thus the displacement vectors shown in Fig. 1 represent in relative magnitude and direction not only the classical amplitudes but also the velocities of the atoms when they are passing (simultaneously) through their equilibrium positions.

[1] H. H. Nielsen, Phys. Rev. **55**, 289 (1939) and J. Chem. Phys. **5**, 818 (1937).
[2] H. A. Jahn, Ann. d. Physik **23**, 529 (1935).
[3] H. A. Jahn and W. H. J. Childs, Nature **141**, 916 (1938); H. A. Jahn, Proc. Roy. Soc. **A168**, 469, 495 (1938); W. H. J. Childs and H. A. Jahn, Proc. Roy. Soc. **A169**, 451 (1939).
[4] E. Bright Wilson, J. Chem. Phys. **4**, 313 (1936).
[5] W. H. J. Childs and H. A. Jahn, Proc. Roy. Soc. **A169**, 451 (1939).

Suppose now the molecule is rotating. Then we know that the particles will be subject to additional accelerations. These are the centrifugal acceleration and the compound centrifugal (or Coriolis) acceleration. The centrifugal acceleration involves the squares of the angular velocity components which are small compared with the vibrational frequencies and hence we need consider only the Coriolis acceleration which is linear in these components. The components of the Coriolis acceleration for each atom are given by

$$J_x=2(\dot{y}\Omega_z-\dot{z}\Omega_y),$$
$$J_y=2(\dot{z}\Omega_x-\dot{x}\Omega_z),$$
$$J_z=2(\dot{x}\Omega_y-\dot{y}\Omega_x),$$

where Ω_x, Ω_y, Ω_z are the components of angular velocity about the three axes. Let us consider rotation about the z axis perpendicular to the plane of the molecule. Then $\Omega_z=\Omega$, $\Omega_x=\Omega_y=0$ and we have

$$J_x=2\Omega\dot{y}, \quad J_y=-2\Omega\dot{x}.$$

Thus we find at $t=0$ when the atoms are passing through their equilibrium positions the following Coriolis accelerations of the atoms:

$$(J_x)_0=0, \qquad (J_x)_1=-2\Omega b_1\omega,$$
$$(J_y)_0=-2\Omega a_0\omega, \quad (J_y)_1=2\Omega a_1\omega,$$

$$(J_x)_2=2\Omega b_1\omega,$$
$$(J_y)_2=2\Omega a_1\omega.$$

If we draw vectors to represent these Coriolis accelerations we find the relation between the mode and the Coriolis acceleration shown in Fig. 2. Of course when the velocity vectors are in the opposite direction (as they will be for half the period) the Coriolis acceleration is also reversed. Thus we see that as the molecule vibrates in the first mode (Q_3) with the frequency ω_3 the Coriolis acceleration will tend to excite the other mode shown (Q_2) but with the same frequency ω_3. When the two frequencies ω_3 and ω_2 are widely separated (as they are in the water molecule) the Coriolis force will not be very successful in generating Q_2, but when they lie close together we may expect a large resonance and a corresponding perturbation of the two modes. It should be pointed out that the actual form of the vibrations ω_1 and ω_2 depends upon the force system, so that ω_1 will in general involve some of Q_2 and since the frequencies ω_3 and ω_1 lie rather close together we may expect a slight perturbation of the rotational levels of these two modes. This has not been observed by Mecke, but he analyzed ω_3 only up to the fourth rotational quantum number for which the Coriolis perturbation would still be small (it increases with the rotational quantum number). There is a simple rule for deriving the Coriolis acceleration when the vectors of a mode are given: If we stand in the direction of the rotation at the foot of the displacement vector and look towards its head, then the Coriolis acceleration is always to the right. We can apply this for example to formaldehyde. For rotation about the figure axis we find at once that the Coriolis acceleration of the mode ν_5 describes the mode ν_6 (see Fig. 5 below). Thus the modes ν_5 and ν_6 are coupled together when the molecule rotates about the figure axis and since these two frequencies lie close together one obtains a large perturbation: this has been observed by Nielsen.

FIG. 2. Mode (1) and Coriolis acceleration (2).

These effects are all included in the general expression for the Hamiltonian of the molecule which has the form

$$H=H_R+H_V$$
$$=(L_x-S_x)^2/I_x+(L_y-S_y)^2/I_y+(L_z-S_z)^2/I_z+H_V,$$

where S_x, S_y, S_z are components of vibrational angular momentum obtained by combining the normal coordinates and their impulses. These components must be subtracted from the components L_x, L_y, L_z of the total angular momentum of the molecule to obtain the components of angular momentum of the equilibrium configuration (with moments of inertia I_x, I_y, I_z) which determine the rotational frequencies.

There is a simple group-theoretical method that gives at once the vibrational angular momenta S_x, S_y, S_z which can and, in general, will appear in the Hamiltonian of any given molecule. Let us take again the water molecule. The group of symmetry is C_{2v} which group has

TABLE I

	E	C_2	σ	σ'
A_1	1	1	1	1
A_2	1	1	−1	−1
B_1	1	−1	1	−1
B_2	1	−1	−1	1

the irreducible representations shown in Table I. The symmetry group is illustrated in Fig. 3. We can classify the vibrations (see Fig. 1) and the infinitesimal rotations of the molecule according to these representations (Fig. 4). Now the vibrational angular momenta have the form

$$q_i p_j - q_j p_i,$$

where the q's are the normal coordinates and the p's are the corresponding impulses. These quantities must transform like angular momenta, i.e. like the rotations R_x, R_y, R_z, that is

$$S_x \sim B_2, \quad S_y \sim B_1, \quad S_z \sim A_2.$$

Now the impulses transform like the corresponding coordinates, so we have merely to investigate the product representations of the normal coordinates. We find

$$B_1 \times B_1 = A_1, \quad A_1 \times A_1 = A_1, \quad A_1 \times B_1 = B_1.$$

Thus the only possible vibrational angular momentum is S_y and this has the form

$$S_y = S_y^{(12)} + S_y^{(13)}$$
$$= \zeta_{12}(q_1 p_2 - q_2 p_1) + \zeta_{13}(q_1 p_3 - q_3 p_1),$$

where the ζ_{12}, ζ_{13} are numerical constants which depend upon the equilibrium configuration and upon the force constants. Thus the complete Hamiltonian for the water-type molecule is given by

$$H = \frac{L_x^2}{I_x} + \frac{(L_y - S_y^{(12)} - S_y^{(13)})^2}{I_y} + \frac{L_z^2}{I_z} + H_V.$$

Formaldehyde has the same group of symmetry C_{2v} and has the modes shown in Fig. 5. From the products

$$A_1 \times A_1 = A_1, \quad A_1 \times B_1 = B_1, \ (R_y)$$
$$B_1 \times B_1 = A_1, \quad A_1 \times B_2 = B_2, \ (R_z)$$
$$B_2 \times B_2 = A_1, \quad B_1 \times B_2 = A_2, \ (R_x)$$

we find that the following components of angular momentum exist:

$$S_x^{(16)}, \quad S_x^{(26)}, \quad S_x^{(46)},$$
$$S_y^{(13)}, \quad S_y^{(15)}, \quad S_y^{(23)}, \quad S_y^{(25)}, \quad S_y^{(43)}, \quad S_y^{(45)},$$
$$S_z^{(36)}, \quad S_z^{(56)},$$

where, for instance, $S_z^{(56)} = \zeta_{56}(q_5 p_6 - q_6 p_5)$. Thus the full Hamiltonian for the formaldehyde molecule is

$$H = \frac{\{L_x - (S_x^{(16)} + S_x^{(26)} + S_x^{(46)})\}^2}{I_x}$$
$$+ \frac{\{L_y - (S_y^{(13)} + S_y^{(15)} + S_y^{(23)} + S_y^{(25)} + S_y^{(43)} + S_y^{(45)})\}^2}{I_y}$$
$$+ \frac{\{L_z - (S_z^{(36)} + S_z^{(56)})\}^2}{I_z}.$$

This Hamiltonian includes all the terms considered by Nielsen in his treatment of di-deuteroformaldehyde and more beside. When the equilibrium configuration and the force constants are known the numerical quantities ζ can be calculated in a simple manner described elsewhere.[6]

As a further example we may take the ethylene molecule. This has the group of symmetry D_{2}[4] and the following vibrations (the numerical classification is that of Dennison and Sutherland,[7] the symmetry classification that of Tisza[8]

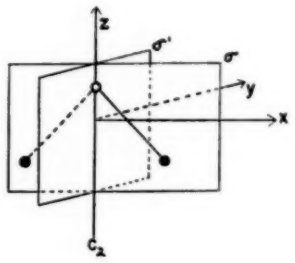

FIG. 3. The group of symmetry for the water molecule.

[6] H. A. Jahn, Ann. d. Physik **23**, 529 (1935); Proc. Roy. Soc. **A168**, 469 (1938).
[7] G. B. B. M. Sutherland and D. M. Dennison, Proc. Roy. Soc. **A148**, 250 (1935).
[8] L. Tisza, Zeits. f. Physik **82**, 48 (1933).

for the group $D_{2p}{}^{i}$, cf. Jahn and Teller[9]):

$$\nu_2(A_{1g}),\quad \nu_4(A_{1g}),\quad \nu_8(A_{1g}),\quad \nu_7(A_{1u}),$$
$$\nu_1(A_{2u}),\quad \nu_3(A_{2u}),\quad \nu_{12}(B_{1g}),\quad \nu_5(B_{1u}),$$
$$\nu_9(B_{1u}),\quad \nu_6(B_{2g}),\quad \nu_{10}(B_{2g}),\quad \nu_{11}(B_{2u}).$$

It is easily verified that the rotations transform as follows:

$$R_x\sim A_{2g},\quad R_y\sim B_{1g},\quad R_z\sim B_{2g},$$

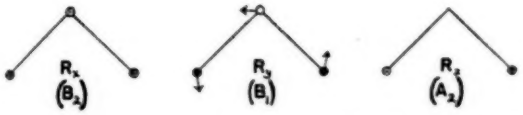

FIG. 4. Symmetry classification of infinitesimal rotations.

where the x axis is along the C−C direction, the y axis in the plane of the molecule and the z axis perpendicular to the latter plane. From the products

$$B_1\times B_2=A_2,\quad A_2\times B_2=B_1,\quad A_2\times B_1=B_2,$$

we find in the above manner the following vibrational angular momenta:

$$S_x=S_x^{(5,11)}+S_x^{(9,11)}+S_x^{(1,7)}+S_x^{(3,7)}+S_x^{(6,12)}+S_x^{(10,12)},$$
$$S_y=S_y^{(2,12)}+S_y^{(4,12)}+S_y^{(8,12)}+S_y^{(5,7)}+S_y^{(7,9)}+S_y^{(1,11)}+S_y^{(3,11)},$$
$$S_z=S_z^{(2,6)}+S_z^{(4,6)}+S_z^{(6,8)}+S_z^{(2,10)}+S_z^{(4,10)}+S_z^{(8,10)}+S_z^{(7,11)}+S_z^{(1,5)}+S_z^{(1,9)}+S_z^{(3,5)}+S_z^{(3,9)}.$$

Consideration of all the above coupling terms will be necessary in a complete analysis of the ethylene spectrum (although, of course, terms coupling widely separated frequencies will be relatively unimportant).

[9] H. A. Jahn and E. Teller, Proc. Roy. Soc. **A161**, 220 (1937).

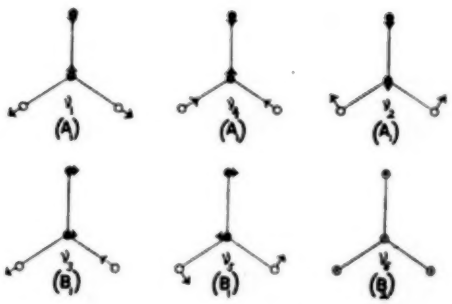

FIG. 5. Normal modes of formaldehyde molecule.

FIG. 6. Two modes of CO_2 molecule coupled by Coriolis forces.

In conclusion it should be pointed out that the above considerations apply also to linear molecules. It is for instance clear from the simple rule given above that the two modes of the CO_2 molecule shown in Fig. 6 are coupled together by Coriolis forces when the molecule is rotating about a direction perpendicular to the axis of the molecule. The existence of this effect would appear to have been overlooked by Adel and Dennison[10] in their dynamical treatment of the CO_2 molecule. It should further be pointed out that the Coriolis forces do not necessarily vanish even for the ground rotational levels of a molecule owing to the presence of the zero-point vibration. Thus it is possible for even the pure rotational spectrum of a polyatomic molecule to be perturbed, if the conditions are fulfilled.

[10] A. Adel and D. M. Dennison, Phys. Rev. **44**, 99 (1933). This shortcoming of the Adel and Dennison Hamiltonian has also been pointed out by Weinberg and Eckart (J. Chem. Phys. **5**, 517 (1937)). The resulting Coriolis perturbation will of course be small in CO_2 since the two coupled frequencies are widely separated.

Separation of Bromine Isotopes by Centrifugation*

RICHARD F. HUMPHREYS†
Sloane Physics Laboratory, Yale University, New Haven, Connecticut
(Received June 14, 1939)

Consideration is given to the high centrifugal field gradients produced by a Beams-type ultracentrifuge as a means of obtaining partial separation of relatively heavy isotopes. Approximate theory is presented for a mixture of two isotopes subjected to "evaporative centrifugation." The theory is capable of predicting the change in abundance ratio for a given set of conditions. To test the feasibility of the method bromine isotopes in the form of ethyl bromide were centrifuged, the result tested spectroscopically. Br^{79} was enriched 11 percent relative to Br^{81}. The agreement with the predicted enrichment was reasonably good.

IF a mixture of gases or liquids is subjected to a gravitational field the heavier molecules tend to concentrate in the direction of the field. For the earth's gravitational field the separation would be negligibly small over any reasonable period of time. However, with the aid of a high speed centrifuge the field can be increased manyfold to make the method useful. The possibility of applying the method to isotopic mixtures was first pointed out by Lindemann and Aston,[1] and later considered in some detail by Mulliken.[2] It can readily be shown that in a centrifugal field gradient the separation factor, θ, which for a mixture of two isotopes can be defined as the ratio of the abundance ratio at the point of minimum field to the abundance ratio at the point of maximum field (that is, at the center and edge of a centrifuge rotor), is given by

$$\theta = \exp\left[(M_2 - M_1)v^2/2RT\right],$$

where v is the peripheral speed, R the gas constant, T the absolute temperature and M_1 and M_2 the light and heavy isotopic masses. The separation factor is thus dependent only on the mass difference of the isotopes, not on the mass of either. This characteristic makes centrifugation applicable to light and heavy isotopes equally well; in addition, those atoms whose isotopes are under investigation may be constituents of any molecule desired since the molecular weight is not of first-order importance. It will be shown subsequently that the molecular weight does play a less important but not negligible part in the choice of molecule to be used. However, this limitation is not severe.

As with many other methods for enriching isotopes the separation increases with decreasing temperature; unfortunately the mechanical difficulties involved with a centrifuge follow the same relation, making it feasible to work only at room temperature.

In reviewing the possibilities of centrifugation of isotopes Mulliken[2] suggested two procedures one might employ: (1) the introduction of gas or liquid at one end of a hollow (or nearly hollow) rotating chamber and its removal at the other end, the operation going on continuously; (2) the introduction of a small amount of *liquid* of comparatively high vapor pressure whose vapor would fill the chamber and undergo separation; the role of the liquid is simply to supply vapor continuously. The vapor would be removed in the same manner as that in which it was introduced, that is, through the hollow shaft supporting the rotor.

Each of these procedures has its advantages. The continuous flow method is essential if liquids are to be centrifuged. However, two major difficulties discourage the use of liquids—first the time required for equilibrium to set in is several hundred or thousand times that needed by a gas; and second vibrations in the centrifuge, even though small, will cause destructive mixing of the separated fractions. Mulliken[2] attempted the centrifugation of mercury, but these difficulties prevented a successful separation. If one therefore restricts himself to a vapor or gas the continuous method will be effective in producing

* Part of a dissertation presented to the Faculty of the Graduate School of Yale University in candidacy for the degree of Doctor of Philosophy.
† Now at Syracuse University, Syracuse, New York.
[1] F. A. Lindemann and F. W. Aston, Phil. Mag. **37**, 523 (1919).
[2] R. S. Mulliken, J. Am. Chem. Soc. **44**, 1033 (1922).

large quantities of separated material. Skarstrom, Carr and Beams[3] have recently obtained by this method 16 cc of carbon tetrachloride liquid in which chlorine 37 was enriched 5 percent. The major disadvantage of the method lies in the mechanical difficulties involved, though these have largely been solved by Beams[4] with his tubular centrifuge.

The second method—evaporative centrifugation—limits the amount of the end product, since only a definite amount of material can be placed initially in the centrifuge rotor. However, the design of the rotor is more favorable to high speeds and hence larger separation factors, as well as permitting a simpler mechanical system. These considerations led to the adoption of this method in the present work.

The following discussion will, then, concern itself with some of the simpler theory of evaporative centrifugation, its application to a specific problem and the results obtained.

Theory

1. Separation factor

It will be convenient to consider only two isotopes present; this is the case commonly encountered, and the generalization to n isotopes adds nothing significant. Let these isotopic gases have partial pressures p_1 and p_2 (the subscript one will always refer to the lighter molecule), and subject them to a constant centrifugal acceleration v^2/r for a sufficiently long time (theoretically infinite) for the composition of the isotopic mixture to reach a steady value; then

$$dp_1=(v^2/r)\rho_1 dr=\rho_1\omega^2 r dr,$$

where ρ is the density of the gas and ω the angular velocity. If M_1 is the molecular weight of isotope 1,

$$\rho_1=M_1 p/RT;\quad 1/p_1 dp_1=(M_1\omega^2 r/RT)dr \quad (1)$$
$$\log\left[p_1(r)/p_1(r_0)\right]=M_1\omega^2(r^2-r_0^2)/2RT.$$

Writing the same equation for isotope 2 and subtracting:

$$\log\frac{p_1(r_0)/p_2(r_0)}{p_1(r)/p_2(r)}=\frac{M_2-M_1}{2RT}(v^2-v_0^2).$$

The mole-fraction may be defined:

$$x_1\equiv p_1/p;\quad x_2\equiv p_2/p.$$

If the rotor is completely hollow $r_0=0$; then

$$\theta=\frac{x_1(0,t)/x_2(0,t)}{x_1(r,t)/x_2(r,t)}=\exp\left[(M_2-M_1)v^2/2RT\right];$$
$$t\to\infty, \quad (2)$$

where to avoid subsequent confusion the variables distance and time are indicated explicitly, though the latter variable enters here only as a limiting condition.

2. Pressure gradient

Except for the very lightest molecules the average molecular weight M can be used to replace either M_1 or M_2 to a fair degree of approximation; hence

$$p(r)/p(0)=e^{Mv^2/2RT}. \quad (3)$$

The pressure ratio from edge to center of the rotor depends on M, not on M_2-M_1. Now, since the vapor is removed at the center a low pressure there will mean a small yield, and in this respect the molecular weight is to be considered. However, compensation for the weight can be made with a compound of high vapor pressure at room temperature, thus increasing $p(r)$ and hence $p(0)$.

3. Interpretation of θ

Equation (2) gives only the ratio of the light to heavy abundance at the center to that at the edge. If one wishes to know the change in abundance of the vapor either at the center or at the edge it is necessary to know one member of this ratio apart from the other. Also, if vapor is removed from the center of the rotor at a finite rate the composition of the mixture will never reach a steady value, so x_1 and x_2 will be functions of time as well as distance. The effect on θ of the introduction of the time variable will be calculated in Section 4; however, it will be convenient in the present section to consider θ defined as a function of time dependent mole-fractions (i.e., by Eq. (2) with the restriction $t\to\infty$ removed), and then to modify the results in Section 4.

Let $N_1(t)$ be the total number of molecules 1 at any time t throughout the rotor, $N(t)$ the total number of all molecules present, and $N_1'(t)$ be

[3] C. Skarstrom, H. E. Carr and J. W. Beams, Phys. Rev. 55, 591 (1939).
[4] J. W. Beams, J. App. Phys. 8, 795 (1937).

the number of molecules 1 removed from the rotor. Likewise, in accordance with previous notation, $N_1(r, t)$ is the number of molecules 1 between r and $r+dr$ at time t; $N(r, t)$ the total number of all molecules between r and $r+dr$ at time t, etc. Then

$$x_1(r, t) = N_1(r, t)/N(r, t);$$
$$x_1(0, t) = N_1(0, t)/N(0, t).$$

As in any enrichment method, the rate of change of composition of the residue depends on the number of molecules removed:

$$\partial N_1(t)/\partial t \sim N_1'(t) \quad \text{or} \quad \frac{\partial N_1(t)/\partial t}{\partial N_2(t)/\partial t} = \frac{N_1'(t)}{N_2'(t)}.$$

However, the composition of the vapor removed will of necessity be the same as that at the center, so

$$N_1'(t)/N_2'(t) = x_1(0, t)/x_2(0, t).$$

Except for the negligibly small number of molecules in the vapor state, the total number of molecules 1 in the rotor will be at the edge in the liquid state. Let r_p be the distance from center to periphery—i.e., $r_p \geqslant r \geqslant 0$. Then

$$N_1(t) \leqq N_1(r_p, t).$$

So

$$\frac{\partial N_1(r_p, t)}{\partial N_2(r_p, t)} = \frac{x_1(0, t)}{x_2(0, t)} = \theta\frac{x_1(r_p, t)}{x_2(r_p, t)} = \theta\frac{N_1(r_p, t)}{N_2(r_p, t)}$$

or

$$\log \frac{N_1(r_p, t)}{[N_2(r_p, t)]^\theta} = \text{constant}.$$

Before centrifuging—at time $t=t_0$,

$$N_1(r_p, t) = N_1(r_p, t_0) = N_1(t_0)$$

(there is no significance to the variable r when $t=t_0$).

$$\frac{N_1(r_p, t)}{[N_2(r_p, t)]^\theta} = \frac{N_1(t_0)}{[N_2(t_0)]^\theta},$$

or

$$\frac{N_1(r_p, t)}{N_2(r_p, t)} = \frac{N_1(t_0)}{N_2(t_0)}\left[\frac{N_2(r_p, t)}{N_2(t_0)}\right]^{\theta-1}. \qquad (4)$$

To solve this, assume $\theta - 1 \ll 1$. This is a reasonable assumption—in the actual experiment, θ was 1.0686. Then

$$N_1(r_p, t)/N_2(r_p, t) \leqq N_1(t_0)/N_2(t_0)$$

or

$$N(r_p, t)/N_2(r_p, t) \leqq N(t_0)/N_2(t_0).$$

So

$$\frac{N_2(r_p, t)}{N_2(t_0)} = \frac{N(r_p, t)}{N(t_0)} = \frac{N(t_0) - N'(t)}{N(t_0)} = 1 - \frac{N'(t)}{N(t_0)}.$$

Put $N'(t)/N(t_0) \equiv F$, the fraction of material removed. Substituting in Eq. (4):

$$N_1(r_p, t)/N_2(r_p, t) = [N_1(t_0)/N_2(t_0)][1-F]^{\theta-1}.$$

It is convenient to abbreviate the abundance ratio with the single symbol:

$$K \equiv N_1/N_2 = x_1/x_2.$$

Therefore:

$$K(r_p, t) = K(0, t)/\theta = K(t_0)[1-F]^{\theta-1}. \qquad (5)$$

$K(t_0)$ is the known initial abundance ratio, θ can be calculated from Eq. (2) (which must be corrected as indicated in the following section); so the altered abundance ratio at either the center or the edge can be calculated for an arbitrary "cut" F.

4. Composition of residue

In the centrifuge rotor there are two opposing gradients set up, the concentration gradient and the pressure gradient. Each of these will cause the molecules to diffuse, the former causing a diffusion toward the edge, the latter causing a diffusion toward the center. If no material is removed from the rotor the number of molecules diffusing per second past a given area due to one cause will equal the number due to the other cause—hence equilibrium is established. However, as soon as vapor is removed at the center by pumping this equilibrium is upset and never regained as long as pumping continues. The effect is to increase the number of molecules moving toward the center per second.

Let Q_c be the quantity diffusing per second due to the concentration gradient, Q_p that due to pressure gradient; let Q be the quantity removed per second. Evidently if the diffusion and rate of pumping are uniform, then

$$(\partial/\partial t)(Q - Q_c + Q_p) = 0$$

or

$$Q-Q_c+Q_p=Q_0. \tag{6}$$

To find Q_c: the quantity diffusing per second in a direction perpendicular to an area A under the influence of a concentration gradient $\partial c/\partial r$ is given by

$$Q_c=-DA\partial c/\partial r,$$

where D is the coefficient of diffusion. So if h is the height of the rotor chamber, we have for molecule 1:

$$Q_c=-2\pi rhD\partial c_1(r, t)/\partial r.$$

But

$$c_1(r, t)=x_1(r, t)p(r)/RT$$

so

$$Q_c=-\frac{2\pi rhD}{RT}\frac{\partial}{\partial r}(x_1p),$$

where the explicit indication of the variables contained in x_1 and p has been dropped temporarily for convenience. If equilibrium is not too violently disturbed by the removal of gas we can make the approximation

$$Q_p\cong Q_c=-\frac{2\pi rhD}{RT}\frac{\partial}{\partial r}(x_1p)=-\frac{2\pi rhD}{RT}\frac{\partial}{\partial r}(p_1).$$

If *Eq.* (6) is now written for isotope 1 Q must be replaced by x_1Q, and the equation becomes

$$x_1Q+\frac{2\pi rhD}{RT}\left\{\frac{\partial}{\partial r}(x_1p)-\frac{\partial}{\partial r}(p_1)\right\}=Q_0. \tag{7}$$

This is the equation of mass motion of isotope 1 when vapor is being removed. It is only approximately true since it contains the approximation that $Q_c=Q_p$. To reduce the equation to only one dependent variable consider the following:

$$\frac{\partial}{\partial r}(x_1p)=p\frac{\partial x_1}{\partial r}+x_1\frac{\partial p}{\partial r}=p\frac{\partial x_1}{\partial r}+x_1\left(\frac{\partial p_1}{\partial r}+\frac{\partial p_2}{\partial r}\right).$$

From Eq. (1) and its companion equation for isotope 2, this becomes:

$$\frac{\partial}{\partial r}(x_1p)=p\frac{\partial x_1}{\partial r}+x_1\frac{\omega^2r}{RT}(M_1p_1+M_2p_2)$$

$$=p\left\{\frac{\partial x_1}{\partial r}+x_1\frac{M\omega^2r}{RT}\right\}.$$

Likewise:

$$\frac{\partial p_1}{\partial r}=p_1\frac{M_1\omega^2r}{RT}=x_1p\frac{M_1\omega^2r}{RT}.$$

Collecting, Eq. (7) now reads:

$$x_1Q+\frac{2\pi hDp}{RT}\left\{r\frac{\partial x_1}{\partial r}+\frac{\omega^2r^2}{RT}(M-M_1)x_1\right\}=Q_0.$$

The mean molecular weight M is given by

$$M=M_1x_1+M_2x_2.$$

So

$$(M-M_1)x_1=x_1x_2(M_2-M_1).$$

Put

$$\alpha\equiv 2\pi hDp/RT.$$

Now

$$D=\eta/\rho=\eta RT/pM,$$

where η is the coefficient of viscosity. Then

$$\alpha=2\pi h\eta/M.$$

Since η is independent of pressure, α is independent of r. (This assumes h is constant along r.) Put

$$\beta\equiv x_1(r, t)x_2(r, t)\omega^2(M_2-M_1)/RT.$$

To a first approximation β can be treated as a constant in both r and t, since $x_1(r, t)$ and $x_2(r, t)$ will at best change by only small amounts, their product even less. Such an assumption is comparable to the one $\theta-1\ll 1$ and is valid for the small separations produced by a single centrifugation. It should be noted that it is this assumption that permits a nontrivial solution of Eq. (7), which now reads

$$x_1Q+\alpha(\beta r^2+r\partial x_1/\partial r)=Q_0.$$

Multiplying by $r^{Q/\alpha-1}$ this becomes:

$$\partial/\partial r(r^{Q/\alpha}x_1)=(Q_0/\alpha)r^{Q/\alpha-1}-\beta r^{Q/\alpha+1}$$

or

$$x_1=Q_0/Q-\beta/2r^2[2\alpha/(Q+2\alpha)].$$

At $r=0$, $x_1(r, t)=x_1(0, t)=Q_0/Q$. So

$$x_1(r, t)-x_1(0, t)=-\tfrac{1}{2}\beta r^2[2\alpha/(Q+2\alpha)]$$

$$=-\frac{x_1(r, t)x_2(r, t)v^2}{2RT}(M_2-M_1)\left(\frac{2\alpha}{Q+2\alpha}\right).$$

But

$$\frac{v^2}{2RT}(M_2-M_1)=\log\theta;$$

put $\Delta x_1 \equiv x_1(r,t)-x_1(0,t)$. Then

$$\Delta x_1=-x_1(r,t)x_2(r,t)[2\alpha/(Q+2\alpha)]\log\theta.$$

If there is equilibrium, $Q=0$:

$$(\Delta x_1)_{Q=0}=(\Delta x_1)_{\max}=-x_1x_2\log\theta$$

so

$$\Delta x_1/(\Delta x_1)_{\max}=2\alpha/(Q+2\alpha)\equiv\epsilon. \tag{8}$$

ϵ is a measure of the equilibrium—or rather the degree of approach to equilibrium—for some rate of pumping Q. The effect of disturbing equilibrium is to introduce a value of ϵ less than one. As one would expect, pumping decreases the separation obtained; it has the effect of reducing the separation factor θ to a value θ', where

$$\log\theta'=\epsilon\log\theta.$$

To obtain values for $x_1(r,t)$ and $x_2(r,t)$:

$$K(r,t)=x_1(r,t)/x_2(r,t)=K(t_0)(1-F)^{\theta'-1};$$

$$x_1+x_2=1$$

(now corrected for nonequilibrium); so

$$x_1(r,t)x_2(r,t)=K(r,t)/[K(r,t)+1]^2$$

and

$$\Delta x_1=-\frac{K(r,t)}{[K(r,t)+1]^2}\log\theta'. \tag{9}$$

The average molecular weight is

$$M=x_1M_1+x_2M_2,$$

so

$$\Delta M=M_1\Delta x_1+M_2\Delta x_2=(M_1-M_2)\Delta x_1$$

or

$$\Delta M=\frac{(M_2-M_1)K(r,t)}{[K(r,t)+1]^2}\log\theta'. \tag{10}$$

This gives the molecular weight gradient along the radius of the rotor in terms of measurable quantities of the system.

5. Variation of composition of residue with time

Equation (5) corrected for effective separation factor becomes:

$$x_1(r,t)/x_2(r,t)=[x_1(t_0)/x_2(t_0)](1-F)^{\theta'-1}.$$

Taking logarithms and differentiating with respect to time:

$$\frac{1}{x_1(r,t)}\frac{\partial x_1(r,t)}{\partial t}-\frac{1}{x_2(r,t)}\frac{\partial x_2(r,t)}{\partial t}=(\theta'-1)\frac{\partial}{\partial t}\log(1-F)$$

or

$$\partial x_1/\partial t=x_1x_2(\theta'-1)\partial[\log(1-F)]/\partial t.$$

Integrating, and remembering that to a first approximation x_1x_2 can be considered constant in time, we obtain

$$x_1(r,t)-x_1(t_0)=x_1(r,t)x_2(r,t)(\theta'-1)\log(1-F).$$

Put

$$\delta x_1(r)\equiv x_1(r,t)-x_1(t_0).$$

(The symbol Δ indicates variation along r, δ variation with t.) Consider the expansion of $\log\theta'$ where $0<\theta'<2$:

$$\log\theta'=(\theta'-1)-\tfrac{1}{2}(\theta'-1)^2+\tfrac{1}{3}(\theta'-1)^3-\cdots \cong(\theta'-1).$$

Therefore

$$\delta x_1(r)=x_1(r,t)x_2(r,t)\log\theta'\log(1-F) =-\Delta x_1\log(1-F). \tag{11}$$

Likewise

$$\delta M(r)=-\Delta M\log(1-F). \tag{12}$$

These equations give the change in the residue as a function of the fraction of material removed.

6. Variation of composition of the distillate

By "distillate" is meant the vapor removed by pumping (which is usually accomplished by vacuum distillation).

$$x_1(0,t)=\frac{N_1(t_0)-N_1(r_p,t)-N_1'(t)}{N(t_0)-N(r_p,t)-N'(t)}.$$

If the cut is small, $N_1'(t)$ will be small compared to $N_1(t_0)$ or $N_1(r_p,t)$; then

$$x_1(0,t)=\frac{N_1(t_0)-N_1(r_p,t)}{N(t_0)-N(r_p,t)} =\frac{x_1(t_0)N(t_0)-x_1(r_p,t)N(r_p,t)}{N(t_0)-N(r_p,t)}$$

$$=[x_1(t_0)-(1-F)x_1(r_p,t)]/F.$$

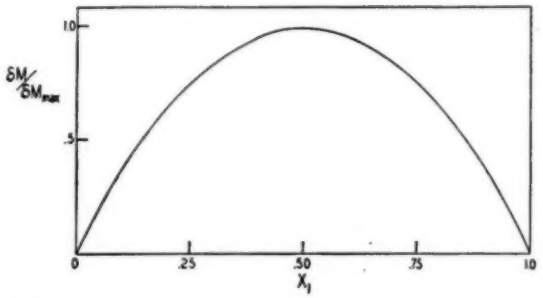

FIG. 1. Variation of change in molecular weight (or isotope abundance) with initial abundance of one isotope.

since $N(t) \cong N(r_p, t)$, and by definition of F:

$1-F=N(r_p, t)/N(t_0)$. Hence:

$$\begin{aligned}\delta x_1(0) &\equiv x_1(0, t) - x_1(t_0) \\ &= -x_1(t_0) + [x_1(t_0) - (1-F)x_1(r_p, t)]/F \\ &= -(1-F)\delta x_1(r)/F.\end{aligned}$$

So

$$\delta x_1(0) = (1-F)\Delta x_1[\log (1-F)]/F \quad (13)$$

and

$$\delta M(0) = (1-F)\Delta M[\log (1-F)]/F. \quad (14)$$

These equations are valid only for small cuts. However, this is the only case of interest since the enrichment in the distillate is appreciable only for small cuts.

7. Variation of composition with abundance ratio

For either the residue or distillate

$$\delta M = Cx_1x_2 = C(x_1 - x_1^2),$$

where C includes factors not dependent on x_1 or x_2. δM is a maximum for $x_1=x_2=\frac{1}{2}$, falls only 25 percent when $x_1=\frac{1}{4}$ or $\frac{3}{4}$, but diminishes rapidly for values of x_1 outside this range as the graph of Fig. 1 illustrates. Hence, as pointed out by Mulliken,[2] the method when applied to a relatively rare isotope yields relatively poorer separations.

Several of the above problems were first worked out by Mulliken[2] on the assumption that equilibrium obtained at all times. The present theory can be made to yield all of his results by assuming $Q=0$. Hence, though the method of attack differs somewhat the results upon simplifying are identical.

EXPERIMENTAL PROCEDURE

The centrifuge constructed for this work was the so-called "vacuum" type air-driven ultracentrifuge developed by Beams.[4] The duralumin rotor was double-cone shaped with an outer diameter of four inches, an inner diameter of 3.5 inches, and an average height of 0.8 inch. When operating at 1500 r.p.s.—about 90 percent of bursting speed—there was produced at the inner diameter a centrifugal field of 388,000 g, a peripheral speed of 400 meters/sec. The details of construction and operation followed closely those recommended by Beams.[4]

In order to illustrate the advantage of centrifugation a heavy isotope is to be desired. It has been pointed out that the separation produced is a maximum for an isotope abundance of one to one. Both these characteristics are combined in the $Br^{79}Br^{81}$ isotopes which have relative abundances of 50.4 : 49.6. For a mass difference of two, a peripheral velocity of 4×10^4 cm/sec. and room temperature, $\theta=1.0686$. This is the separation factor for equilibrium. It must next be decided what degree of equilibrium will be permitted—i.e., what value of ϵ (Eq. (8)) will be arbitrarily assumed; this in turn is governed by the rate of pumping Q. Assume ϵ to be 0.9. This reduces the separation factor to its effective value, 1.0615. To calculate 2α the molecule containing the bromine isotopes must be decided upon. Its chief characteristic must be a high vapor pressure at room temperature; in addition, of course, it must be nonreactive with the centrifuge, readily obtainable, etc. Such a compound is found in ethyl bromide, whose vapor pressure at room temperature is 386 mm. The other constituents of the molecule have isotopic abundances small compared to that of bromine. The coefficient of viscosity for C_2H_5Br is 1.87×10^{-4} poise. Then

$$2\alpha = 43.12\times10^{-6} \text{ g mol/sec.}$$
$$Q = 4.78\times10^{-6} \text{ g mol/sec.}$$

As with ϵ the value of F rests on an arbitrary choice, depending on the quantity of separated material desired and the initial quantity added to the rotor. In this work 10 cc (14 g) of liquid was introduced into the rotor, one cc removed. If this one cc is the first cc pumped out it will be enriched with light isotope, if the last cc the heavy will have gained. A plot of enrichment $K(0, t)$ against cut F, related by Eq. (5), is given in Fig. 2. The enrichment changes slowly for the first tenth or two and quite rapidly for the last

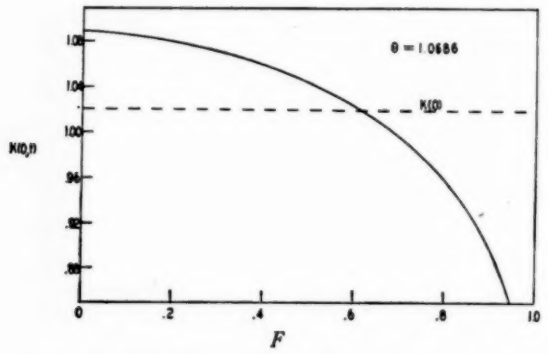

FIG. 2. Variation of isotopic abundance ratio at the center of rotor with fraction of material removed.

tenth. A conspicuous feature of the curve is its lack of symmetry with the $K(0)$ line—the first fraction removed will not have as large an enrichment in Br^{79} as the last fraction will have in Br^{81}. To obtain an equal enrichment of Br^{79} the first fractions must be recentrifuged. Now from the value of Q just calculated it is seen that to pump one cc of liquid requires 45 minutes (for $\epsilon=0.9$). Hence, the first cc necessitates only 45 minutes of running but must be recentrifuged, the last cc requires 7.5 hours of continuous running, any break in which will vitiate the results. The choice of these two procedures rests on the choice of isotope whose enrichment is desired and on the mechanical difficulties involved in operating the centrifuge.

In the present work an enrichment of Br^{79} was attempted, collecting one cc from five centrifugations and recentrifuging, removing one cc. Thus $F_1=0.1$; $F_2=0.2$. The change in abundance ratio can be calculated by applying Eq. (13) twice; it is thus found that the ratio will change from 50.4 : 49.6 to 53.1 : 46.9, an increase of 11 percent. This corresponds to a decrease in molecular weight (Eq. (14)) of 0.054 unit.

The collection system was designed to handle small quantities of a volatile liquid with a minimum loss. All transport of material was done by vacuum distillation. A calculation with Eq. (3) shows a pressure ratio of 40 to one from edge to center of the rotor; this means a pressure of ethyl bromide of one cm at the center; therefore to distill the ethyl bromide into the rotor it is only necessary to start the centrifuge rotating. To distill the material out of the rotor liquid air is used to cool a trap for solidifying the vapor. To adjust the rate of removal to one cc of liquid per 45 minutes capillary tubing was introduced into the line; this capillary was by-passed when distilling liquid into the rotor. A system of traps which could be permanently sealed off permitted segregation of different fractions.

RESULTS

The enrichment obtained was determined spectroscopically by means of relative intensity measurements of isotopic lines in the absorption spectrum of Br_2. For this molecule the isotope splitting of lines is a maximum, but the structure of the bands, though well analyzed, is very complex.[5] An alternative molecule is HBr^+ whose spectrum is open and unambiguous, but for bands near the system origin has only negligibly small isotope splitting, and thus requires interferometric apparatus for satisfactory resolution. This latter complication was thought to outweigh the advantage of increased accuracy; furthermore the absorption spectrum of Br_2 entails no loss of material, an important feature when dealing with small quantities.

The ethyl bromide was converted to bromine by adding an alcoholic solution of silver nitrate, washing and drying the silver bromide which precipitated out, and then heating the AgBr with concentrated sulphuric acid and manganese dioxide to liberate Br_2. This last operation was performed in an appendix tube connected to a 1.5-meter absorption tube. Five-hour exposures were required with the bromine vapor at a pressure of 66 mm to produce satisfactory spectrograms. The dispersion instrument was a 21-foot concave grating with 30,000 lines to the inch, mounted in an Eagle mounting. The (9,2) band at 6050A was found to be relatively free of overlapping bands. Standard photometric technique using a step filter calibrated with a photoelectric cell was applied to nine lines to obtain their relative intensities. These lines yielded 26 intensity ratios which could be compared to corresponding ratios obtained with normal bromine.

The result of these comparisons indicated an increase in the abundance ratio of everywhere from 8.8 to 13.1 percent with an average value of 11 percent, a mean deviation from the average

[5] W. G. Brown, Phys. Rev. **39**, 777 (1932).

of 1 percent. It will be recalled that the theory predicted a change of 11 percent.

When attempts were made to obtain an enrichment of Br^{81} chemical reaction of the C_2H_5Br with the duralumin rotor occurred. Apparently, under high centrifugal stress a sort of Grignard reaction was induced; the loss of C_2H_5Br was serious enough to prevent a successful separation of the last one cc. Recently it has been found that an alumilite coating (an anodic treatment of aluminum oxide) will protect the duralumin from reaction, at least for a while. It is hoped that this will permit long runs without reaction.

Conclusions

The agreement between the predicted and experimental values of the enrichment is not too significant in view of the rather spacious assumptions made in the theory and the wide spread of deviations found in the data. The major cause of these latter variations can be found in the photometric determination of line intensities in such a complex spectrum as Br_2. It is evident, though, that the agreement is good qualitatively and reasonably good quantitatively.

Compared with other methods for separating *heavy* isotopes the enrichment is sufficiently large to give some promise to centrifugation as a method of separating isotopes.

The author wishes to acknowledge his indebtedness to Professor Lars Onsager for assistance received with the theory here presented, and to Professor W. W. Watson for his direction of this research and for his able advice and assistance.

OCTOBER 1, 1939 PHYSICAL REVIEW VOLUME 56

The Accommodation Coefficient of Helium on Nickel*

Barbara Raines
Department of Physics, Bryn Mawr College, Bryn Mawr, Pennsylvania
(Received July 26, 1939)

The thermal accommodation coefficient of helium on gas-free "A" nickel was measured at the temperatures 90, 195, 273 and 369°K, and was found to be 0.048, 0.060, 0.071 and 0.077, respectively (±0.004). In the presence of the gas the accommodation coefficient rose rapidly to the equilibrium values 0.413, 0.423, 0.360 and 0.343, respectively (±0.012). Using the theory of A. F. Devonshire and the observed values of α_0, calculations were made of the two constants of the interaction potential between a helium and a nickel atom. The results obtained were $\kappa=(0.75\pm0.05)\times10^8$ cm^{-1} for the exponential decay constant, and $D=(430\pm60)$ cal./mol for the heat of adsorption of helium on nickel. At the two lower temperatures the thermal conductivity of "A" nickel was measured. The values obtained were (0.74±0.04) watt/cm²/deg. at 90°K, and (0.71±0.04) watt/cm²/deg. at 195°K.

FOLLOWING the work of Roberts[1] who showed that the accommodation coefficient of a gas on a clean (that is, gas-free) metal surface was much smaller than that on a gas-covered surface, investigations of the exchange of energy between a gas and a hot solid have proceeded along two lines. In the first, interest is centered on the properties of the clean metal; in the second, on the detection and investigation of films of adsorbed gas. The present work belongs in the former category and is concerned with surface films only to the extent that they must be removed.

Experimental Details

1. Apparatus

In most respects the apparatus used and the procedure followed was similar to that of Roberts.[1]

The metal to be investigated was in the form

* This paper represents the publication in part of a dissertation submitted to the faculty of Bryn Mawr College in partial fulfillment of the requirements for the degree of Doctor of Philosophy.

[1] J. K. Roberts, Proc. Roy. Soc. **A129**, 146 (1930); **A135**, 192 (1932); **A142**, 518 (1933).

of a filament of nickel "A" wire, 14.86 cm long and 0.00423 cm in diameter. The filament, held taut by tungsten springs, was mounted along the axis of a Pyrex tube 1 cm in diameter. The tube was enclosed in a constant temperature bath so that the walls of the tube and the ends of the wire were maintained at a fixed temperature while the wire was heated above its surroundings by the passage of an electric current. (Liquid air, CO_2-snow-and-acetone, shaved ice and water provided three fixed temperatures. For the highest temperature (369°K) an SAE 20 oil bath was used.) The bath temperature was measured by means of two chromel-alumel thermocouples placed less than 0.5 cm from the tungsten-to-glass seals of the experimental tube.

The potential drop across the tube and across a 10-ohm standard resistance in series with the tube was measured by means of a Queen Gray potentiometer. From these measurements the fundamental experimental quantities, namely, the resistance of the tube and the power input, were determined.

The vacuum system was designed so that the pressure in the experimental tube was controlled by means of two stopcocks, *A* and *B*, in series, placed between the high and low vacuum sides of the mercury diffusion pump. When stopcock *A* was closed the pressure in the tube was maintained at about 10^{-6} mm Hg. When stopcock *A* was open, helium circulated through the tube at a pressure (of the order of 10^{-3} mm Hg) determined by the setting of stopcock *B*. Pressures were measured by means of a McLeod gauge in shunt with the tube.[2] The helium was purified by circulation over a misch metal arc. After a few hours of operation the helium was spectroscopically pure, except for the presence in the misch metal bottle of mercury vapor which was prevented from reaching the tube by the interposition of traps. These traps were filled with liquid air when tube measurements at that temperature were being made; at other times CO_2-snow-and-acetone was used as the refrigerant.

[2] The values of the accommodation coefficient reported here differ somewhat from those presented in a preliminary report (Phys. Rev. **55**, 684 (1939)) because later consideration showed that a different pressure correction should have been applied, to take into account the difference in temperature between the McLeod gauge and the tube.

2. Procedure

After the initial bake-out at 450°C the wire was flashed repeatedly in vacuum until further flashing at 950°C produced no further change in the resistance at 0°C. Some of the difficulties encountered in this process of aging the nickel wire have been described in a previous paper.[3] When, after prolonged heat treatment, the wire became stable, the vacuum system was cut off from the fore pump and helium introduced. The system was then ready for the investigation proper.

It has been amply shown[1, 4] that, at the temperatures at which the present work was done (under 400°K), the surface of the metal cannot be kept free from contamination in the presence even of spectroscopically pure helium. It is necessary, therefore, to begin either with a hot wire or with a previously cleaned wire in vacuum, and to measure the accommodation coefficient as a function of time, in order that α_0, the accommodation coefficient for a clean wire, may be determined by extrapolation. The former method has been used by Roberts;[1] the latter, by Mann and Newell.[5] Both have been tried by the author and the second found to possess distinct advantages.

Whichever method is adopted the primary measurement is that of the variation of the resistance of the wire with time. If the wire is flashed in the presence of the gas, and the zero of time taken when the flashing current is cut off, then the resistance drops rapidly because of the cooling of the wire at the same time that it drops because of the gradual increase in the accommodation coefficient which results from the building up of a surface film on the metal. Even if a determination is made of the time taken for the disturbance due to flashing to die down (in Roberts' case this was about four minutes), and if only later values of the resistance are used to determine α, it is still necessary, in order to find α_0, to extrapolate over a considerable interval (about four minutes) during which the accommodation coefficient can be expected to have been changing most rapidly. If, on the other

[3] B. Raines, Phys. Rev. **54**, 481 (1938).
[4] W. B. Mann, Proc. Roy. Soc. **A146**, 776 (1934).
[5] W. B. Mann and W. C. Newell, Proc. Roy. Soc. **A158**, 397 (1937).

hand, after flashing in vacuum, the resistance is measured as a function of time until it becomes stable, and *then* gas is admitted, any change in resistance thereafter is due to the additional heat loss to the gas. This loss is proportional to αp (the product of accommodation coefficient and pressure) and is known to be zero at the time the gas was admitted. A simple auxiliary experiment suffices to determine the variation of pressure with time after admission of the gas. Hence α, the ratio of the ordinates of the αp and p curves, can be determined for times as little as 15 sec. after the time of admission of the gas. Although αp and p both approach zero as time approaches zero, their ratio does not, and the intercept value (see Fig. 2) gives α_0, the required accommodation coefficient for the gas on a clean wire. The results reported in the present paper were obtained by this method.

Figure 1 shows a typical curve for the variation of the resistance of the tube with time after flashing.* It can be seen that the change in resistance due to cooling took place over a longer time than did the change in resistance due to increasing heat loss to the gas. Hence, in this work, it was impossible to use the first method of determining α_0.

After taking the data for the curve shown in Fig. 1, the resistance R was measured as a function of power input Q. The temperature excess of the wire was always less than 10°C, so that $R=f(Q)$ was a straight line whose intercept value gave R_0, the resistance of the wire at bath temperature. In this connection it should be noted that all measurements of resistance were taken with the current flowing first in one and then in the reverse direction, in order to eliminate errors due to thermal e.m.f.'s. The order of magnitude of these e.m.f.'s was such that when this precaution was not observed, the curve of (apparent) resistance against power showed large departures from linearity. The tube was then re-evacuated and its resistance in vacuum again determined. In each case $(R-R_0)$ agreed closely with that found just before the gas was admitted, showing that the wire had returned to its former condition, and that the contamination had been superficial.

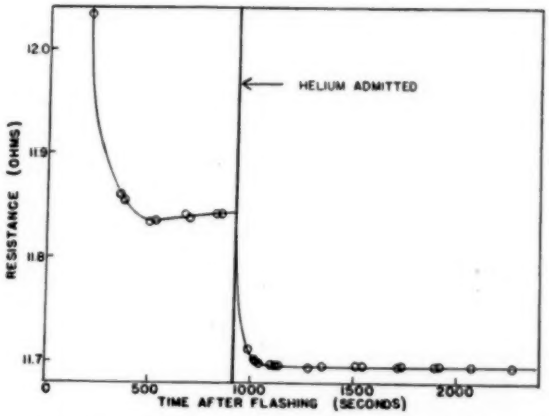

FIG. 1. Variation of the resistance of the wire (273°K) with time after flashing. The drop in resistance after helium is admitted is due entirely to loss of heat to the gas.

RESULTS

The equation for the distribution of temperature along a current-bearing wire whose ends are maintained at a fixed temperature has been developed by Roberts and extended by Michels and Cox[6] to a filament supported by springs. Michels and Cox, however, made no correction for the increase in resistivity due to heating of the wire. When this correction is made, and account is taken of heat lost to the gas as well as by radiation and by conduction through the ends, the differential equation obtained

$$d^2t/dx^2-At+B=0,$$

and the solution:

$$t=\frac{B}{A}\left[1+\frac{\sinh A^{\frac{1}{2}}(x-L)-\sinh A^{\frac{1}{2}}x}{\sinh A^{\frac{1}{2}}L}\right]$$

remain the same in form, but the constants A and B have the values

$$A=\frac{8e\sigma T^3}{aK}+\frac{2}{aK}\left(\frac{2R}{\pi\mu T}\right)^{\frac{1}{2}}\alpha p-\frac{I^2\rho_0 C}{\pi^2a^4K}$$

and

$$B=I^2\rho_0/\pi^2a^4K-A\Delta T$$

for the filament, and

$$A_s=\frac{8e_s\sigma T^3}{a_sK_s}+\frac{2}{a_sK_s}\left(\frac{2R}{\pi\mu T}\right)^{\frac{1}{2}}\alpha p-\frac{I^2\rho_{s0}C_s}{\pi^2a_s^4K_s}$$

* The slight but unmistakable increase in resistance between 500 and 900 sec. is to be attributed to a real change in the resistivity of the wire. This creep of the resistance of the nickel to a stable value was always observed after flashing. In this curve it is unnoticeable after 900 sec. but it sometimes persisted longer.

[6] W. C. Michels and M. Cox, Physics **7**, 153 (1935).

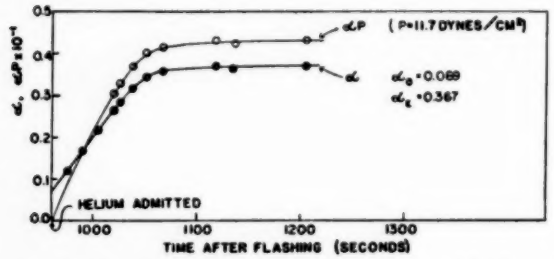

FIG. 2. The αp curve shows the variation with time of the heat lost to the gas. The α curve is obtained by dividing αp by the pressure which attains its equilibrium value (11.7 dynes/cm²) one minute after admission of the gas.

and

$$B_s = I^2\rho_{s0}/\pi^2 a_s^4 K_s$$

for the springs.

The mean temperature excess for the filament is*

$$\bar{t} = \frac{B}{A}\left[1+\frac{2(1-\cosh A^{\frac{1}{2}}L)}{A^{\frac{1}{2}}L\sinh A^{\frac{1}{2}}L}\right]$$

and for the springs,*

$$\bar{t}_s = \frac{a^2K}{a_s^2K_s}\frac{B}{A^{\frac{1}{2}}}\frac{(\cosh A^{\frac{1}{2}}L-1)}{\sinh A^{\frac{1}{2}}L}\frac{(1-\operatorname{sech} A_s^{\frac{1}{2}}L_s)}{A_sL_s} + \frac{B_s}{A_s}\left[1-\frac{\tanh A_s^{\frac{1}{2}}L_s}{A_s^{\frac{1}{2}}L_s}\right].$$

The temperature excess at the junction of filament and springs is:*

$$\Delta T = \frac{a^2K}{a_s^2K_s}\frac{B}{A^{\frac{1}{2}}}\frac{(\cosh A^{\frac{1}{2}}L-1)}{\sinh A^{\frac{1}{2}}L}\frac{\tanh A_s^{\frac{1}{2}}L_s}{A_s^{\frac{1}{2}}} + \frac{B_s}{A_s}(1-\operatorname{sech} A_s^{\frac{1}{2}}L_s).$$

In order to compute the heat loss to the gas, from which αp and then α are determined, it is necessary to know the losses due to radiation and to conduction through the ends. In addition to easily-measured properties of the nickel wire (such as resistance and diameter), these losses depend, respectively, on the total emissivity (e) and the thermal conductivity (K) of the wire. When the pressure is reduced to about 10^{-6} mm Hg, the gas loss is negligible, and (from the value of $(R-R_0)$ just before the gas was admitted) either the radiation loss (and hence e) or the conduction loss (and hence K) can be determined provided the other is known.

A search of the literature revealed no data on the total emissivity of nickel in the required temperature range, and it therefore remained to select from the many determinations of the thermal conductivity of nickel (above room temperature) the set of data most likely to be representative of the specimen of nickel used in this experiment. The data of van Dusen and Shelton[7] on commercial malleable nickel were chosen and after making a slight extrapolation to 0°C, the values of total emissivity shown by the circles of curve I, Fig. 3, were obtained. For the two lower temperatures (195 and 90°K), the radiation loss is small, and it was therefore thought preferable to estimate e and to compute K. Hence a smooth curve (curve I, Fig. 3) was passed through the computed points and (0, 0), roughly following the variation to be expected if $e \propto (\rho T)^{\frac{1}{2}}$. As questionable as the procedure looks at first glance, in all probability it produces a very small error, for the variation in e indicated by the dotted lines of curve I, Fig. 3 would cause only a two-percent variation in K.

The mean values of thermal conductivity found were 0.74 watt/cm²/deg. at 90°K and 0.71 watt/cm²/deg. at 195°K. The internal consistency was about one percent, but the probable error can conservatively be estimated at five percent to allow for systematic errors. It can be seen (curve II, Fig. 3) that the values

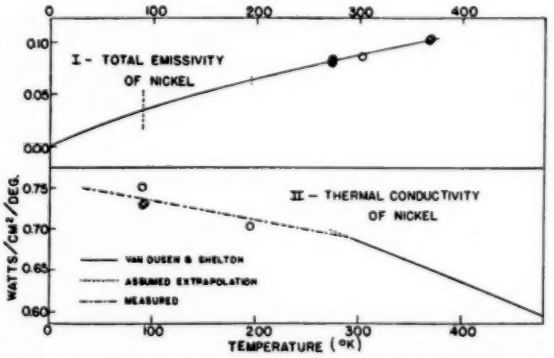

FIG. 3. At 273°K and above, the total emissivity of nickel was determined, using values of thermal conductivity obtained by van Dusen and Shelton. Below 273°K the thermal conductivity was determined, using values of the total emissivity from curve I.

* Because of typographical or algebraic errors in the Michels and Cox paper, the expressions for $\bar{t}$, $\bar{t}_s$, and ΔT are incorrectly printed. They should read as above.

[7] M. S. van Dusen and S. M. Shelton, Nat. Bur. Stand. J. Research 12, 429 (1934).

obtained join fairly smoothly onto those of van Dusen and Shelton.

The Accommodation Coefficient

The results for the accommodation coefficient of helium on grade "A" nickel are shown in Table I.

The results are in fair agreement with Roberts'[1] observed value of 0.085 for α_0 (He on Ni) for a temperature somewhat above room temperature. Nevertheless, the fact that he gets a bigger α_0 for a smaller equilibrium value (0.20) lends point to the argument that changes in α might have been more rapid, during the first four minutes after flashing, than was indicated by the best extrapolation that could be made.

That the wire was stable when the measurements (of Table I) were made can be inferred not only from the consistency of the determinations at one temperature, but from the smooth variation from highest to lowest temperature, despite the chronological order in which the determinations were made.

Among the many theories of the thermal accommodation coefficient which have appeared in recent years, that of Devonshire[8] is the only one which takes into account, as an integral part of the development, the attractive field which is known to exist between a solid and a gas. Hence the interpretation of the results presented here will be confined to considerations suggested by his treatment. His formula for the thermal accommodation coefficient contains as parameters two constants of the interaction potential between a gas and a solid atom: D, the heat of adsorption of the gas on the solid, and κ, the exponential decay constant. Using $\kappa=0.75\times10^8$ cm^{-1}, $D=428$ cal./mol, and applying the correction factor 1.04 to raise slightly the absolute values of α_0, one obtains theoretical values for the accommodation coefficient which are in striking agreement with the experimental results. This is shown clearly in Table II. The estimation of the precision of this determination of the field constants is, however, a matter of some difficulty. On the one hand, the experimental values of the accommodation coefficient have not been corrected for the roughness of the surface of the wire. They are therefore too high by a factor which is larger than 1, and possibly larger than 2.[1] On the other hand, as Devonshire points out, because of his use of a one-dimensional model, the theoretical values are too large by a factor between 1 and 2. Hence it was thought advisable to find another pair of values of D and κ which would give the observed temperature variation as before, but which would require a correction factor of approximately 1.5 to bring the absolute values into agreement with experiment. Then the difference between these two sets of values could be used as an estimate of the probable error. The values $\kappa=0.70\times10^8$ cm^{-1}, $D=373$ cal./mol were found to satisfy these requirements. On this basis, the constants of the interaction potential between helium and nickel can be given as $\kappa=(0.75\pm0.05)\times10^8$ cm^{-1} and $D=(430\pm60)$ cal./mol.

In conclusion it is a pleasure to thank Professor Walter C. Michels for his interest and advice during the course of this work. I am indebted also to a bequest of the late Marion E. Reilly which made possible the purchase of some of the essential apparatus.

Table I. *Accommodation coefficient of helium on nickel.*

	Accommodation Coefficient		
T°K	α_0 gas-free surface	α_e equilibrium value, gas-covered surface	Chronological order of determinations
369	0.077±0.004	0.343±0.012	7
273	0.069	0.357	1
	0.073	0.362	2
195	0.060	0.423	3
90	0.056	0.395	4
	0.046	0.417	5
	0.042	0.426	6

Table II. *Comparison of observed accommodation coefficients with those computed from Devonshire's theory.*

	Accommodation Coefficient He-Ni		
		Computed (Devonshire's theory)	
T (°K)	Observed (mean values)	$\kappa=0.75\times10^8$ cm^{-1} $D=428$ cal./mol corr. fact. 1.04	$\kappa=0.70\times10^8$ cm^{-1} $D=373$ cal./mol corr. fact. 1.56
369	0.077	0.077	0.080
273	0.071	0.070	0.071
195	0.060	0.061	0.060
90	0.048	0.047	0.044

[8] A. F. Devonshire, Proc. Roy. Soc. **A158**, 269 (1937).

Variational Atomic Wave Functions

LEO GOLDBERG
Harvard College Observatory, Cambridge, Massachusetts,

AND

ALBERT M. CLOGSTON
George Eastman Research Laboratory of Physics, Massachusetts Institute of Technology, Cambridge, Massachusetts

(Received August 3, 1939)

The energy tables constructed by Morse, Young, and Haurwitz to facilitate the variational computation of wave functions for atoms containing $1s$, $2s$, and $2p$ electrons have been extended to include $3p$ and $3d$ electrons. The best parameters, total energies, and term values are given for the states $(1s3d)$ $^1D, ^3D$; $(2p^2)$ $^3P, ^1D, ^1S$; and $(1s^23d)$ ^2D of the atoms He, Li, Be, B, C, N, O, F and Ne, and for $(1s3p)$ $^1P, ^3P$ of He I. It is shown that the observed energies of the $1snd$ states of He I are very accurately reproduced with the use of hydrogenic radial wave functions for both the $1s$ and nd electrons.

IN an earlier paper, Morse, Young and Haurwitz[1] described the construction of a set of tables that were employed to calculate simple, variational wave functions for atomic states involving $1s$, $2s$, and $2p$ electrons. The tables have now been extended[2] to include $3p$ and $3d$ electrons, and the present note gives the results of variational calculations on the states $1s3p$, $1s3d$, $2p^2$, and $1s^23d$. The following wave functions were utilized in the computations:

$$1s \quad u_1(r)=(\mu^3a^3/\pi)^{\frac{1}{2}}e^{-\mu ar},$$

$$2p \quad u_3(r)=(\mu^5c^5/\pi)^{\frac{1}{2}}r\cos\theta e^{-\mu cr},$$

$$3p \quad u_6(r)=(2\mu^7/15\pi N^2)^{\frac{1}{2}}r\cos\theta \times[(5/\mu)Ae^{-\mu dr}-re^{-\mu r}], \tag{1}$$

$$3d \quad u_9(r)=(\mu^7f^7/18\pi)^{\frac{1}{2}}r^2(3\cos^2\theta-1)e^{-\mu fr}.$$

The constant A, which makes u_6 orthogonal to u_3, is given by:

$$A=(d+c)^5/(1+c)^6. \tag{2}$$

In order to avoid the use of more than three parameters in the calculations for the $1s3p$ configuration, we have made the following simplification to eliminate the parameter c. An inspection of the results obtained by Morse, Young and Haurwitz[1] for the $1s2s$ and $1s2p$ configurations shows that the screening of the inner electron by the outer one is negligible for those states. We have accordingly assumed in the $1s3p$ calculations for He I that $a\mu=2.00$. The value of $c\mu$ in the $1s3p$ calculations must be equivalent to that obtained for $1s2p$. Therefore, the ratio $c/a=\beta$ is taken as constant for $1s2p$ and $1s3p$. Eq. (2) then becomes

$$A=(d+\beta a)^5/(1+\beta a)^6, \tag{3}$$

where $\beta(^3P^0)=0.275$, and $\beta(^1P^0)=0.245$.

The procedure followed in obtaining the best values of the energies and the parameters is precisely that outlined in the earlier paper. We define the following integrals:

$$\mu^2T_n=-\int \bar{u}_n\nabla^2u_n dv, \quad \mu V_n=2\int (u_n^2/r)dv,$$

$$\mu V_{nm}=2\int [u_n^2(r_1)u_m^2(r_2)/r_{12}]dv_1dv_2, \tag{4}$$

$$\mu X_{nm}=2\int [\bar{u}_n(r_1)\bar{u}_n(r_2)u_m(r_1)u_m(r_2)/r_{12}]dv_1dv_2.$$

The energy W of any atomic state is then

$$W=\mu^2T+\mu V, \tag{5}$$

where T is a linear combination of the T's, and V a linear combination of the V's and X's. Both T and V are independent of μ, and hence the energy is minimized analytically with respect to this parameter. We obtain

$$\mu=-V/2T, \tag{6}$$

and

$$W=-V^2/4T. \tag{7}$$

[1] Morse, Young and Haurwitz, Phys. Rev. **48**, 948 (1935).

[2] The extensions to the tables are being mimeographed; those interested in obtaining copies should write to the Physics Department, Massachusetts Institute of Technology, Cambridge, Massachusetts.

TABLE I. *Wave function parameters and energies.*

ATOM	He	Li	Be	B	C	N	O	F	Ne
				TWO-ELECTRON STATES					
				$(2p^2)$ ^3P *State*					
$2c\mu$	1.672	2.672	3.672	4.672	5.672	6.672	7.672	8.672	9.672
W_{cal}	1.398	3.570	6.741	10.913	16.085	22.257	29.429	37.601	46.772
$\text{Term}_{cal}\times10^{-6}$	−0.2856	−0.5959	−1.016	−1.546	−2.185	−2.935	−3.794	−4.762	−5.841
				$(2p^2)$ ^1D *State*					
$2c\mu$	1.630	2.630	3.630	4.630	5.630	6.630	7.630	8.630	9.630
W_{cal}	1.328	3.458	6.587	10.717	15.847	21.976	29.106	37.236	46.365
$\text{Term}_{cal}\times10^{-6}$	−0.2932	−0.6082	−1.033	−1.567	−2.212	−2.966	−3.829	−4.802	−5.886
				$(2p^2)$ ^1S *State*					
$2c\mu$	1.566	2.566	3.566	4.566	5.566	6.566	7.566	8.566	9.566
W_{cal}	1.227	3.293	6.360	10.426	15.492	21.559	28.625	36.692	45.758
$\text{Term}_{cal}\times10^{-6}$	−0.3043	−0.6262	−1.058	−1.599	−2.250	−3.011	−3.882	−4.862	−5.952
				$(1s3d)$ ^3D *State*					
a	6.00	4.50	4.00	3.75	3.60	3.50	3.43	3.38	3.33
$a\mu$	2.00	3.00	4.00	5.00	6.00	7.00	8.00	9.00	10.00
$3\mu f$	1.00	2.00	3.00	4.00	5.00	6.00	7.00	8.00	9.00
W_{cal}	4.1111	9.4447	17.0006	26.7789	38.7790	53.0022	69.4465	88.113	109.005
W_{exp}	4.1113	9.4450							
Term_{cal}	12190	48800	109800	195210	304960	439190	597680	780600	988200
Term_{exp}	12209	48834							
				$(1s3d)$ ^1D *State*					
a	6.00	4.50	4.00	3.75	3.60	3.50	3.43	3.38	3.33
$a\mu$	2.00	3.00	4.00	5.006	6.00	7.00	8.00	9.00	10.00
$3\mu f$	1.00	2.00	3.00	4.00	5.00	6.00	7.00	8.00	9.00
W_{cal}	4.1111	9.4443	16.9997	26.7772	38.7768	52.9989	69.4428	88.108	108.999
W_{exp}	4.1112	9.4447							
Term_{cal}	12190	48760	109700	195030	304720	438830	597280	780000	987500
Term_{exp}	12206	48804							

	$He(1s3p)$ $^3P^0$ *State*	$He(1s3p)$ $^1P^0$ *State*
a	6.29	6.15
$a\mu$	2.00	2.00
d	1.54	1.00
$d\mu$	0.490	0.325
3μ	0.954	0.975
W_{cal}	4.115	4.109
W_{exp}	4.116	4.110
Term_{cal}	12600	12000
Term_{exp}	12730	12080

ATOM	Li	Be	B	C	N	O	F	Ne
			THREE-ELECTRON STATES					
			$(1s^23d)$ ^2D *State*					
a	8.06	5.54	4.69	4.27	4.01	3.84	3.72	3.63
$a\mu$	2.69	3.69	4.69	5.69	6.69	7.69	8.69	9.69
$3f\mu$	1.00	2.00	3.00	4.00	5.00	6.00	7.00	8.00
W_{cal}	14.5556	27.6399	44.9458	66.4740	92.2244	122.1970	156.3919	194.8106
W_{exp}	14.6710	27.7520	45.0603	66.5721				
Term_{cal}	12200	48800	109900	195200	305000	439200	597700	780900
Term_{exp}	12203	48828	109861	195292	305210	439506	598004	
$^2D_{3/2}{}^3-D_{5/2\ cal}$	0.036	0.58	2.91	9.26	22.4	46.7	86.2	147
$^2D_{3/2}-{}^2D_{5/2\ exp}$				11.3			108	

The results of the present calculation are shown in Table I. No difficulty was encountered in obtaining energy minima for any but the $3\,^1P^0$ level. For this state the energy was first computed over the range from $d=2.00$ to $d=1.00$. It appeared from the run of the energies that the minimum lay close to the value $d=1.00$. This value of d corresponds to the same average screening in both the inner and the outer parts of the electron orbit. In order that the minimization might be carried out accurately, the energies were computed for values of d less than

unity. These computations indicated a point of inflection at $d=1.00$. The failure of the energy to minimize properly is probably due to the fact that the $3\,{}^1P^0$ function was made orthogonal to an approximate $2\,{}^1P^0$ function rather than to the true one. It is difficult to visualize a value of d less than unity, which would mean a more effective screening for r small than for r large. We have consequently adopted the value $d=1.00$ as close to the correct one. The resulting energy, obtained from the minimization with respect to a, is in satisfactory agreement with the observed term value. Furthermore, the average effective charge, 3μ, is 0.975, as compared with the value 0.97 obtained for the $2\,{}^1P^0$ level.

The quantity $3\mu f$ may be regarded as the average effective charge on the $3d$ electron. Table I shows that $3\mu f=Z$ for the $1s3d$ and $1s^23d$ configurations throughout the He I and Li I isoelectronic sequences. This result means that the screening by the inner electrons is probably negligible for the entire array of $1snd$ and $1s^2nd$ configurations. We may consequently seek to derive general expressions for the energy integrals by adopting hydrogenic $1s$ and nd wave functions. We write the hydrogenic functions in the following form:

$$u_{1s}=(\mu^3/\pi)^{\frac{1}{2}}e^{-\mu r}, \tag{8}$$

$$u_{nd}=\left[\frac{5\mu^7(n+2)\,!}{2^3n^8 4\pi(n-3)\,!(5\,!)^2}\right]^{\frac{1}{2}}(3\cos^2\theta-1)r^2 \times e^{-\mu r/2n}F(-n+3,\,6,\,\mu r/n), \tag{9}$$

where F is the confluent hypergeometric function:

$$F(\alpha,\gamma,x)=1+\frac{\alpha}{1!\gamma}x+\frac{\alpha(\alpha+1)}{2!\gamma(\gamma+1)}x^2+\cdots. \tag{10}$$

The parameter μ is retained as a scale constant, which may be evaluated from (6). The functions (9) will be exactly hydrogenic, provided that $\mu=Z$. The extent to which μ deviates from Z measures the degree by which the functions deviate from orthogonality.

To calculate the energies, we need to evaluate the following integrals:

$$T_{nd}=\frac{N^2}{\mu^2}\int_0^\infty r^6e^{-\mu r/n}(\mu/r-\mu^2/4n^2) \times F^2(-n+3,\,6,\,\mu r/n)dr, \tag{11}$$

$$V_{nd}=\frac{2N^2}{\mu}\int_0^\infty r^5e^{-\mu r/n}F^2(-n+3,6,\mu r/n)dr, \tag{12}$$

$$V_{1snd}=\frac{2N^2}{\mu}\int_0^\infty r^5e^{-\mu r/n}(1-\mu re^{-2\mu r}-e^{-2\mu r}) \times F^2(-n+3,\,6,\,\mu r/n)dr, \tag{13}$$

$$X_{1snd}=\frac{16}{5}\mu^2N^2\int_0^\infty r_2^6\exp\left[-\mu\left(\frac{2n+1}{2n}\right)r_2\right] \times F(-n+3,\,6,\,\mu r_2/n) \times\left[\int_{r_2}^\infty r_1\exp\left[-\mu\left(\frac{2n+1}{2n}\right)r_1\right] \times F(-n+3,\,6,\,\mu r_1/n)dr_1\right]dr_2, \tag{14}$$

where

$$N^2=\mu^7(n+2)\,!/(n-3)\,!(5\,!)^2. \tag{15}$$

The quantities T_{nd} and V_{nd} are made up of integrals of the form

$$\int_0^\infty r^{-k}R^2(nd)dr, \tag{16}$$

where $R(nd)$ is the radial part of the hydrogenic nd wave function. Values of this integral for different values of k have been tabulated by Condon and Shortley.[3] With the aid of their Table II,[5] we find

$$T_{nd}=1/4n^2, \quad V_{nd}=1/n^2. \tag{17}$$

The quantity V_{1snd} may be evaluated by the process of integrating (13) term by term and applying the well-known[4] transformations among the hypergeometric functions. We obtain

$$V_{1snd}=\frac{1}{n^2}\left\{1-\frac{n(n^2-1)(n^2-4)(2n)^{2n-6}}{5\,!(2n+1)^{2n}} \times\left[\frac{7n+4}{2n+1}F\left(-n+3,\,-n+2,\,6,\,\frac{1}{4n^2}\right)+\frac{4n^2-23n+33}{24n^2(2n+1)}F\left(-n+2,\,-n+2,\,7,\,\frac{1}{4n^2}\right)\right]\right\}, \tag{18}$$

[3] E. U. Condon and G. H. Shortley, *The Theory of Atomic Spectra*, p. 117.

[4] *Cf.* Forsyth, *Differential Equations*, p. 192.

where F is the ordinary hypergeometric function of four variables. Although the exchange integral (14) is easily evaluated for a particular value of n, we have been unable to obtain a simple, closed expression for n generally. Table II contains the results of energy calculations for the $1s3d$ and $1s4d$ configurations of He I, obtained with the use of the hydrogenic energy integrals. The agreement with experiment is excellent. Indeed, the calculated $1s4d$ energies are slightly below the experimental values, which is due to the departure of the hydrogenic functions from exact orthogonality. It may be noted that the parameter $\mu(4d)$, which would possess the value 2 if the functions were exactly orthogonal, departs from that figure only in the fifth decimal.

TABLE II. *Results for* He I *1s3d and 1s4d.*

	1s3d	*1s4d*		*1s3d*	*1s4d*
$\mu(3\,^3D)$	2.00000	2.00003	$\mu(3\,^1D)$	2.00000	2.00002
$W(3\,^3D)_{\text{cal}}$	4.11114	4.06261	$W(3\,^1D)_{\text{cal}}$	4.11109	4.06257
$W(3\,^3D)_{\text{exp}}$	4.11126	4.06257	$W(3\,^1D)_{\text{exp}}$	4.11123	4.06255

The wave functions derived in this investigation have been utilized by one of us[5] to calculate transition probabilities for a number of lines of He I.

It is a pleasure to record our thanks to Dr. P. M. Morse for his interest and guidance in this problem, and to Dr. D. H. Menzel for many valuable discussions of the properties of hypergeometric functions.

[5] Goldberg, Astrophys. J., in press.

OCTOBER 1, 1939 PHYSICAL REVIEW VOLUME 56

Numerical Calculations of the Reflection of Electrons by Metals

L. A. MACCOLL
Bell Telephone Laboratories, New York, New York

(Received July 17, 1939)

The specular reflection of electrons by metallic surfaces is considered. It is assumed that the potential energy of an electron is constant ($=-V_0$) in the interior of the metal, and account is taken of the image force acting on an electron outside the metal (Nordheim's problem). The reflection coefficient R is computed for the range of values of V_0 which is of interest in connection with real metals, and for the range of values of energy of the electrons in which R has appreciable values. In the Appendix there are given some values of the function $\Gamma'(iy)/\Gamma(iy)$, for real values of y, which were computed incidentally.

1. INTRODUCTION

THE chief purpose of this article is to give the results of some numerical calculations of the reflection coefficient for a beam of electrons impinging on the plane face of a thick metallic body. We make use of the crude and simple assumption that the potential energy of an electron is constant in the interior of the metal, and we take account of the electrostatic image force acting on an electron outside the metal. Most of the analytical features of the problem have been discussed in an article by Nordheim;[1] but his work was not carried to the point of obtaining numerical results, such as are given here.

2. GENERAL FORMULA FOR THE REFLECTION COEFFICIENT

We employ a rectangular coordinate system, and assume that the metallic body occupies the space to the left of the plane $x=0$. The potential energy of an electron at the point (x, y, z) is assumed to be given by the equations:

$$V(x, y, z) = -V_0, \quad x \leqq x_0,$$
$$= -\epsilon^2/4x, \quad x \geqq x_0.$$

[1] L. Nordheim, Proc. Roy. Soc. London **A121**, 626–639 (1928). Unfortunately, Nordheim's article contains a number of typographical errors, which render the formulae unreliable. All formulae used in the present work have been derived independently.

Here ϵ denotes the absolute value of the electronic charge; and x_0 is determined by the equation $V_0=\epsilon^2/(4x_0)$, so that $V(x, y, z)$ is continuous. V_0 is a positive parameter, the value of which is to be selected in accordance with the metal under consideration.

We confine our attention to electrons having total energy E. One solution of the wave equation,

$$\nabla^2\psi+k^2(E-V)\psi=0, \quad k^2=8\pi^2m/h^2,$$

for these electrons is represented by the equations:

$$\begin{aligned}\psi&=B_1\exp\{ik[-x(E_x+V_0)^{\frac{1}{2}}\\&\qquad+(p_yy+p_zz)/(2m)^{\frac{1}{2}}]\}, \quad x\leqq x_0,\\&=[A_2W_{\lambda,\frac{1}{2}}(\xi)+B_2W_{-\lambda,\frac{1}{2}}(-\xi)]\\&\qquad\times\exp[ik(p_yy+p_zz)/(2m)^{\frac{1}{2}}], \quad x\geqq x_0.\end{aligned} \tag{1}$$

Here p_y and p_z denote arbitrary constants, and the symbols E_x, ξ, and λ, are defined by the equations

$$\begin{aligned}E_x&=E-(p_y^2+p_z^2)/(2m),\\\xi&=2ikxE_x^{\frac{1}{2}},\\\lambda&=-ik\epsilon^2/(8E_x^{\frac{1}{2}}).\end{aligned}$$

The symbols $W_{\lambda,\frac{1}{2}}(\xi)$ and $W_{-\lambda,\frac{1}{2}}(-\xi)$ denote the usual confluent hypergeometric functions.[2] The three constants B_1, A_2, and B_2, are subject to the two relations,

$$\begin{aligned}&B_1\exp[-ikx_0(E_x+V_0)^{\frac{1}{2}}]\\&\quad=A_2W_{\lambda,\frac{1}{2}}(2ikx_0E_x^{\frac{1}{2}})+B_2W_{-\lambda,\frac{1}{2}}(-2ikx_0E_x^{\frac{1}{2}}),\\&-(E_x+V_0)^{\frac{1}{2}}B_1\exp[-ikx_0(E_x+V_0)^{\frac{1}{2}}]\\&\quad=2E_x^{\frac{1}{2}}[A_2W'_{\lambda,\frac{1}{2}}(2ikx_0E_x^{\frac{1}{2}})\\&\qquad-B_2W'_{-\lambda,\frac{1}{2}}(-2ikx_0E_x^{\frac{1}{2}})],\end{aligned} \tag{2}$$

which are consequences of the requirement that the functions ψ, $\partial\psi/\partial x$, $\partial\psi/\partial y$, and $\partial\psi/\partial z$, be continuous at every point of the plane $x=x_0$.

The physical significance of the solution (1) can be determined easily with the aid of the following asymptotic representations of the functions $W_{\pm\lambda,\frac{1}{2}}(\pm\xi)$:

$$W_{\pm\lambda,\frac{1}{2}}(\pm\xi)\sim e^{\mp\frac{1}{2}\xi}(\pm\xi)^{\pm\lambda}\left[1+\sum_{n=1}^{\infty}\frac{[\frac{1}{4}-(\pm\lambda-\frac{1}{2})^2][\frac{1}{4}-(\pm\lambda-\frac{3}{2})^2]\cdots[\frac{1}{4}-(\pm\lambda-n+\frac{1}{2})^2]}{n!(\pm\xi)^n}\right]. \tag{3}$$

It is found that the wave function

$$A_2W_{\lambda,\frac{1}{2}}(\xi)\exp[ik(p_yy+p_zz)/(2m)^{\frac{1}{2}}]$$

represents an incident beam of electrons moving toward the surface of the metal, and that the wave function

$$B_2W_{-\lambda,\frac{1}{2}}(-\xi)\exp[ik(p_yy+p_zz)/(2m)^{\frac{1}{2}}]$$

represents a reflected beam of electrons moving away from the surface. (For $x<x_0$ our wave function ψ represents a transmitted beam of electrons moving toward the left from the plane $x=x_0$.) It is clear that E_x is the total energy of an electron diminished by the kinetic energy associated with the component of momentum parallel to the surface of the metal.

The intensities of the incident and reflected beams are proportional to $|A_2|^2$ and $|B_2|^2$, respectively; and hence the reflection coefficient is $R=|B_2/A_2|^2$. By Eqs. (2), we have the following formula for the reflection coefficient:

$$R=\left|\frac{2E_x^{\frac{1}{2}}W'_{\lambda,\frac{1}{2}}(2ikx_0E_x^{\frac{1}{2}})+(E_x+V_0)^{\frac{1}{2}}W_{\lambda,\frac{1}{2}}(2ikx_0E_x^{\frac{1}{2}})}{-2E_x^{\frac{1}{2}}W'_{-\lambda,\frac{1}{2}}(-2ikx_0E_x^{\frac{1}{2}})+(E_x+V_0)^{\frac{1}{2}}W_{-\lambda,\frac{1}{2}}(-2ikx_0E_x^{\frac{1}{2}})}\right|^2. \tag{4}$$

3. The Limit of R as E_x Approaches Zero

The limit of R as E_x approaches zero is of interest, because this is the condition of grazing incidence, and also because this is the condition under which R has its greatest value. In order to

[2] Demonstrations of the properties of the confluent hypergeometric functions which we use are to be found in: E. T. Whittaker and G. N. Watson, *Modern Analysis* (Cambridge University Press, 4th ed., 1927), Chapter XVI.

calculate the limit, we go back to the equation

$$\frac{\partial^2\psi}{\partial x^2}+k^2\left[E_x+\frac{\epsilon^2}{4x}\right]\psi=0,$$

set E_x equal to zero, and obtain a reflection coefficient R_0 by means of a calculation which is independent of the above, but is parallel to it. We find that R_0 is given by the formula

$$R_0=\left|\frac{f_1'(x_0)+ikV_0^{\frac{1}{2}}f_1(x_0)}{f_2'(x_0)+ikV_0^{\frac{1}{2}}f_2(x_0)}\right|^2, \tag{5}$$

where

$$f_1(x)=x^{\frac{1}{2}}[J_1(k\epsilon x^{\frac{1}{2}})-iY_1(k\epsilon x^{\frac{1}{2}})],$$
$$f_2(x)=x^{\frac{1}{2}}[J_1(k\epsilon x^{\frac{1}{2}})+iY_1(k\epsilon x^{\frac{1}{2}})].$$

Here J_1 and Y_1 denote the usual Bessel functions.

It can be proved that R_0 is in fact equal to $\lim_{E_x\to 0} R$. Since the proof is rather long, when it is given completely and rigorously, it will be omitted.[3]

4. Numerical Calculations and Results

Our numerical results are given graphically, in a self-explanatory form, by the curves of Figs. 1 and 2. Only a few remarks about the calculations are necessary.

The values of the confluent hypergeometric functions and their derivatives, which were required, were computed by means of the formula

$$W_{\lambda,\frac{1}{2}}(\xi)=\frac{1}{\Gamma(1-\lambda)}e^{-\frac{1}{2}\xi}$$
$$+e^{-\frac{1}{2}\xi}\sum_{n=1}^{\infty}\left[\frac{\Gamma'(n-\lambda)}{\Gamma(n-\lambda)}-\frac{\Gamma'(n+1)}{\Gamma(n+1)}-\frac{\Gamma'(n)}{\Gamma(n)}\right]$$
$$\times\frac{\Gamma(n-\lambda)\xi^n}{n!(n-1)!\Gamma(-\lambda)\Gamma(1-\lambda)}$$
$$+e^{-\frac{1}{2}\xi}\log\xi\sum_{n=1}^{\infty}\frac{\Gamma(n-\lambda)}{n!(n-1)!\Gamma(-\lambda)\Gamma(1-\lambda)}\xi^n,$$

[3] The author merely established the equality $R_0=\lim_{E_x\to 0} R$ on the basis of general function-theoretic considerations. A paper by W. C. Taylor (J. Math. and Phys. **18**, 34–49 (1939)), which has just appeared, contains formulae, relating specifically to the confluent hypergeometric functions, from which the equality can be inferred at once.

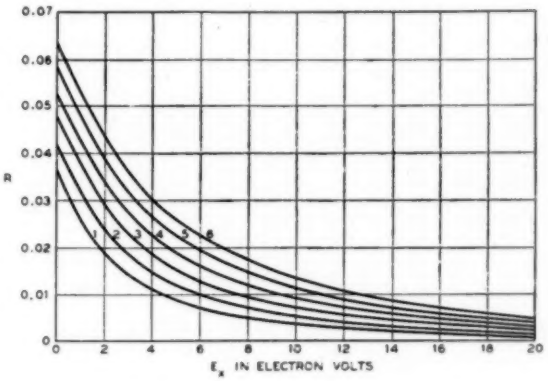

FIG. 1. Reflection coefficient R as a function of E_x. (Curves 1, 2, 3, 4, 5, 6 are for V_0 equal to 10, 12, 14, 16, 18, 20 electron volts, respectively.)

and the formula which is obtained by applying the ordinary formal operations of differentiation with respect to ξ to this.[4] This formula was obtained by a process which is indicated, but not carried out completely, by Whittaker and Watson.[5] In order to make use of these formulae (with the aid of the available tables, and of the equations $\Gamma(z+1)=z\Gamma(z)$ and $\Gamma'(z+1)/\Gamma(z+1)=\Gamma'(z)/\Gamma(z)+1/z$), it was necessary first to compute a short table of values of $\Gamma'(z)/\Gamma(z)$ for pure imaginary values of z. This was done by means of the relation

$$\frac{\Gamma'(z)}{\Gamma(z)}=-\gamma-\frac{1}{z}+\sum_{n=1}^{N}(-1)^{n+1}\zeta(n+1)z^n$$
$$+(-1)^N z^{N+1}\sum_{n=1}^{\infty}\frac{1}{n^{N+1}(n+z)},$$

using a value of N large enough so that the series

$$\sum_{n=1}^{\infty}\frac{1}{n^{N+1}(n+z)}$$

converged with satisfactory rapidity. (γ denotes Euler's constant, and ζ denotes the Riemann zeta-function.)

The substantial accuracy of the complicated numerical calculations was strongly indicated by the agreement between the values of the reflection coefficient, for $E_x=0$, calculated directly by

[4] For imaginary values of λ and ξ, $W_{-\lambda,\frac{1}{2}}(-\xi)$ is merely the conjugate of $W_{\lambda,\frac{1}{2}}(\xi)$.

[5] See also Nordheim's paper.

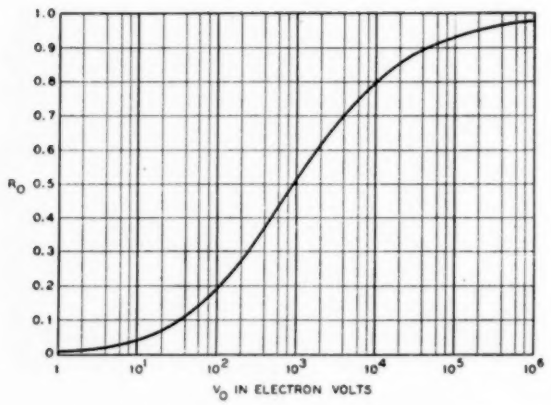

FIG. 2. $R_0\left(=\lim_{E_x\to 0} R\right)$ as a function of V_0.

means of Eq. (5), and the values obtained by extrapolating the curves calculated by means of Eq. (4) to the line $E_x=0$. Actually, it is estimated that the calculated values of R are correct to better than one-tenth percent in neighborhood of $E_x=1$ electron volt, and to about one percent in the neighborhood of $E_x=20$ electron volts.

The asymptotic formulae (3) are of no value in computing R for such values of E_x as those shown in Fig. 1, but they do enable us to determine the asymptotic behavior of R for very large values of E_x. This behavior is represented by the formula

$$R\sim\frac{V_0^4}{4\epsilon^4k^2E_x^3}.$$

The reflection coefficient R_0 given by Eq. (5) is a function of the single variable V_0. The values of V_0 appropriate to the cases of real metals lie between ten and twenty electron volts. However, in order to show the nature of the function R_0 more completely, we have plotted it, in Fig. 2, for a considerably greater range of values of V_0. It is easily shown, by means of the known representations of the Bessel functions for large and small values of their arguments, respectively, that when V_0 is small we have, approximately,

$$R_0=\frac{V_0}{4k^2\epsilon^4},$$

and that when V_0 is large we have

$$R_0\sim 1-\frac{\pi k\epsilon^2}{V_0^{\frac{1}{2}}}.$$

In conclusion, we call attention to the fact that if we had left the image force out of account, that is, if we had assumed the potential energy to be

$$V(x,y,z)=-V_0, \quad x<0,$$
$$=0, \quad x>0,$$

the reflection coefficient would have been given by the equation

$$R=\left|\frac{(E_x+V_0)^{\frac{1}{2}}-E_x^{\frac{1}{2}}}{(E_x+V_0)^{\frac{1}{2}}+E_x^{\frac{1}{2}}}\right|^2.$$

For the values of V_0 and E_x which are of interest, this formula gives values of R which are greater than those given by (4) by a factor which is of the order of ten. Hence, when actual values of R are required, we can by no means neglect the effect of the image force.

APPENDIX

The values of $\Gamma'(iy)/\Gamma(iy)$, for real values of y, which we have computed incidentally, may conceivably be useful in other work. Hence, we record them here. The eight decimal places shown are believed to be quite correct.

y	$\Gamma'(iy)/\Gamma(iy)$
0.1	$-0.56529779+i(10.16342116)$
0.2	$-0.53073041+i(5.32064142)$
0.3	$-0.47675489+i(3.79986145)$
0.4	$-0.40786794+i(3.09770369)$
0.5	$-0.32888636+i(2.71268857)$
0.6	$-0.24419658+i(2.47826542)$
0.7	$-0.15733613+i(2.32420192)$
0.8	$-0.07088340+i(2.21654578)$
0.9	$+0.013452015+i(2.13738747)$
1.0	$+0.09465032+i(2.07667405)$

LETTERS TO THE EDITOR

Prompt publication of brief reports of important discoveries in physics may be secured by addressing them to this department. Closing dates for this department are, for the first issue of the month, the eighteenth of the preceding month, for the second issue, the third of the month. Because of the late closing dates for the section no proof can be shown to authors. The Board of Editors does not hold itself responsible for the opinions expressed by the correspondents.

Communications should not in general exceed 600 words in length.

Concentration of Heavy Carbon by Thermal Diffusion

In the recent paper by Furry, Jones and Onsager[1] on the theory of isotope separation by the method of thermal diffusion definite predictions are made on the possible concentration of C^{13} with methane as the carrier. Using experimental conditions very similar to those postulated by these authors, except for length of column, I find that the C^{13} content of the methane is just doubled, whereas according to the theory the concentration should be at least some five- or sixfold. Since Bramley and Brewer,[2] using columns of about the same length, also obtain a separation factor of 2.0, this discrepancy between theory and experiment may to a considerable extent be real and not solely the effect of gas impurities.

The apparatus consists of three units in series, all made of copper pipe, the bottom of one unit being connected to the top of the following unit by two large-bore tubes, one of which is heated in order to set up convective circulation. The first two units are each one meter in length, one immediately above the other, while the final unit is 10 feet long, connected to the second unit by $\frac{3}{4}$" convection tubes some 7 feet in length. In each unit the inner pipe is $\frac{1}{2}$" O.D. concentrically mounted by means of fine centering pins inside a 1" I.D. pipe. The two shorter units have the inner cylindrical surfaces heated by means of inside spiral Chromel ribbon heaters, while the 10-foot unit is heated on the outside. The hot surfaces have been maintained at about 330°C and are outgassed before introduction of the methane. The power consumption is 2 kw with 1 gallon of water per min. for cooling. Tank methane is purified by the method of Storch and Golden[3] and stored in a water-sealed gasometer from which it is introduced, dried, into the apparatus at just above atmospheric pressure. At this "light" end gas is continuously valved-off into the room at a rate of 100 cc/hr., the rate of withdrawal at the "heavy" end being 3 cc/hr.

Samples drawn off at intervals of two, four, six, and eight days of continuous operation were changed to CO_2 and analyzed by means of a mass spectrometer. These analyses indicate a maximum C^{13}/C^{12} ratio of 2.02 percent at 4 days, the ratio in the subsequent samples being slightly below this value. Analysis shows the ethane content of the methane to be so small (tenths of 1 percent) that it could not lower the C^{13} concentration to such an extent. It is thought that the introduction of fresh gas at the rate of 100 cc/hr. is sufficient to maintain about normal CH_4 at the light end and thus make nearly full use of the separation factor of the apparatus. If the convection tubes between units do not function perfectly, the concentration may be due solely to the 10-foot column and the result is then in essential agreement with that of Bramley and Brewer.

To obtain a larger separation factor together with a larger speed of production a multistage apparatus with successive units decreasing in size is under construction.

I wish to thank Professor L. Onsager for much valuable discussion on the applications of the theory, and Professor H. C. Urey for the analyses which were made in his laboratory.

WILLIAM W. WATSON

Sloane Physics Laboratory,
Yale University,
New Haven, Connecticut,
September 15, 1939.

[1] W. H. Furry, R. C. Jones and L. Onsager, Phys. Rev. **55**, 1083 (1939).
[2] A. Bramley and A. K. Brewer, J. Chem. Phys. **7**, 553 (1939).
[3] H. H. Storch and P. L. Golden, J. Am. Chem. Soc. **54**, 4662 (1932).

The Heat of Fission of Uranium

The heat produced in a 13-g sample of metallic uranium when it was exposed to intense beams of slow neutrons from the Berkeley cyclotron was measured by a resistance thermometer.[1] The number of fissions produced in 0.07 mg of the element was measured with a pulse amplifier under the same geometrical conditions and at either the same neutron intensity or at an intensity bearing a known ratio to it. From these data the energy liberated per fission can be calculated. The weighted average of the measurements is 175 Mev per fission with an estimated probable error of 10 percent. The uranium sample was surrounded by thin brass and copper so that all soft radiations, such as α-particles and recoil nuclei, and most of the beta-rays would be absorbed. All neutrons and most gamma-rays escaped. It is hoped to continue and extend the work and to present the details in a later paper.

The apparatus was built at Princeton and used for preliminary work there. I am deeply indebted to Professor E. O. Lawrence for permission to continue the work in Berkeley and to him and to practically the entire staff of the Radiation Laboratory for their unfailingly cordial helpfulness; also to my colleague, Professor M. G. White, for suggestions and advice.

MALCOLM C. HENDERSON

Palmer Physical Laboratory,
Princeton University,
Princeton, New Jersey,
September 12, 1939.

[1] S. W. Watson and M. C. Henderson, Proc. Roy. Soc. **A118**, 318 (1928).

The Upward Radiation Produced by Cosmic Rays at High Altitudes

In order to investigate the effect of lead on the cosmic radiation at high altitudes, the following experiment was performed. A single Geiger counter was caused to occupy four positions relative to lead blocks. This was accomplished by mounting the counter on an arm which, when rotated by a small electric motor, carried the counter through a repeating cycle of four successive positions. The counts were scaled down and then transmitted by short wave radio to a station on the ground, by means of technique previously described. The counter walls were of such thickness that electrons below about 10^6 volts would not be counted. The position of the counter with respect to the lead was also transmitted, as were barometric and temperature data. The flight reached a minimum pressure of 23 mm Hg (approx. 80,000 ft.), and repeated the counting rate ratios on the descent, thus providing a check at corresponding pressures. The accuracy of the data is indicated by the standard deviations in column A of Table I.

TABLE I. *Counting rate in each of four positions with respect to lead as indicated in Fig. 1 as a function of pressure.*

PRESSURE INTERVAL (MM HG)	A	B	C	D
23–100	10.0±0.5	16.8	14.3	15.8
100–200	12.5±0.5	13.6	13.1	13.0
200–400	4.7±0.3	5.2	4.3	5.5
400–760	0.7±0.2	0.8	0.8	0.7

The counter occupied the four different positions A, B, C, and D with respect to lead as shown in Fig. 1, and remained in each position for approximately one minute. The counting rates in each position are presented in Table I as a function of pressure. The counts were averaged for each position over four pressure intervals, and the average includes observations obtained on the down-flight as well as on the up-flight.

Let x equal the counting rate of the counter due to all the radiation incident upon it in the absence of lead (position A), p equal the transmission (combined absorption and shower production) coefficient for downward rays through the lead, z the production coefficient of upward radiation produced by rays which impinge on the lead, and y the coefficient of production of upward radiation produced in the lower block of lead by rays which have passed through the upper block. Then the counting rates of the counter in the four positions A, B, C, and D will be given by $A=x$; $B=x(p+y+1)$; $C=x(p+1)$; $D=x(z+1)$. Hence it follows that $(D/A)-1=z$; $(C/A)-1=p$; $(B-C)/A=y$, and thus we may determine the coefficients from the data. Further it follows that if $z=y$, $(C+D)=(B+A)$.*

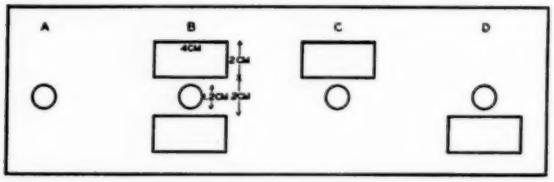

FIG. 1. Four positions of counter with respect to lead blocks during the flight.

TABLE II. *Shower production and absorption coefficient (p) and upward radiation production coefficients (z and y) derived from the observations.*

PRESSURE INTERVAL (MM HG)	p	z	y
23–100	0.43	0.58	0.25
100–200	0.05	0.04	0.04
200–400	−0.09	0.17	0.19

The values of the coefficients p, z, and y at the different altitudes are shown in Table II. It will be seen that p is positive at high altitudes and becomes negative at low altitudes. This is in agreement with cascade theory, since at high altitudes many showers are produced in the lead, while at low altitudes more rays are absorbed than are added as showers. Further, A decreases rapidly with elevation at altitude above the maximum of the familiar cosmic-ray intensity-altitude curve, while B, C and D show no clearly marked maxima.

It will also be seen that at low altitudes z is almost exactly equal to y and the relation $(C+D)=(B+A)$ holds. At the high altitudes, however, z is considerably larger than y. The difference between z and y must be due to the screening by the upper block of the lower block in B, with the result that fewer upward ejections are produced in the lower block.

The observations indicate that the counting rate at the highest altitude in position D, with lead below the counter, is much greater than in position A with no lead present. Since it seems improbable that rays coming up from below would be of sufficient number or energy to produce such abundant upward showers in the lead block, it appears that ionizing radiation is ejected upward from the lead by downward directed rays. This effect is presumably due to reflection of electrons, to nuclear disintegrations, and to wide angle showers in the lead. A large effect due to reflection, which these observations indicate, suggests the presence of many electrons of low energy in the radiation at high altitudes.

These experiments were partially supported by the Carnegie Institution of Washington. Thanks are due also to W. F. G. Swann for helpful discussions and to Victor Legallais for construction of the apparatus.

S. A. KORFF
E. T. CLARKE

Bartol Research Foundation of the Franklin Institute,
Swarthmore, Pennsylvania,
September 14, 1939.

* This algebra assumes that the radiation is incident on the apparatus from the top hemisphere. If we assume that $x=x_1+x_2$ where x_1 is incident radiation from above and x_2 from below, and since $z\leqslant 1$, then $(x_2/x)\leqslant 0.2$. For $z=0.6$, $x_2=0$. Since z is presumably considerably less than 1, (x_2/x) appears to be a small quantity and is for the present neglected.

Point Projector Electron Microscope

Electron images of high magnification and resolution can be obtained by making use of the quasi-rectilinear propagation of the field emission from a minute cathode close to the object being examined. The cathode here takes the form of an etched tungsten or molybdenum point similar to those used by Eyring, Makeown and Millikan[1] for cold emission measurements and by E. W. Muller[2] for the study of the variation of work function with crystalline orientation as well as of adsorption phenomena.

The "point projector microscope" thus constituted is essentially a transmission microscope. Consequently the specimens must be prepared so as to be transparent, wholly or partly, to electrons of the velocity corresponding to the applied voltage. Suitable methods of preparation for this purpose have been indicated by L. Marton[3] and H. Ruska.[4]

The magnification of the device depends on the ratio of the distance from the cathode to the viewing screen (or photographic plate) to the distance from the cathode to the object. The latter can readily be varied externally, permitting a wide range of magnifications.

As this type of microscope involves no electron-optical lens elements, the images obtained are free from the ordinary aberrations. The limit of resolution depends solely on the distribution of initial velocities of the field electrons and on Fresnel diffraction by the object, making it possible to proceed beyond the resolution of the light microscope by some orders of magnitude.

Figure 1, (a), (b) and (c), shows images of a 400-mesh

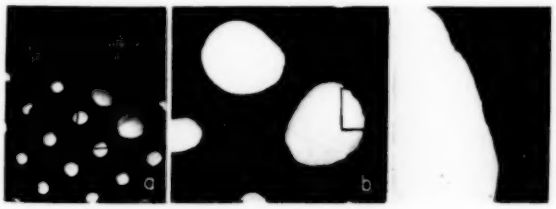

FIG. 1. Electronic projections of 400-mesh copper screen. The area of (c) is marked on (b) and that of (b) is marked on (a).

electroplated copper screen (0.0008 inch thick) magnified electron-optically 200, 600 and 3000 times, respectively, obtained with a sealed-off point projector microscope. While sharp images of the edge of a hole were observed on the luminescent screen with magnifications up to 8000 times, the mechanical steadiness of the image was here inadequate to permit photography with the increased exposures required at the relatively low lens aperture (f: 4.5) available.

A more detailed description of the device and its operation will be published elsewhere.

G. A. MORTON
E. G. RAMBERG

Electronic Research Laboratory,
RCA Manufacturing Company,
Camden, New Jersey,
September 11, 1939.

[1] C. F. Eyring, S. S. Makeown and R. A. Millikan, Phys. Rev. **31**, 900 (1928).
[2] E. W. Muller, Zeits. f. Physik **106**, 541 (1937).
[3] L. Marton, Bull. Acad. Belg. Cl. d. Sc. **22**, 1336–1344 (1936).
[4] H. Ruska, Naturwiss. **27**, 287–292 (1939).

Search for Weak Lines in the Molybdenum L Spectrum

Cecil J. Burbank[1] has recently reported the observation of nondiagram lines in the L group of 47 Ag resulting from electron bombardment sufficiently energetic to produce K ionization. The theory of such emission, treated by R. D. Richtmyer[2] is in harmony with Burbank's observations.

An unsuccessful search for similar lines in the spectrum of 42 Mo has just been conducted, with the Burbank apparatus with certain improvements. Since Burbank was greatly troubled by high order reflections of short wave radiation, tending to swamp the weak satellites, we thought it necessary to suppress such radiation and completely succeeded in doing so by interposing a total reflector of magnesium on glass between the silver target and the spectrometer crystal. It was possible to adjust the angle of incidence so that the wave-length region investigated was reflected to the gypsum crystal of the spectrograph almost completely while all radiations capable of higher order reflection were entirely cut off. This technique made possible the use of heavy targets instead of thin layers as used by Burbank.

All of the lines listed by Siegbahn[3] in the region investigated (from $L\gamma_1$ to $L\alpha_2$) were observed and in addition a line, thought to be new, having the wave-length 4979 x.u. was found between β_2 and β_3. Since this line does not disappear when the tube is operated at a potential below the K-excitation voltage it is not a satellite of the type studied by Burbank. The region between β_4 and α_1 was investigated very carefully since the analogy of silver indicated that the strongest satellites of the type sought should appear there. Although exposure conditions appeared at least as favorable as in Burbank's cases none of the expected lines was recorded.

The Auger transitions which result in the double ionization prerequisite to the emission of these satellites are more probable in elements of low atomic number and we had therefore expected the lines to be more intense in the molybdenum than in the silver spectrum. The results indicate that such is not the case.

WERNER VEITH
PAUL KIRKPATRICK

Stanford University,
California,
September 11, 1939.

[1] C. J. Burbank, Phys. Rev. **56**, 142 (1939).
[2] R. D. Richtmyer, Phys. Rev. **56**, 146 (1939).
[3] M. Siegbahn, *Spektroskopie der Röntgenstrahlen*.

Disintegration of N^{14} and N^{15} Produced by Deuteron Bombardment

A mixture of 80 percent N^{14} and 20 percent N^{15} gas has been bombarded with 1.07-Mev deuterons from the Cornell cyclotron. The ranges of the protons and alpha-particles emitted at 90° were measured by means of a shallow ionization chamber and a pulse amplifier. The nitrogen gas at reduced pressure was contained in a target cell of about 1.5 cm² volume. This cell was separated from the cyclotron chamber by a thin aluminum foil. On the side of the cell another aluminum window allows particles emitted in a direction at 90° to the deuteron beam to enter

the range cell. The range cell was 6.86 cm long with a mica foil on the end away from the target cell. The pressure in the range cell could be varied, allowing a change of about 6 cm in the air equivalent of the range cell. The ionization chamber and foil holder were fastened next to the exit window of the range cell. The entire assembly of target cell, range cell, foil holder and ionization chamber were screwed firmly together so that no relative motion of the parts could take place.

The pressure in the range cell could be read to about 1 mm Hg. The set of mica foils used in this experiment were all from one sheet and the stopping power in mg/cm²/cm of air was measured for two thin foils. The air equivalents of the thicker foils were obtained using the value 1.42_5 mg/cm²/cm air for 5-Mev alpha-particles. The value 1.07 Mev for the energy of the deuterons was computed from the physical constants of the cyclotron. A high bias was used on the counting Thyratron of the amplifier and a correction made for the bias and depth of the ionization chamber using the specific ionization curves for alpha-particles[1] and protons.[2]

Two proton groups have been measured by Cockcroft and Lewis[3] from the $N^{14}(dp)N^{15}$ reaction. These proton groups were measured in the present work and, in addition, a group of protons of 66.1-cm range was observed. This 66-cm group was observed both with the $N^{14}-N^{15}$ mixture and with ordinary tank nitrogen in the target cell, but was not observed with CO^2 as the target gas or with the target cell evacuated. Thus there is reason to assign the 66-cm proton group to the $N^{14}(dp)N^{15}$ reaction.

With the same $N^{14}-N^{15}$ mixture in the target cell three groups of alphas were observed. Two of these have been found previously[3, 4] and are from the $N^{14}(d\alpha)C^{12}$ reaction. The other group (5.09-cm range) can be attributed to the $N^{15}(d\alpha)C^{13}$ reaction since it appeared with no target gas except the one containing N^{15}. Further, the Q value, 7.40 Mev, checks sufficiently well with the Q value 7.55 calculated from the mass values.[5] In addition to the three homogeneous groups the intense continuous distribution of alphas arising from the reaction $N^{14}+H^2\rightarrow 4He^4$ was found below 3.9-cm range.

Because of the relatively large number of alpha-particles in the region below 6 cm it was not possible with the present equipment to detect the short range ($\sim$3.5 cm) proton group expected from the $N^{15}(dp)N^{16}$ reaction. It is hoped that with a target of much higher N^{15} concentration it will be possible to detect protons in this region below 6 cm.

TABLE I. *Experimental results of deuteron bombardment of* N^{14} *and* N^{15}.

REACTION	RANGE CM 15°, 760 MM	Q VALUE MEV	EXCITATION LEVEL MEV
$N^{14}(d\alpha)C^{12}$	11.59	13.21	C^{12} gr. st.
	6.37	8.86	4.35
$N^{14}(dp)N^{15}$	90.76	8.41	N^{15} gr. st.
	66.10	6.88	1.53
	20.99	3.10	5.31
$N^{15}(d\alpha)C^{13}$	5.09	7.40	C^{13} gr. st.

The results of the present experiment are shown in Table I. The Q values obtained from range measurements are all lower by about 0.15 Mev than those obtained from mass values.[5] Repeated checks on the method used in measuring the ranges indicate that a systematic error is not likely in this part of the experiment. It is possible that there is an error in the energy value 1.07 Mev of the incident deuterons, although this figure was checked by direct measurement of the deuteron ranges.

The writers are deeply indebted to Professor H. C. Urey of Columbia University for the supply of N^{15} gas, and to Professor R. F. Bacher for his continued encouragement in this work.

M. G. HOLLOWAY
B. L. MOORE

Department of Physics,
Cornell University,
Ithaca, New York,
September 3, 1939.

[1] M. G. Holloway and M. S. Livingston, Phys. Rev. **54**, 18 (1938).
[2] Parkinson, Herb, Bellamy and Hudson, Phys. Rev. **52**, 75 (1937).
[3] J. D. Cockcroft and W. B. Lewis, Proc. Roy. Soc. **154**, 261 (1936).
[4] Lawrence, McMillan and Henderson, Phys. Rev. **47**, 273 (1935).
[5] M. S. Livingston and H. A. Bethe, Rev. Mod. Phys. **9**, 373 (1937)

A Radioactive Isomer of Sr^{87}

In connection with studies soon to be reported of the radioactive isotopes of Sr and Y we have given particular attention to a period of 2.7 ± 0.2 hours which appears to be associated with an excited state of stable Sr^{87}.

Stewart, Lawson and Cork[1] reported a 3-hour Sr period produced by Sr+d and Sr+n (slow). They assigned it to an isomeric state of Sr^{89}, rejecting other possible assignments because the activity was electron rather than positron emitting. Cloud-chamber observations showed an apparently continuous spectrum with an upper limit of 610 kev. Our cloud-chamber measurements are similar to theirs, but the beta-ray spectrograph shows that the spectrum consists only of a strong line at $H\rho 2340$ (360 kev). (The broadening of the spectrum in the cloud chamber is undoubtedly due to the scattering which is important at these low energies.) These electrons are evidently K and L conversion electrons accompanying a 370-kev gamma-ray emitted in a K-electron capture or an isomeric transition. This removes the necessity of assignment to Sr^{89}.

We further find that this same period with the same electron spectrum is produced strongly by Rb+p at 6 Mev. Only a $p-n$ reaction could account for the yield, which restricts the assignment to either Sr^{85} or Sr^{87*}. There is also a strong period of $\sim$60 days produced in this reaction. In view of the argument below this may be assigned to Sr^{85}.

Finally an 85 ± 5-hour yttrium activity (produced either by Sr+p or Sr+d) shows the same electron line. When Sr is extracted from an aged sample of this activity the Sr fraction decays with the 2.7-hour period while the Y fraction grows with this period. The only Y isotopes which could be produced by both Sr(p, n) and Sr(d, n) are Y^{87} and Y^{88}. The latter has already been assigned[1] a 2-hour (e^+) period, since it is produced also by Y+fast neutrons. Stewart *et al.*[1] reported a 60-hour Y period from Sr+d which they identified with the 60–70-hour Y^{90}, produced by Y+n and Y+d, postulating a $Sr^{88}(d, \gamma)Y^{90}$ reaction.

Since the Y decay curves are complicated by the growth of the 2.7-hour Sr and by a very long Y period we believe that they were also observing this 85-hour period. This activity does not show the high energy beta-rays of Y^{90}.

We conclude that both the 85-hour and 2.7-hour periods must be assigned to isobars of mass 87. Then Y^{87} decays by K-electron capture to the excited Sr^{87*} which goes to the ground state Sr^{87} with the 2.7-hour period and the emission of a partially converted 370-kev gamma-ray. Absorption measurements in Pb show the expected absorption coefficient for this gamma-ray and Al absorption curves indicate a conversion factor of about 15 percent. The 2.7-hour activity emits x-rays also which show high mass absorption coefficients in both Se and Br indicating they are Sr rather than Rb K x-rays. The same Sr^{87*} is also produced directly by $Rb^{87}(p, n)$ and $Sr^{86}(n, \gamma)$. In the $Sr+d$ and $Sr+p$ bombardments it is probably produced only by the decay of Y^{87}, which accounts for the low and variable yield.[1]

The question arises whether Sr^{87*} is formed by the decay of naturally radioactive Rb^{87}. We extracted Sr from 5 g of RbCl but found no activity as much as 0.1 percent of that expected if every Rb^{87} atom decayed to Sr^{87*}. Furthermore, Libby and Lee[2] have found the maximum energy of the electrons from Rb^{87} to be 132 kev. There is thus no evidence for the 360-kev electrons from Sr^{87*} and it seems probable that only the decay to the ground state of Sr^{87*} is energetically possible.

It is interesting that in three of the five known pairs of adjacent isobars there is now known an excited radioactive state in one of the pair (In^{113} and In^{115} being the other cases[3]). In each case the period of the excited state is in the neighborhood of 2–4 hours and the energy is in the range 330–390 kev above the ground state.

L. A. DuBridge
John Marshall

University of Rochester,
Rochester, New York,
September 14, 1939.

[1] Stewart, Lawson and Cork, Phys. Rev. **52**, 901 (1937).
[2] W. F. Libby and D. D. Lee, Phys. Rev. **55**, 245 (1939).
[3] S. W. Barnes and P. W. Aradine, Phys. Rev. **55**, 50 (1939); S. W. Barnes, Phys. Rev. **56**, 414 (1939).

THE AMERICAN INSTITUTE OF PHYSICS

INCORPORATED

ADMINISTRATIVE STAFF

HENRY A. BARTON, *Director*

MADELINE M. MITCHELL, *Publications Manager*

Office: 175 Fifth Avenue, New York, New York

JOURNALS

THE PHYSICAL REVIEW
REVIEWS OF MODERN PHYSICS
JOHN T. TATE, *Editor*
J. W. BUCHTA, *Assistant Editor*

JOURNAL OF APPLIED PHYSICS
ELMER HUTCHISSON, *Editor*

THE JOURNAL OF THE OPTICAL SOCIETY OF AMERICA
THE REVIEW OF SCIENTIFIC INSTRUMENTS
F. K. RICHTMYER, *Editor*

JOURNAL OF THE ACOUSTICAL SOCIETY OF AMERICA
FLOYD A. FIRESTONE, *Editor*

THE JOURNAL OF CHEMICAL PHYSICS
HAROLD C. UREY, *Editor*
JOSEPH E. MAYER, *Assistant Editor*

THE AMERICAN PHYSICS TEACHER
DUANE ROLLER, *Editor*

GOVERNING BOARD

For The American Physical Society:

JOHN T. TATE, *Chairman*
University of Minnesota

GEORGE B. PEGRAM, *Secretary*
Columbia University

KARL T. COMPTON
Massachusetts Institute of Technology

For The Optical Society of America:

E. C. CRITTENDEN
National Bureau of Standards

A. C. HARDY
Massachusetts Institute of Technology

W. B. RAYTON
Bausch & Lomb Optical Company

For The Acoustical Society of America:

FLOYD A. FIRESTONE
University of Michigan

HARVEY FLETCHER
Bell Telephone Laboratories

WALLACE WATERFALL
The Celotex Corporation

For The Society of Rheology:

WHEELER P. DAVEY
Pennsylvania State College

MELVIN MOONEY
United States Rubber Products, Inc.

R. L. PEEK, JR.
Bell Telephone Laboratories

For The American Association of Physics Teachers:

PAUL E. KLOPSTEG
Central Scientific Company

FREDERIC PALMER, JR.
Haverford College

F. K. RICHTMYER
Cornell University

The American Institute of Physics is a membership corporation of which five societies are the founding members. These five societies are the principal national societies devoted to pure and applied physics in America. Their names, and those of their representatives who form the Governing Board of the Institute, are given above. The principal work of the Institute is the publication of journals sponsored by the societies or by itself. The names and the editors of the journals are also listed above.

The broad purpose of the Institute is to represent, in all matters of wide or common interest, the five thousand or more members and subscribers associated with the Founder Societies and the journals. It aims to advance the science and profession of physics, and to promote cooperation between pure research, the applied sciences and the industries. To achieve these aims, it is greatly in need of an endowment and is empowered by law to administer grants and funds of any kind.

CONTENTS

PHYS. REV. 56 (1939) OCTOBER 1

Excitation of Neutrons by Uranium . . . . . W. H. ZINN AND LEO SZILARD 619

Induced Radioactivity in Beryllium . . . . . KASIMIR FAJANS AND DAVID W. STEWART 625

Induced Radioactivity in Strontium and Yttrium; Nuclear Isomers in Strontium . . . . . DAVID W. STEWART 629

Time Distribution of Cosmic-Ray Bursts . . . . . PIARA S. GILL 633

Slow Mesons in the Cosmic Radiation . . . . . C. G. MONTGOMERY, W. E. RAMSEY, D. H. COWIE AND D. D. MONTGOMERY 635

Transition Effect for Large Bursts of Cosmic-Ray Ionization and the Number of Primary Electrons of Very High Energy . . C. G. MONTGOMERY AND D. D. MONTGOMERY 640

Theory of the Diffuse Scattering of X-Rays by Crystals in the Region of the K Critical Absorption Wave-Length . . . . . G. E. M. JAUNCEY 644

Evidence of a Periodic Deviation from the Schottky Line. I . . . . . R. L. E. SCHWARZ AND T. E. PHIPPS 652

Evidence of a Periodic Deviation from the Schottky Line. II . . . . . D. TURNBULL AND T. E. PHIPPS 663

Periodic Deviation from the Schottky Line . . . . . H. M. MOTT-SMITH 668

Zeeman Effect in the Hyperfine Structure of Iodine. II . . . . . ARTHUR S. FRY AND RUSSELL A. FISHER 669

Hollow Cathode Source for the Zeeman Effect . RUSSELL A. FISHER AND ARTHUR S. FRY 675

Interferometer Wave-Lengths of Certain Lines in the Secondary Spectrum of Hydrogen . . . . . LEWIS S. COMPTON, ROYAL M. FOWLER AND NORTON A. KENT 678

Note on Carbide Coupling Tones in Polyatomic Molecules . . . . . H. A. JAHN 680

Separation of Bromine Isotopes by Centrifugation . . . . . RICHARD F. HUMPHREYS 684

Accommodation Coefficient of Helium on Nickel . . . . . BARBARA RAIVID 691

Variational Atomic Wave Functions . . . LEO GOLDBERG AND ALBERT M. CLOGSTON 695

Numerical Calculations of the Reflection of Electrons by Metals . . . . L. A. MACCOLL 699

Letters to the Editor:

Concentration of Heavy Carbon by Thermal Diffusion . . . . . WILLIAM W. WATSON 703

Short Fission of Uranium . . . . . MALCOLM C. HENDERSON 703

Upward Radiation Produced by Cosmic Rays at High Altitudes . S. A. KORFF AND E. T. CLARKE 704

Point Projector Electron Microscope . . . . . G. A. MORTON AND E. G. RAMBERG 705

Search for Weak Lines in the Molybdenum *L* Spectrum . WERNER VEITH AND PAUL KIRKPATRICK 705

Disintegration of F^{19} and Ne^{20} Produced by Deuteron Bombardment . . . . . M. G. HOLLOWAY AND S. L. MOORE 705

Radioactive Isomer of Sr^{87} . . . . . L. A. DUBRIDGE AND JOHN MARSHALL 706

LANCASTER PRESS, INC., LANCASTER, PA.